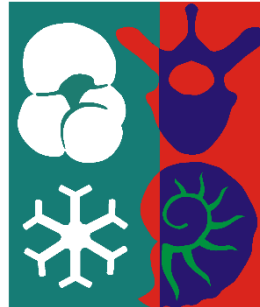




ARISTOTLE UNIVERSITY OF THESSALONIKI
Interinstitutional Program of Postgraduate Studies in
PALAEOLOGY – GEOBIOLOGY



KONSTANTINOS LASKOS
Biologist

THE VALLESIAN LARGE-SIZED *PALAEOTRAGUS* (GIRAFFIDAE,
MAMMALIA) FROM NORTHERN GREECE

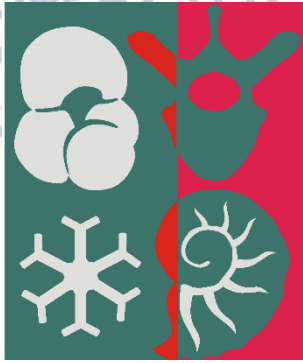
MASTER THESIS

DIRECTION: Macropalaeontology
Directed by Aristotle University of Thessaloniki



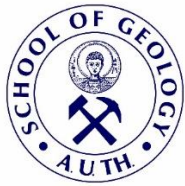
THESSALONIKI/ATHENS/PATRAS/MYTILINI
2020



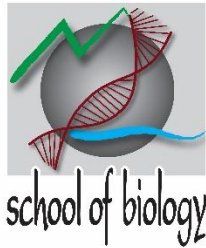


Interinstitutional
Program of
Postgraduate
Studies in
PALAEOLOGY – GEOBIOLOGY

supported by:



Τμήμα Γεωλογίας ΑΠΘ
School of Geology AUTH



Τμήμα Βιολογίας ΑΠΘ
School of Biology AUTH



National and
Kapodistrian
University of
Athens
Faculty of Geology
and
Geoenvironment

Τμήμα Γεωλογίας & Γεωπεριβάλλοντος
ΕΚΠΑ

School of Geology & Geoenvironment
NKUA



Τμήμα Γεωλογίας Παν/μίου Πατρών
School of Geology, Patras Univ.



UNIVERSITY OF THE AEGEAN

Τμήμα Γεωγραφίας Παν/μίου Αιγαίου
School of Geography, Aegean Univ.





KONSTANTINOS LASKOS
ΚΩΝΣΤΑΝΤΙΝΟΣ ΛΑΣΚΟΣ
Πτυχιούχος Βιολόγος

THE VALLESIAN LARGE-SIZED *PALAEOTRAGUS* (GIRAFFIDAE,
MAMMALIA) FROM NORTHERN GREECE

ΟΙ ΜΕΓΑΛΟΣΩΜΟΙ *PALAEOTRAGUS* (GIRAFFIDAE, MAMMALIA) ΑΠΟ ΤΟ
ΒΑΛΛΕΖΙΟ ΤΗΣ ΒΟΡΕΙΑΣ ΕΛΛΑΔΑΣ

Υποβλήθηκε στο ΔΠΜΣ Παλαιοντολογία-Γεωβιολογία

Ημερομηνία Προφορικής Εξέτασης: 17/03/2020
Oral Examination Date: 17/03/2020

Three-member Examining Board

Professor Kostopoulos S. Dimitrios, Supervisor
Associate Professor Iliopoulos Georgios, Member
Assistant Professor Rousiakis Sokratis, Member

Τριμελής Εξεταστική Επιτροπή

Καθηγητής Κωστόπουλος Σ. Δημήτριος, Επιβλέπων
Αναπληρωτής Καθηγητής Ηλιόπουλος Γεώργιος, Μέλος
Επίκουρος Καθηγητής Ρουσιάκης Σωκράτης, Μέλος



© Konstantinos Laskos, Biologist, 2020

All rights reserved.

THE VALLESIAN LARGE-SIZED *PALAEOTRAGUS* (GIRAFFIDAE, MAMMALIA) FROM NORTHERN GREECE – *Master Thesis*

© Κωνσταντίνος Λάσκος, Πτυχιούχος Βιολόγος, 2020

Με επιφύλαξη παντός δικαιώματος.

ΟΙ ΜΕΓΑΛΟΣΩΜΟΙ *PALAEOTRAGUS* (GIRAFFIDAE, MAMMALIA) ΑΠΟ ΤΟ ΒΑΛΛΕΖΙΟ ΤΗΣ ΒΟΡΕΙΑΣ ΕΛΛΑΔΑΣ – *Μεταπτυχιακή Διπλωματική Εργασία*

Citation:

Laskos K., 2020. – The Vallesian large-sized *Palaeotragus* (Giraffidae, Mammalia) from Northern Greece. Master Thesis, Interinstitutional Program of Postgraduate Studies in Palaeontology-Geobiology. School of Geology, Aristotle University of Thessaloniki, 73 pp.

It is forbidden to copy, store and distribute this work, in whole or in part, for commercial purposes. Reproduction, storage and distribution are permitted for non-profit, educational or research purposes, provided the source of origin is indicated. Questions concerning the use of work for profit-making purposes should be addressed to the author.

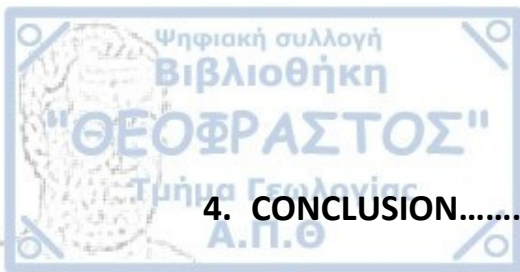
The views and conclusions contained in this document express the author and should not be interpreted as expressing the official positions of the Aristotle University of Thessaloniki.

Cover Figure: <https://alchetron.com/Palaeotragus>



CONTENTS

Acknowledgements.....	i
Abstract.....	ii
Περίληψη.....	iii
Museums Abbreviations.....	iv
1. INTRODUCTION.....	1
1.1 Phylogeny.....	1
1.1.1 <i>Early Pecora diversification</i>.....	1
1.1.2 <i>Giraffidae diversification</i>.....	1
1.2 Giraffidae Biogeography.....	5
1.3 The Greek Giraffid Record.....	9
1.4 The Genus <i>Palaeotragus</i> and its Species.....	12
1.5 Objectives of Present Study.....	15
2. METHODOLOGY.....	16
2.1 Description and System of Measurements.....	16
2.2 Studied and Comparative Material.....	19
2.3 Sites.....	20
2.3.1 <i>Axios Valley</i>.....	21
2.3.2 <i>Nikiti</i>.....	24
2.4 Statistical Analyses and Illustrations.....	25
3. SYSTEMATIC PALAEOLOGY.....	26
3.1 Description.....	26
3.1.1 <i>Site: Nikiti-1 (NKT)</i>.....	26
3.1.2 <i>Site: Pentalophos (PNT)</i>.....	33
3.1.3 <i>Site: Ravin de la Pluie (RPI)</i>.....	38
3.1.4 <i>Site: Xirochori (XIR)</i>.....	39
3.2 Comparison.....	40
3.2.1 <i>The taxonomy of Late Miocene Eurasian Palaeotragus</i>.....	40
3.2.2 <i>Comparison of the Greek Vallesian Large Palaeotragus</i>.....	53
3.2.2.1 <i>Nikiti-1 (NKT)</i>.....	53
3.2.2.2 <i>Pentalophos (PNT)</i>.....	57
3.2.2.3 <i>Ravin de la Pluie (RPI)</i>.....	59
3.2.2.4 <i>Xirochori (XIR)</i>.....	59



4. CONCLUSION.....60

REFERENCES.....62

PLATES



ACKNOWLEDGEMENTS

First of all, I am deeply grateful to my supervisor Professor Dimitris S. Kostopoulos. Not only he gave me the opportunity to get occupied with such an interesting subject, but he provided me with plenty of photographic material with *Palaeotragus* specimens from various sites of Eurasia and he provided me with plenty of old papers that were really important, but it would be almost impossible to find on my own. Of course, the most important thing was that after talking with me for hours he guided me to understand and apply the process of a paleontology research, which was previously something new to me, and he helped the ideas that I had in my mind to settle. The help of the member of examining board Associate Professor Giorgos Iliopoulos was also crucial. I had the opportunity to examine with him some graphs and my material and he was also a person that made a significant contribution to help me decide. Finally, I have to thank Dr Sokratis Rousiakis, also member of the examining board, as his corrective feedback to my final text was constructive.

I have to thank my fellow postgraduate students Katerina Kafetzidou, Antipas Klitsas and Marianna Kokotini. We had contact throughout the process of our researches, often exchanging view on each other's subject and had someone who could relate to when something did not go well. I have to thank Katerina a little more, as we shared the same office and I could not have asked for a better companionship.

MSc Anastasia Gkeme was also an important contributor, as she lent me her camera and I was able to take photos of my material.

I am also grateful to my friends Natasha and Thaleia, both graduates of the school of English Language and Literature. I asked oftentimes for their advice to better express what I wanted to say in the English language. Next, I thank my friend Ilias (Yaki), who also lent me his camera to take some additional photos of my material.

Last but not least, I could not forget to mention my family, that supported me financially with the postgraduate program of studies and they generally were my support throughout the accomplishment of my thesis.



ABSTRACT

The genus *Palaeotragus* is the most common giraffid genus in the Late Miocene of Eurasia and numerous species have been described. However, the validity of many of these species has been repeatedly questioned. A metric examination of these species showed that all the large-sized *Palaeotragus* should be considered synonyms to *Palaeotragus coelophrys*, with the exception of *Palaeotragus berislavicus*, and possibly *P. asiaticus*. A morphological examination of several dental specimens did not reveal any feature that could provide diagnostic information, as the premolar morphology demonstrates high variation, while the molar morphology demonstrates no variation.

Systematic excavations in the Late Miocene sites of Axios Valley (from 1972 to 2012) and Nikiti (from 1991 to 2005), revealed rich faunal assemblages. Members of the Giraffidae family are represented in almost all the different sites. The genus *Palaeotragus* is the most common giraffid of the aforementioned areas.

A large-sized *Palaeotragus* skull and several postcranial bones, which were previously classified as *Palaeotragus cf. rouenii* and later as *Palaeotragus sp.*, from the Vallesian site Nikiti-1 are re-evaluated here. According to metric and morphological comparisons the Nikiti *Palaeotragus* is distinguished by both *Palaeotragus rouenii* and *Palaeotragus coelophrys*. Based on metric comparisons, Nikiti *Palaeotragus* showed several similarities with *Palaeotragus berislavicus*, therefore a classification as *Palaeotragus aff. berislavicus* is suggested.

A review of old along with a study of new fossil remains of large-sized *Palaeotragus* from the Vallesian of Axios Valley (sites Ravin de la Pluie, Xirochori and Pentalophos), suggests that, based on their size, Ravin de la Pluie specimens are better classified as *Palaeotragus cf. coelophrys*, Pentalophos specimens are better referred to as *Palaeotragus coelophrys* and the single mandible from Xirochori to as *Palaeotragus sp.*

Το γένος *Palaeotragus* είναι το πιο κοινό της οικογένειας Giraffidae στο Άνω Μειόκαινο της Ευρασίας και πολλά είδη του έχουν περιγραφεί. Παρόλα αυτά, η εγκυρότητα πολλών από τα είδη έχει επανειλημμένα αμφισβητηθεί. Στην παρούσα έρευνα, μια επανεξέταση των μετρικών χαρακτηριστικών των ειδών αποκάλυψε ότι όλοι οι μεγαλόσωμοι αντιπρόσωποι του γένους *Palaeotragus* θα έπρεπε να θεωρηθούν συνώνυμα του *Palaeotragus coelophrys*, με εξαίρεση τον *Palaeotragus berislavicus* και πιθανόν τον *Palaeotragus asiaticus*. Μορφολογική εξέταση αρκετών οδοντικών δειγμάτων δεν αποκάλυψε κάποιο στοιχείο με διαγνωστική αξία, καθώς η ποικιλομορφία στην μορφολογία των προγομφίων εμφανίζεται πολύ υψηλή, ενώ των γομφίων πολύ χαμηλή.

Συστηματικές ανασκαφές στην Κοιλάδα του Αξιού (από το 1972 έως το 2012) και στην Νικήτη (από το 1991 ως το 2005), αποκάλυψαν πλούσιες πανίδες. Μέλη της οικογένειας Giraffidae αντιπροσωπεύονται στις περισσότερες από τις θέσεις. Το γένος *Palaeotragus* είναι το πιο κοινό γένος της οικογένειας στις προαναφερθείσες θέσεις.

Ένα κρανίο και διάφορα μετακρανιακά οστά, που είχαν ταξινομηθεί στο παρελθόν ως *Palaeotragus cf. rouenii* ή *Palaeotragus sp.*, από την πανίδα του ύστερου Βαλλέζιου της θέσης Νικήτη-1 επανεξετάζονται εδώ. Μετρικές και μορφολογικές συγκρίσεις έδειξαν ότι ο *Palaeotragus* της Νικήτης διαφέρει τόσο από τον *Palaeotragus rouenii* όσο και από τον *Palaeotragus coelophrys*. Σύμφωνα με μετρικές συγκρίσεις, παρουσιάζει αρκετές ομοιότητες με τον *Palaeotragus berislavicus*, και επομένως προτείνεται η ταξινόμησή του ως *Palaeotragus aff. berislavicus*.

Μία αναθεώρηση παλαιότερου και μελέτη νέου υλικού μεγαλόσωμων *Palaeotragus* από τις θέσεις Ravin de la Pluie, Πεντάλοφος και Ξηροχώρι, που ανήκουν στο Βαλλέζιο της Κοιλάδας του Αξιού, έδειξε ότι δείγματα της πρώτης θέσης θα πρέπει να ταξινομηθούν ως *Palaeotragus cf. coelophrys*, δείγματα της δεύτερης ως *Palaeotragus coelophrys* και δείγματα της τρίτης ως *Palaeotragus sp.*



MUSEUMS ABBREVIATIONS

AeMNH	Aegean Museum of Natural History, Mytilinii, Samos
AMNH	American Museum of Natural History, New York
AMPG	Athens Museum of Palaeontology and Geology, Athens
AUTh	Aristotle University of Thessaloniki, Thessaloniki
CMNH	Carnegie Muesum of Natural History, Pittsburgh
CRGEM	Central Research Geological Exploration Museum, Saint-Petersbourg
EU	Ege University, Izmir
HUM	Howard University Museum, Washington
MCML	Musée Cantonal de Géologie, Lausanne
MNHN	Muséum National d'Histoire Naturelle, Paris
MMTT	Natural Museum for Natural History, Tehran
MNHN	Muséum National d'Histoire Naturelle, Paris
MSU	Moldova State University, Chisinau
MTA	Natural History Museum of Ankara, Ankara
NMHL	National History Museum of London, London
NHMW	Museum of Natural History of Vienna, Vienna
NMENH	National Museum of Ethnography and Natural History, Chisinau
NMNSU	National Museum of Natural Sciences of Ukraine, Kyiv
OSU	Odessa State University, Odessa
PIN	Palaeontological Institute, Moscow
RSGMU	Russian State Geological Prospecting University, Moscow
SIZK	Schmalhausen Institute of Zoology of National Academy of Sciences of Ukraine, Kyiv



1.1.1 Early Pecora diversification

During the Eocene/Oligocene boundary (33.9 Ma) a drop in world's temperature and humidity, resulted to a spreading of grasslands. Small herbivores' biodiversity dropped, but new niches were created for larger herbivores, facilitating the radiation of Pecora during Early/Middle Oligocene (31.6-28.9 Ma). Molecular data (Irwin *et al.* 1991, Hassanin & Douzery 2003) are in accordance with the fossil record (Vislobokova 1997) about the timing of this radiation.

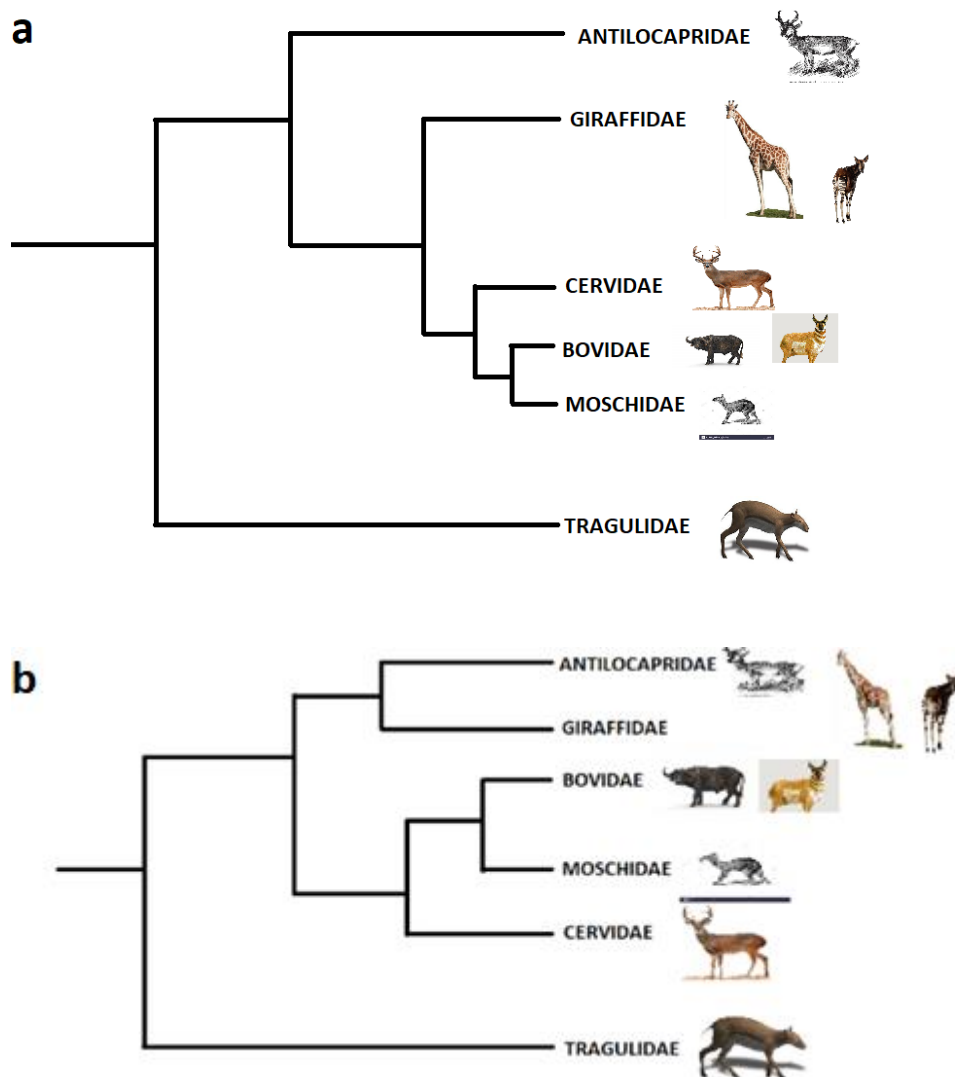
According to Mitchell & Skinner (2003) a pecoran family of the Oligocene, called Gelocidae, radiated later, during Early Miocene, giving rise to all extant pecoran families. At that time the intensifying global cooling and drying triggered the main part of Pecora evolution including the emergence of the families Antilocapridae, Moschidae, Bovidae, Cervidae, and Giraffidae. Among different groups of taxa radiated from Gelocidae, the members of Palaeomerycinae bear ossicones and therefore this subfamily is considered as the most possible ancestor of Giraffoidea (Jannis & Scott 1987, Mitchell & Skinner 2003).

The exact phylogenetic relationships among Giraffidae as well as with the rest of the families of Pecora are not yet clear. There is a possibility that Giraffidae are in the same clade with Antilocapridae, while Cervidae, Bovidae and Moschidae are in a different (sister) clade. Another scenario suggests that Antilocapridae were the first to split from the rest of the Pecora, followed by Giraffidae (Fig. 1) (Hassanin & Douzery 2003, Hassanin *et al.* 2012).

1.1.2 Giraffidae diversification

Several efforts have been made in order to understand the evolution of the giraffids (Hamilton 1978, Solounias 2007, Rios *et al.* 2017). However, there is no consensus about the exact Giraffoidea phylogeny, as different authors used different characters in order to reconstruct the phylogeny of the group. The presence of only

two living Giraffidae genera, does not allow molecular comparisons, making the reconstruction of their phylogeny difficult. Moreover, the stratigraphic data are not so relevant with the assessment of relations inside Giraffidae (Hamilton 1978). Thus, constructing a true phylogenetic scenario for Giraffidae is problematic and further research is needed. However, there is some agreement among different researchers (Hamilton 1978, Solounias 2007, Rios *et al.* 2017) in recognizing at least six subfamilies: Canthumerycinae, Okapiinae, Sivatheriinae, "Samotheriinae", "Palaeotragiinae" and Giraffinae.



Figures 1a, b: Two possible phylogenetic scenarios for Ruminantia, based on DNA analyses of extant Ruminants that place Giraffidae in different positions (Hassanin & Douzery 2003, Hassanin *et al.* 2012).

Bonis *et al.* (1997) described specimens of *Georgiomeryx georgalasi* Paraskevaïdis, 1940 from the island of Chios (dated at MN 5; 16.0-13.7 Ma), in an attempt to shed light in early giraffid evolution. The relations between the basal

giraffids are interpreted in Figure 2. *Georgiomeryx* had a more giraffid like P₄ with "...closed anterior valley, and a lingually open posterior valley...", than *Canthumeryx* Hamilton, 1973, so it was assumed to be a more advanced giraffid, closer to the taxa that thrived during the Late Miocene. Bonis *et al.* (1997) concluded that *Georgiomeryx*, as well as *Canthumeryx* and *Injanatherium* Heintz *et al.*, 1981 are basal, primitive giraffids and that each of the genera constitutes a monophyly. Another taxon that according to Bonis *et al.* (1997) shows a mix of ruminant plesiomorphies and giraffid apomorphies is *Giraffokeryx* Pilgrim, 1910. That genus assumed to be either a sivathere (Hamilton 1978, Solounias 2007) or a basal giraffid close to *Injanatherium*, as they both have two pairs of ossicones (Bonis *et al.* 1997, Rios *et al.* 2017). The genus is also proposed as the link between Canthumerycinae and the rest of Giraffidae (Mitchell and Skinner 2003). Most recent reviews suggest that *Canthumeryx*, *Georgiomeryx*, *Injanatherium* and *Giraffokeryx* are included in the subfamily of Canthumerycinae that diverged early on giraffid evolutionary history (Solounias 2007, Rios *et al.* 2017).

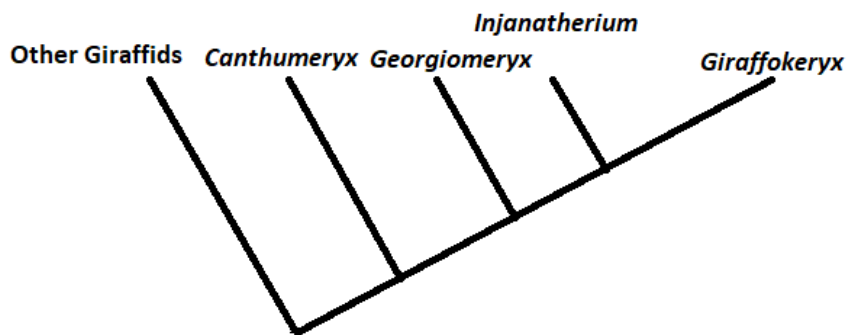


Figure 2: Cladogram of relationships among basal Giraffidae (adopted from Bonis *et al.* 1997).

Concerning the more advanced giraffids (Fig. 3), there is also consensus that *Okapia* Lankester, 1902, including today's okapi (*Okapia johnstoni* Sclater, 1901) and the fossil *Okapia stillei* (Dietrich, 1941) represents a primitive taxon. Okapiinae are distinguished from other giraffids, mainly because they lack apomorphies, being more primitive than most fossil giraffids (Colbert 1938). Colbert (1938) analyzed a plethora of other skull and dental characters of *Okapia*, showing that similarities with other giraffids should be regarded as plesiomorphies. *Okapia's* postcranial skeleton is also

primitive. According to Hamilton (1978), the Okapiinae's metapodials have proportions that are closer to bovids or cervids than to giraffids. Therefore, the lengthening (and the secondary shortening in Sivatheriinae) of the metapodials is an apomorphic feature for the other subfamilies. Another convincing evidence that favors the possibility that *Okapia* is primitive, is the fact that according to molecular clock *Okapia* and *Giraffa* Brünnich, 1772 split about 15.2 Ma (Hassanin *et al.* 2012), early on Giraffidae's radiation.

Sivatheriinae are probably a monophyletic subfamily. Their main synapomorphies are the existence of two pairs of large, complex ossicones and a secondary shortening of their metapodials (Hamilton 1978), whereas typical Sivatheriinae reach extremely large size. This is the case of *Sivatherium giganteum* Falconer & Cautley, 1836, *Shansitherium tafeli* Killgus, 1922, *Sivatherium cingulatum* Houghton, 1922, *Sivatherium maurisium* Pomel, 1892, *Helladotherium duvernoyi* Gaudry, 1860, *Bramatherium megacephalum* Lydekker, 1876, *Birgerbohlinia schaubi* Crusafont-Pairó, 1952 and *Decennatherium pachecoi* Crusafont-Pairó, 1952.

The subfamilies "Samotheriinae", "Palaeotragiinae" and Giraffinae seem to consist a monophyletic group, sharing the synapomorphy of neck's and limbs' elongation, which is weak in "Samotheriinae" but extreme in Giraffinae (Hamilton 1978, Solounias 2007, Danowitz *et al.* 2015a, b). However, this point of view is not universally accepted (Rios *et al.* 2017).

The first subfamily to branch out is that of "Samotheriinae", with a slight elongation of neck and limbs (Danowitz 2015a, b). Hamilton (1978) proposed some dental features as synapomorphies, but several scholars consider them as polyphyletic (Hamilton 1978, Geraads 1986, Solounias 2007). The "Samotheriinae" lineage contains species such as *Samotherium boissieri* Forsyth-Major, 1888, *Samotherium neumayri* Rodler & Weithofer, 1890, *Samotherium sinense* Bohlin, 1926 and *Samotherium major* Bohlin, 1926.

"Palaeotragiinae" and Giraffinae are proposed as sister taxa, sharing a more extreme lengthening of the metapodials and of their neck (Hamilton 1978, Solounias 2007, Danowitz *et al.* 2015a, b). "Palaeotragiinae" probably consist a polyphyletic or

paraphyletic group (Geraads 1986, Hou *et al.* 2014, Danowitz *et al.* 2015b). It is accepted that they do not share any apomorphy that differentiates them from other giraffids (Hamilton 1978, Solounias 2007). They could be defined as giraffids with intermediate neck and limb elongation. The type species is *Palaeotragus rouenii* Gaudry, 1861 from Pikermi, Greece. *Palaeotragus coelophrys* Rodler & Weithofer, 1890 is another species that is widely accepted as valid. "Palaeotrugiinae" are going to be further discussed later.

Finally, Giraffinae are considered as the more evolved subfamily of that Pecora lineage. The extreme lengthening of the metapodials and neck is proposed as their main synapomorphy (Hamilton 1978, Solounias 2007, Rios *et al.* 2017). If that opinion is followed, then *Giraffa*, including today's *Giraffa camelopardalis* Linnaeus, 1758, *Bohlinia* Matthew, 1929, including *Bohlinia attica* Gaudry & Lartet, 1856 and *Bohlinia nikitiae* Kostopoulos *et al.*, 1996 and *Honanotherium* Bohlin, 1926 should be grouped together. It should be noted that not all authors accept that grouping inside Giraffinae (e.g., Solounias 2007).

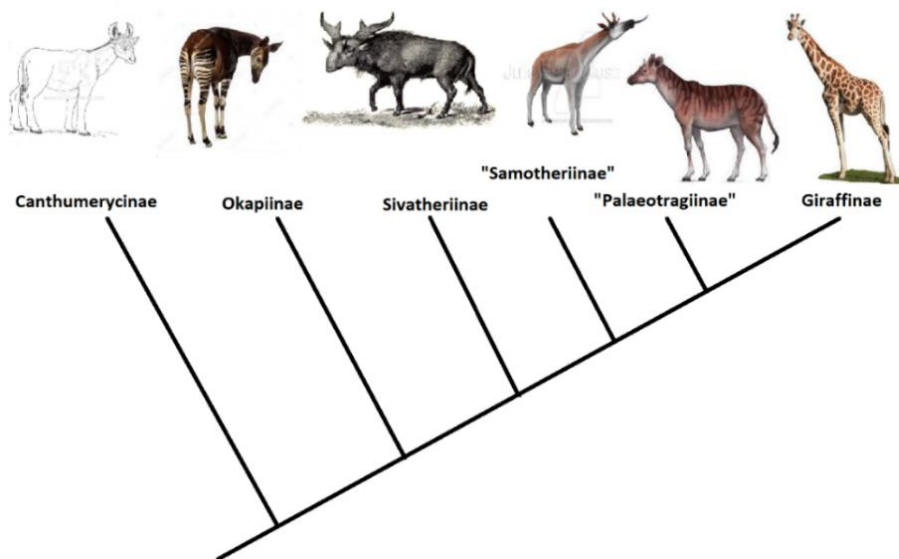
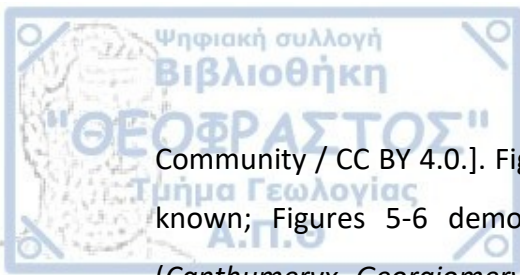


Figure 3: Phylogeny of the family Giraffidae [adopted from Hamilton (1978)]

1.2 Giraffidae Biogeography

The Palaeobiogeography of Giraffidae is demonstrated here based on data collected in NOW Database [Data(<http://www.helsinki.fi/science/nov/>)] by The NOW



Community / CC BY 4.0.]. Figure 4 maps the overall expansion of Miocene Giraffidae known; Figures 5-6 demonstrate the Miocene expansion of Canthumerycinae (*Canthumeryx*, *Georgiomeryx*, *Giraffokeryx* and *Injanatherium*) and “Samotheriinae” (*Samotherium* species); Figures 7-9 demonstrate the Miocene and also the Plio-Pleistocene expansion of Sivatheriinae (*Sivatherium*, *Decennatherium*, *Bramatherium*, *Birgerbohlinia* species), “Palaeotrugiinae” and Giraffinae (*Giraffa*, *Bohlinia* and *Honanotherium* species).

Giraffidae were a widespread family (Fig. 4) known by a variety of localities in the Old World. They were extremely abundant during the Turolian in Eastern Mediterranean (Koufos 2003) and in Africa from Miocene to today. They were absent from Central and Western Africa during the Miocene (Harris *et al.* 2010). They are also well-known from the Miocene of Asia, especially from sites of Central Eastern (China, Mongolia, Kazakhstan) and Central South (India, Pakistan, Nepal) Asia (Fortelius *et al.* 2006). The family of Giraffidae has an African origin and some of its oldest members migrated to Eurasia through Levante (Koufos 2003). However, only Canthumerycinae and Okapiinae originated in Africa, whereas Sivatheriinae, “Samotheriinae”, “Palaeotrugiinae” and Giraffinae have a Eurasian origin (Mitchell & Skinner 2003).

The Canthumerycinae are the less abundant subfamily and although they were present in all the three continents, they show a fragmentary distribution (Fig. 5). They are relatively abundant in Turkey, in South-Central Asia, in Middle East, in North-East Africa and in Kenya. There are only two references for their presence in Europe; the first one is in Serbia (Ciric & Thenius 1959, Pavlovic 1969) and the second in Chios (Bonis *et al.* 1997).

Samotherium species are mostly found in Eurasia’s Late Miocene, spreading from East China to the Balkans and there is a reference for their presence in Italy (Marra *et al.* 2011). A few fossiliferous localities in Africa contain fossils referred to as *Samotherium* (in Kenya, Algeria and Libya) (Harris *et al.* 2010) (Fig. 6).

The Sivatheriinae are widespread in the Miocene of the Mediterranean; *Decennatherium* and *Birgerbohlinia* are common in Spain, while *Helladotherium* is abundant in Balkans and Anatolia. They are also widespread in the Plio-Pleistocene of

North-Western and Eastern Africa with the genus *Sivatherium*. Finally, they are represented in the Late Miocene of South-Central Asia by *Hydaspitherium*, *Bramatherium* and *Sivatherium* (Fig. 7).

“Palaeotraginae” are abundant in the Late Miocene of Eurasia from Balkans to China. They are also present in Miocene localities of North-Western and Eastern Africa and in the Plio-Pleistocene of Balkans (Fig. 8).

Finally, in the Late Miocene, Giraffinae were represented in China with *Honanotherium*, in Eastern Mediterranean with *Bohlinia* and possibly in India and Pakistan (Mitchel & Skinner 2003, Aftab *et al.* 2016) with the species *Giraffa priscilla* Pilgim, 1911. After Miocene, they are mostly known from Africa with the genus *Giraffa* (Fig. 9). The only exceptions are references of *Giraffa* from the site Çalta, Turkey, dated at the Early Pliocene (Sen 1977, Geraads 1998).

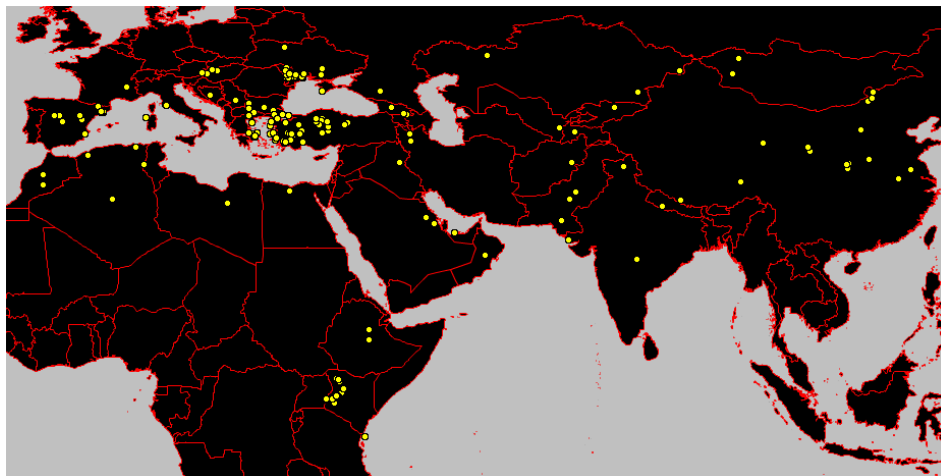


Figure 4: Total geographic expansion of Miocene Giraffidae (recovered in January 2020 from NOW Database)

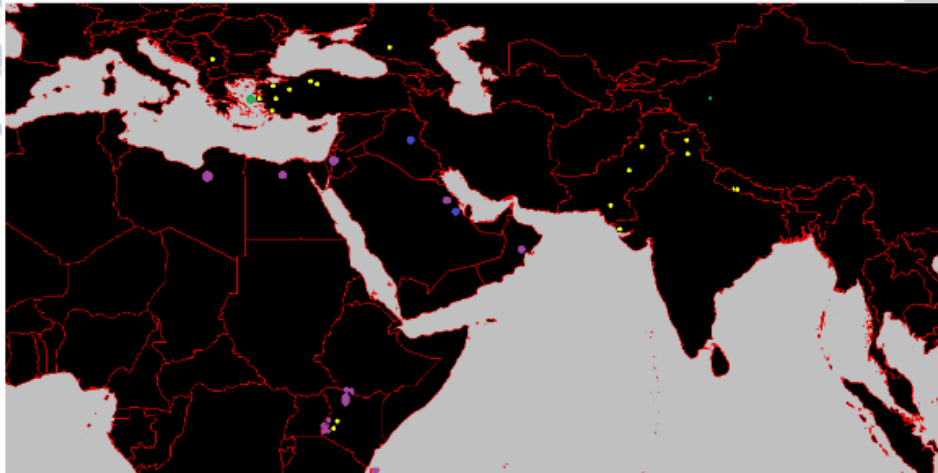


Figure 5: *Canthumerycinae* species expansion during Miocene. Yellow: Giraffokeryx, Purple: Canthumeryx, Green: Georgiomeryx, Blue: Injanatherium (recovered in January 2020 from NOW Database)

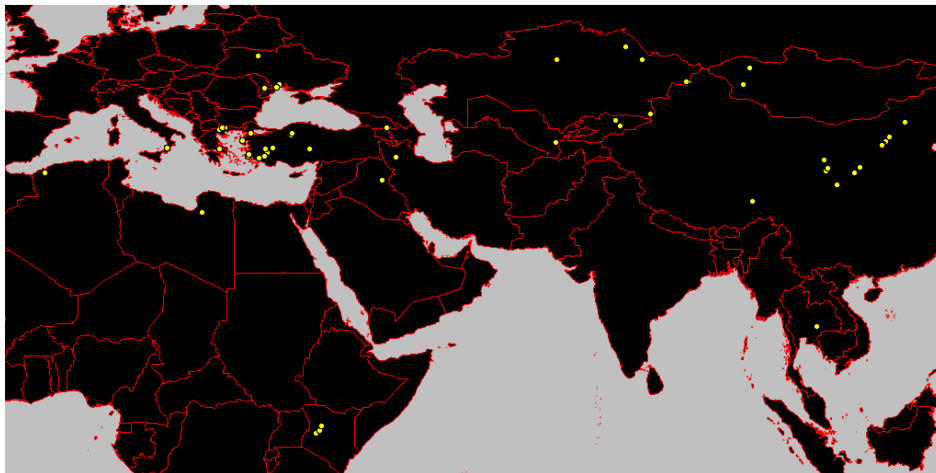


Figure 6: *Samotherium* species expansion during Miocene (recovered and modified in January 2020 from NOW Database)

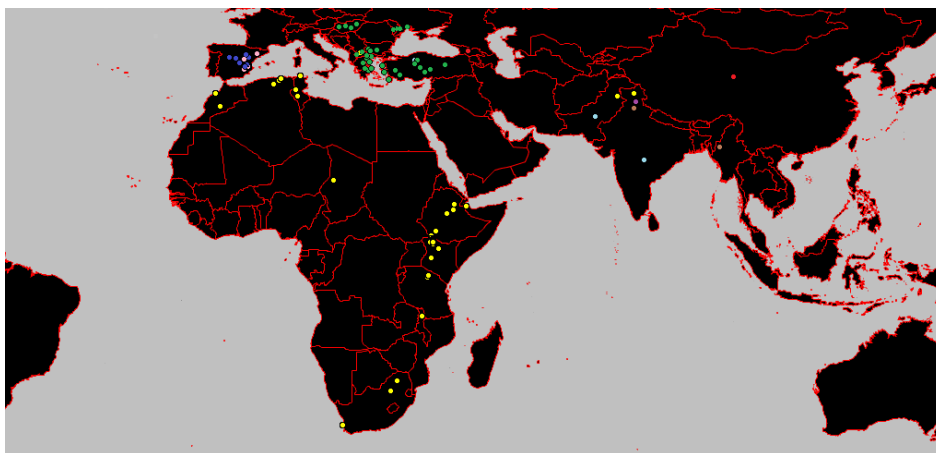


Figure 7: *Sivatheriinae* species expansion during Miocene and Plio-Pleistocene. With Yellow: *Sivatherium* species, Pink: *Birgerbohlinia schaubi*, Green: *Helladotherium* species, Blue: *Decennatherium*, Brown: *Hydaspathierium*, Light Blue: *Bramatherium*, Red: Unidentified (recovered and modified in January 2020 from NOW Database)

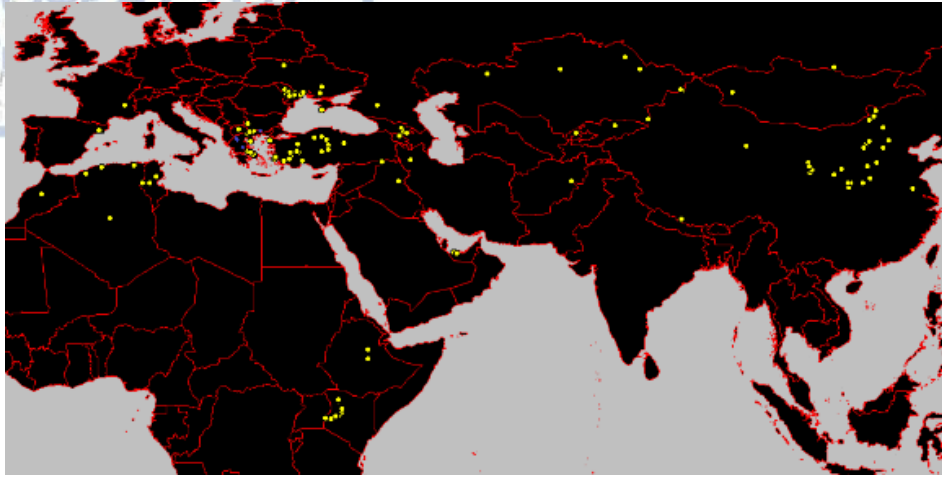


Figure 8: "Palaeotragiinae" species expansion during Miocene and Plio-Pleistocene. Yellow: Miocene site with Palaeotragus, Blue: Palaeotragus inexpectatus (recovered in January 2020 from NOW Database)

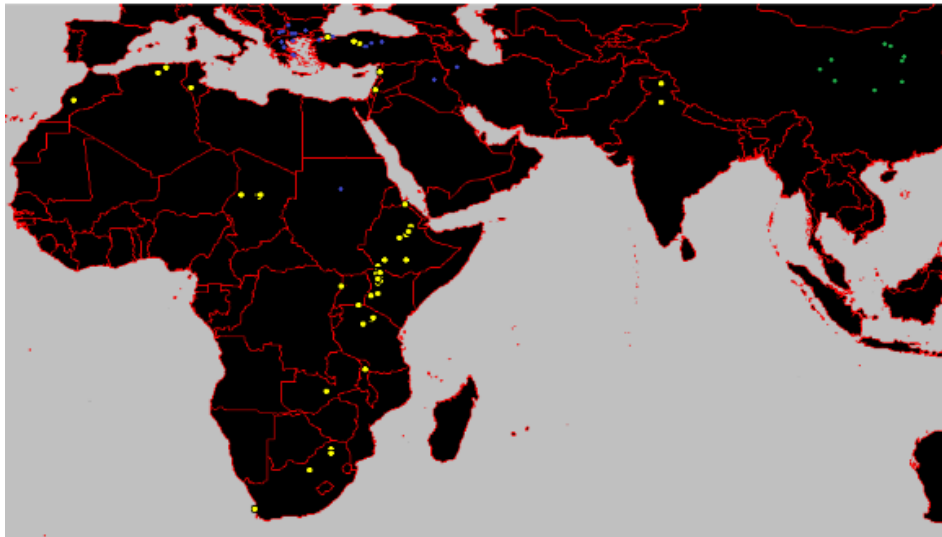
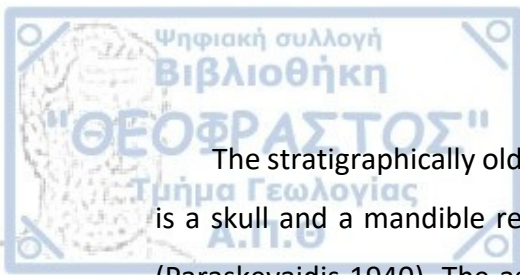


Figure 9: Giraffinae species expansion during Miocene and Plio-Pleistocene. Yellow: Giraffa, Blue: Bohlinia, Green: Honanotherium (recovered in January 2020 from NOW Database)

1.3 The Greek Giraffid Record

Giraffids have a long and rich fossil record in Greece spanning from Middle Miocene (MN 5) to Pleistocene (MN 17) (Table 1, Fig. 10). The study of Greek giraffids goes back to the times of Duvernoy (1854) and Gaudry & Lartet (1856) and still is of great interest due to giraffids' high taxonomic diversity and their well-preserved fossils.



The stratigraphically oldest giraffid specimen that has found until today in Greece is a skull and a mandible referred to *Georgiomeryx* from Thymiana locality in Chios (Paraskevaïdis 1940). The assemblage in which *Georgiomeryx* was found is dated to the Late Orleanian (MN5), at a time of great faunal interchange with Africa. Chios *Georgiomeryx* represents the first datum of giraffids in the Eastern Mediterranean (Koufos 2003).

Sivatheriinae are mostly known in Greece by *Helladotherium*, which first appeared in the Late Vallesian fauna of Nikiti-1 (Koufos 2000). The genus was also common during Turolian, disappearing from Greece at the end of this age (Koufos 2003) and it is the only known giraffid from the island of Rhodes (Boni 1943, fide Koufos 2006). *Palaeogiraffa* Bonis & Bouvrain, 2003 is an enigmatic genus of a medium to large-sized giraffid with slender metapodials. *Palaeogiraffa macedoniae* (Geraads, 1989), from Xirochori, was previously described as *Decennatherium* (Geraads 1979) and Bonis & Bouvrain (2003) clarified that this species, should be assigned to a new genus *Palaeogiraffa*. It is known exclusively from Northern Greece and Eastern Thrace.

The first appearance of *Samotherium* is dated on the Early Turolian of Samos (Koufos 2003). During the Turolian the genus was very common in Asia Minor and present in adjacent territories in continental Greece. It finally disappeared from Greece during the Late Miocene (Schmidt-Kittler *et al.* 1995).

The first datum of *Palaeotragus* in the Eastern Mediterranean is in Middle Sinap (Turkey), dated at 10.6 Ma (Lunkka *et al.* 1992, Kappelman *et al.* 2003), at the end of Early Vallesian. In Greece *Palaeotragus* oldest record comes from Pentalophos site, discussed in this work, whereas its last occurrences are from the Early Pleistocene faunas of continental Greece and Lesvos island (Kostopoulos 1996, Athanassiou 2014).

Finally, Giraffinae are represented in the Greek record by *Bohlinia*, which first appeared in Eastern Mediterranean at Ravin de la Pluie (Axios Valley) during the Late Vallesian (MN 10) and continued throughout the Turolian. It disappeared at the end of Miocene (Bonis & Koufos 1999).

Table 1: Giraffidae occurrences in Greece (localities and age).

	Site	<i>Georgiomeryx georgiiasi</i>	<i>Bobhina attica</i>	<i>Bobhina cf. attica</i>	<i>Bobhina nikitiae</i>	<i>Bobhina sp.</i>	<i>Helalodotherium duvernoyi</i>	<i>Helalodotherium cf. duvernoyi</i>	<i>Helalodotherium sp.</i>	<i>Palaeotragus rouenii</i>	<i>Palaeotragus cf. rouenii</i>	<i>Palaeotragus sp.</i>	<i>Palaeotragus aff. berislavicus</i>	<i>Palaeotragus inexpectatus</i>	<i>Palaeotragus coelophrys</i>	<i>Palaeotragus cf. coelophrys</i>	<i>Palaeotragus quadricornis</i>	<i>Samotherium major</i>	<i>Samotherium boissieri</i>	<i>Samotherium cf. boissieri</i>	<i>Samotherium sp.</i>	<i>Palaeoaiiuffa macedoniae</i>	<i>Palaeoaiiuffa namiri</i>	<i>Palaeoaiiuffa maior</i>	Chronology	
Axios Valley	RZO						x			x															MN 11	
	PXM						x																			MN 11
	VTK		x																							MN 12
	VAT		x							x										x						MN 11
	DIT - DTK		x								x															MN 13
	PNT															X*							x			MN 9
	RPI			x								x					X*							x		MN10
	XIR												X*											x		MN10
Nikiti	NKT		x		x		x						X*													MN10
	NIK						x			x																MN11
Eastern Macedonia	MTH							x																		MN13
	MAR																					x				MN 13/MN14
	Thermo- pigi						x			x		x														MN 12
Thessaly	PER						x			x																MN11
	ALF						x																			MN11/MN13
Attica	PIK		x				x			x																MN12
	CHO									x																MN12
	PYV						x																			MN9/MN13
Evia	Kerasia		x			x	x			x		x							x			x				MN11/MN12
	AHG									x																MN11/MN13
	HAL						x																			MN12
Rhodes	RHO					x																			MN9/MN13	
Pleistocene Sites	VTF														x											MN17
	VOL														x											MN17
	SES														x											MN17
	DFN														x											MN17
Chios (THB)		x																							MN 5	
Kryopigi						x			x																MN10	
Samos						x			x		x						x	x	x						MN 12/ MN 13	

RZI: RZI: Ravin de Zouaves-1, RZO: Ravin de Zouaves-5, PXM: Prochoma, VAT: Vathylakkos-3, DTK, DIT: Ditiko-1, 2 respectively, PNT: Pentalophos, RPI: Ravin de la Pluie, NKT: Nikiti-1, NIK: Nikiti-2, MTH: Ano Metochi-2,3, MAR: Maramena, PER: Perivolaki, ALF: Alifakas, PIK: Pikermi, CHO: Chomateres, PYV: Pyrgos Vasilissis, Kerasia: KRS, KRS-1, KRS-3, KRS-4, AHG: Achmet AGA, RHO: Rhodes, VTF: Vatera-F VOL: Volakas, SES: Sesklon, DFN: Dafnero, THB: Thymiana B, Samos: Qx, Q5, Q6 MLN, MYT, MTLA, MTLB, MTLA (Iliopoulos 2003, Koufos 2006, Kostopoulos 2009, Lazaridis 2015, Koufos et al. 2016, Xafis et al. 2019)

*Studied in present study

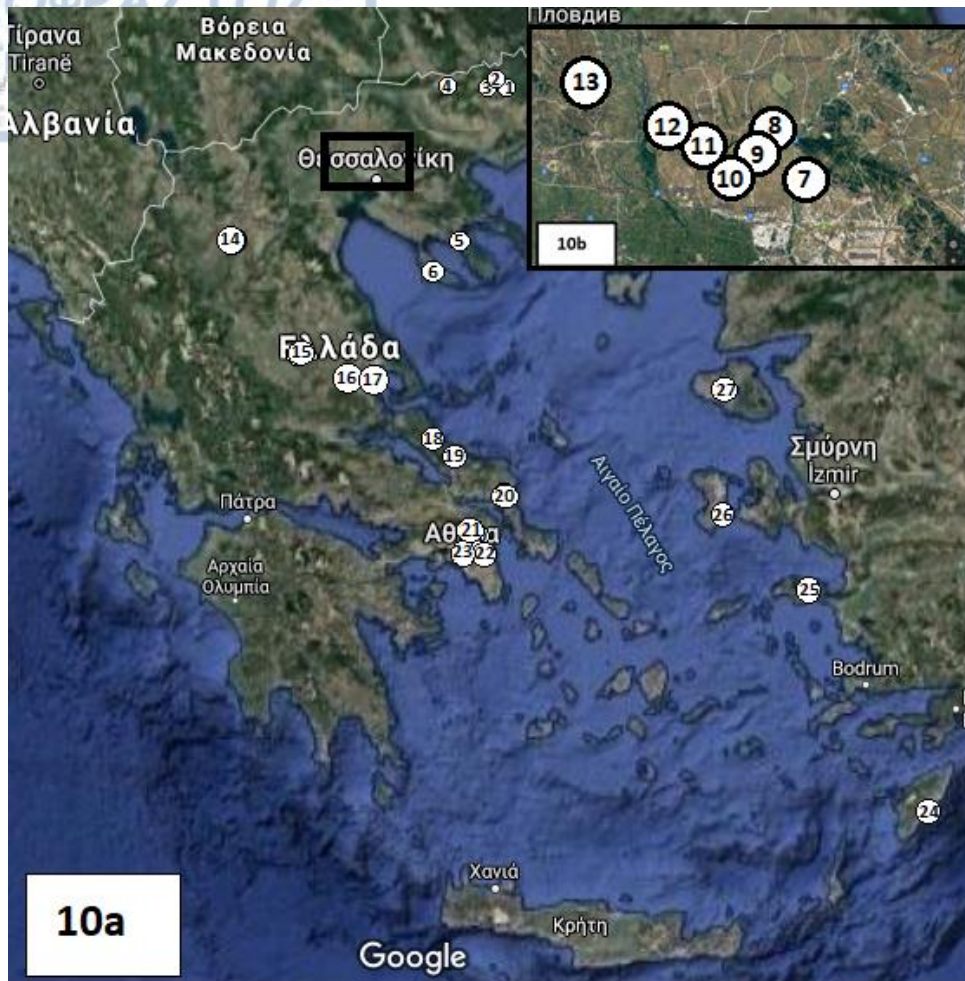


Figure 10: Localities in Greece (a) and Axios Valley (b) with Giraffid assemblages. 1: Maramena, 2: Volax, 3: Ano Metochi, 4: Thermopigi, 5: Nikiti-1, 6: Kryopigi, 7: Pentalophos, 8: Xirochori, 9: Ravin de la Pluie & Ravin de Zouaves-1, 10: Ravin de Zouaves-5, 11: Vathylakkos, 12: Prochoma, 13: Dytiko, 14: Dafnero, 15: Alifakas, 16: Perivolaki, 17: Sesklon, 18: Kerasia, 19: Achmet Aga, 20: Halmyropotamos, 21: Pikermi, 22: Chomateres, 23: Pyrgos Vassilisis, 24: Rhodes, 25: Samos-Mytilini localities, 26: Thymiana, 27: Gavathas

1.4 The Genus *Palaeotragus* and its Species

Palaeotragus expanded from North Africa to Black Sea and from Balkans to China and it especially thrived in the Turolian communities of Eastern Mediterranean. "Palaeotragiinae" is probably a polyphyletic or paraphyletic subfamily that contains the species of the genus *Palaeotragus*. According to several authors (Geraads 1986, Godina 2002, Hou *et al.* 2014, Danowitz *et al.* 2015b), *Samotherium* species should be probably grouped within "Palaeotragiinae" subfamily.

Numerous species have been described as *Palaeotragus* from the Old World's Miocene. *Palaeotragus tungurensis* Colbert, 1936 is a Middle Miocene species described from China districts. It is the oldest *Palaeotragus* representative, although it is not sure if it is valid (e.g., Solounias 2007). The type specimens are dated at 12.85-11.2 Ma (Colbert 1936). Other Middle Miocene *Palaeotragus* taxa are the small-sized *P. lavocati* Heintz, 1976 from Morocco's MN 6 and the middle-sized *P. robinsoni* Crusafont-Pairó, 1979, from Tunisia's MN7-8 (Harris *et al.* 2010). *Palaeotragus germaini* Arambourg, 1959 is a species described from the Late Miocene of Africa (North Africa and Kenya). Unidentified *Palaeotragus* specimens have been described from Ethiopia, Kenya and Tunisia too (Robinson & Black 1974, Bishop & Pickford 1975, Nakaya *et al.* 1987, Haile-Selassie 2009).

The vast majority of *Palaeotragus* species has been described from the Late Miocene of Eurasia (Figs 11, 12). The type species is *Palaeotragus rouenii*, originally from Pikermi (Gaudry 1861), that is characterized by small size and long, slender metapodials. Another important and generally accepted taxon is *Palaeotragus coelophrys*, originally from Maragheh, Iran (Rodler & Weithofer 1890). Late Miocene palaeotragines include, however, many more reported species: *Palaeotragus microdon* Koken, 1885 from Shansi, China, *Palaeotragus quadricornis* Bohlin, 1926 from Samos, Greece, *Palaeotragus expectans* Borissiak, 1914 from Sevastopol, Ukraine, *Palaeotragus pavlowae* Pavlow, 1913 from Grebeniki, Ukraine, *Palaeotragus asiaticus* Godina, 1975 from Ortok, Kyrgyzstan, *Palaeotragus berislavicus* Korotkevitch, 1957 from Berislav, Ukraine, *Palaeotragus moldavicus* Godina, 1979 from Starye Bogeny, Moldova, *Palaeotragus hoffstetteri* Ozansoy, 1965 from Sinap, Turkey and *Palaeotragus borissiaki* Alexeiev, 1930 from Eldari, Georgia. It should be noted that the validity of all these species has often been questioned by some experts (Geraads 1974, 1986). Others not only accept that over-segregation, but also propose the presence of three sub-genera (Godina 1975, 1979). The taxonomy of Late Miocene Eurasian *Palaeotragus* species will be later comprehensively discussed.

Palaeotragus priasovicus Godina & Bajgusheva, 1985 and *Palaeotragus inexpectatus* (Samson & Radulesco, 1966) from the Eurasian Plio-Pleistocene are considered synonyms with each other and with *Mitilanotherium*, *Macedonitherium*

and *Sogdianotherium* species and they are all assigned as *Palaeotragus* (Kostopoulos & Athanassiou 2005, van der Made & Morales 2011, Athanassiou 2014).

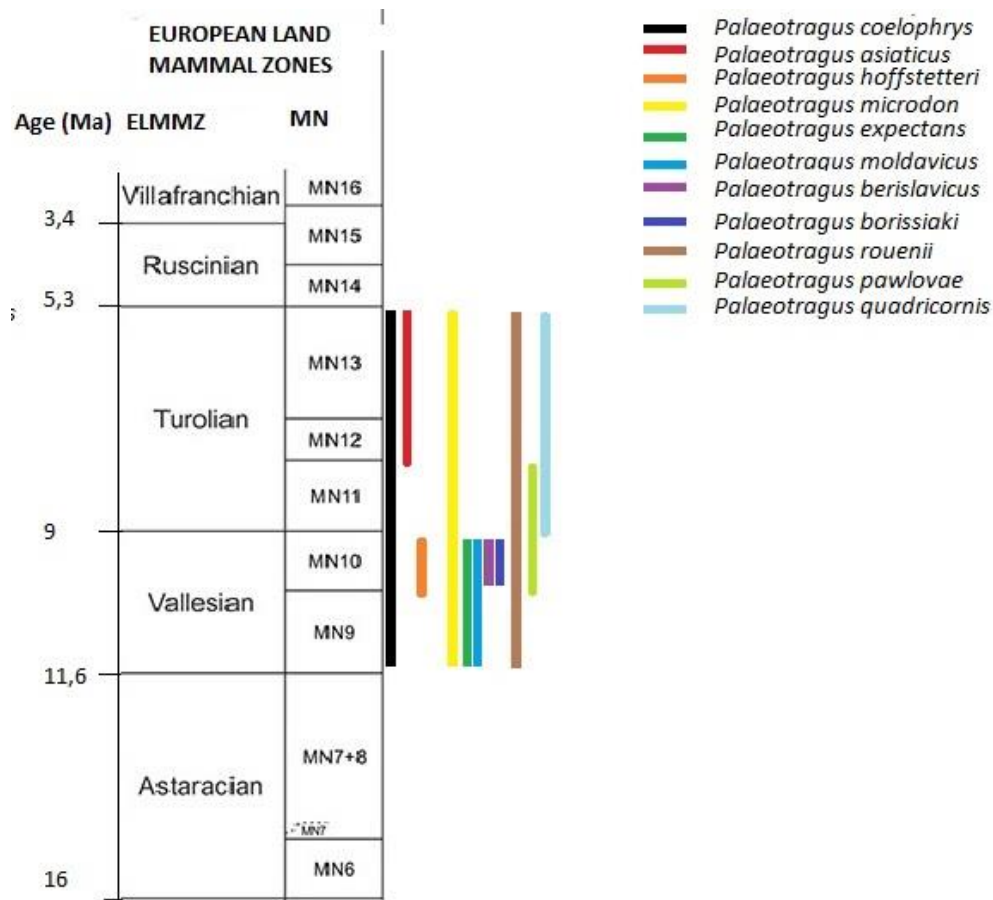


Figure 11: Late Miocene Eurasian Palaeotragus chronologic expansion

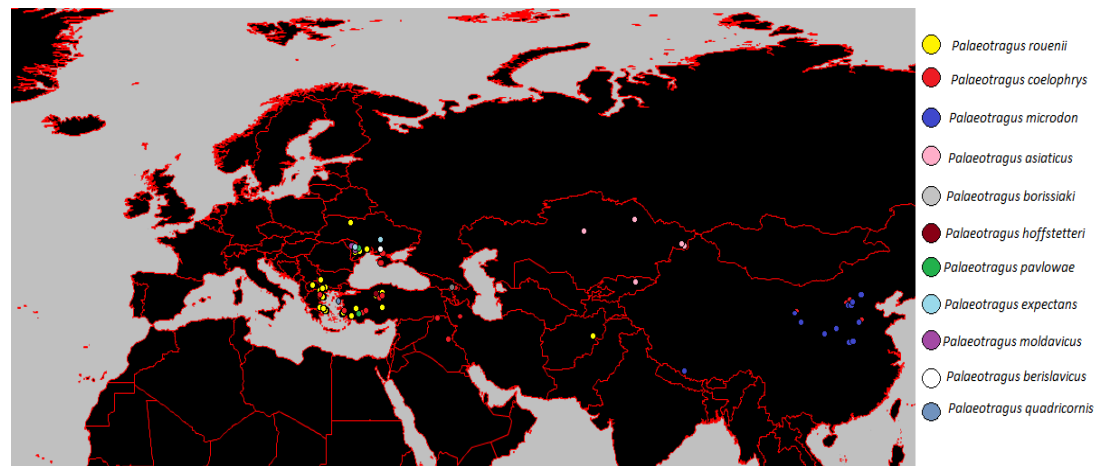


Figure 12: Late Miocene Eurasian Palaeotragus geographic expansion (recovered in January 2020 from NOW Database)



1.5 Objectives of Present Study

The main aim of the present study is a re-evaluation of the fossils attributed to the giraffid genus *Palaeotragus* from the fossil sites of Nikiti-1 (NKT), Pentalophos (PNT), Ravin de la Pluie (RPI) and Xirochori (XIR), all of them including a Vallesian fauna. The NKT material has been originally described as *Palaeotragus cf. rouenii* (Kostopoulos *et al.* 1996) and later considered as *Palaeotragus sp.* (Koufos *et al.* 2016). The PNT material has been previously referred to *Palaeotragus coelophrys* (Koufos 2006, Konidaris 2013) but never described. The large-sized *Palaeotragus* material from RPI has been attributed to *Palaeotragus cf. coelophrys* by Geraads (1978). Using statistic methods and based mainly on dental and postcranial morphology and proportions, the validity of the aforementioned taxonomy will be tested. As for the Xirochori specimen, a classification will be suggested. In order to properly classify those specimens, a taxonomic revision of Late Miocene Eurasian large sized *Palaeotragus* will be attempted.

2. METHODOLOGY

2.1 Description & System of Measurements

For the description of the adult dental material, the nomenclature proposed by Gentry *et al.* (1999) is followed (Fig. 13). For the description of the deciduous lower premolars, the nomenclature by Geraads *et al.* (2013) is followed (Fig. 14).

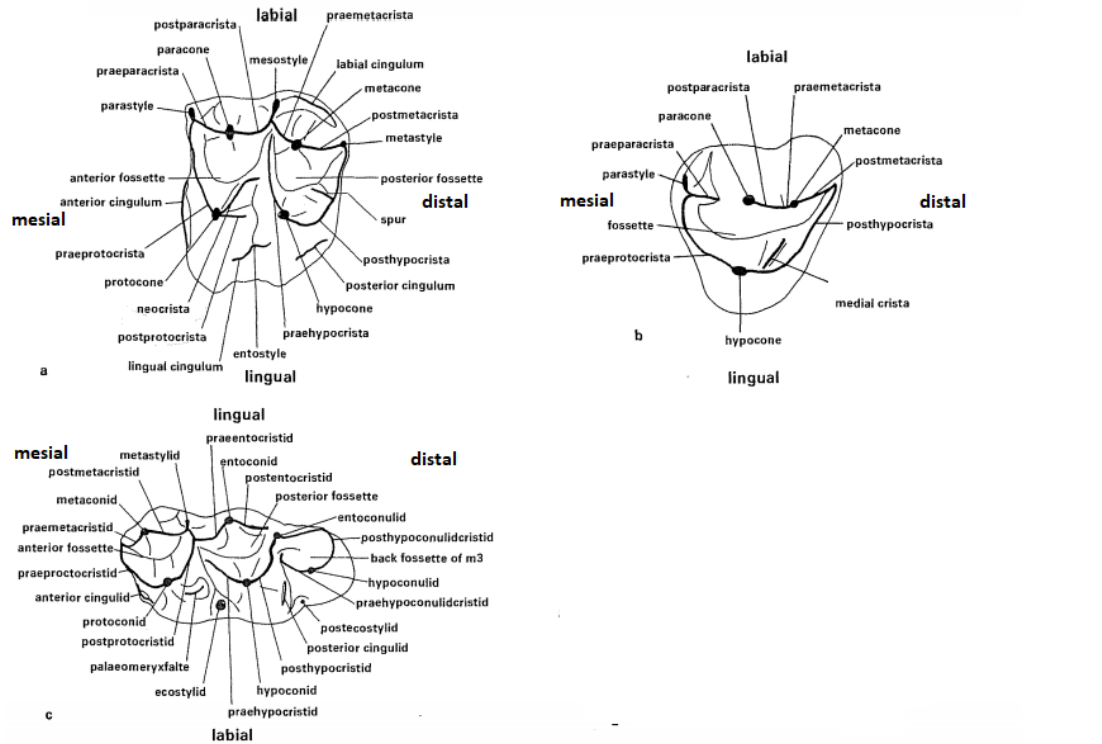


Figure 13: Terminology of adult ruminant cheek teeth: (a) upper molar; (b) upper premolar, (c) lower third molar (modified from Gentry *et al.* 1999)

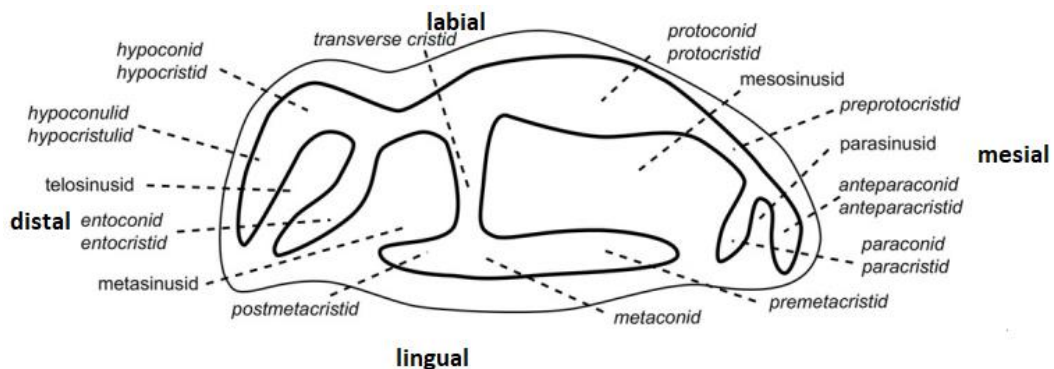


Figure 14: Terminology of lower deciduous ruminant premolar (modified from Geraads *et al.* 2013).

Lower dentition is noted by using the number of the tooth as an index (e.g., M₁ is a lower first molar). Upper dentition is noted by using the number of the tooth as an exponent (e.g. M¹ is an upper first molar).

The features that were measured, are the following: The length of the total toothrow (LPM), the length of the premolar row (LP) and the length of the molar row (LM). For each individual upper premolar, its length (LP^x) and its width (WP^x) were measured. The same was applied for the studied lower deciduous premolars. On account of the upper molars, we measured their length (LM^x), the greatest width of their anterior (mesial) lobe (WaM^x) and the greatest width of their posterior (distal) lobe (WpM^x). The same measurements were taken for the lower molars too. As for the M_3 , which consists of three lobes, the measurements include the greatest width of the anterior lobe (WaM_3), the greatest width of the middle lobe (WmM_3) and the greatest width of the posterior lobe (WpM_3). All measurements were taken with a digital caliper at 0.01 mm precision.

Terminology by Rios *et al.* (2016) is followed for the description of the metapodials (Figs 15, 16). Terminology by Schmid (1972) was used for the description of the rest postcranial bones.

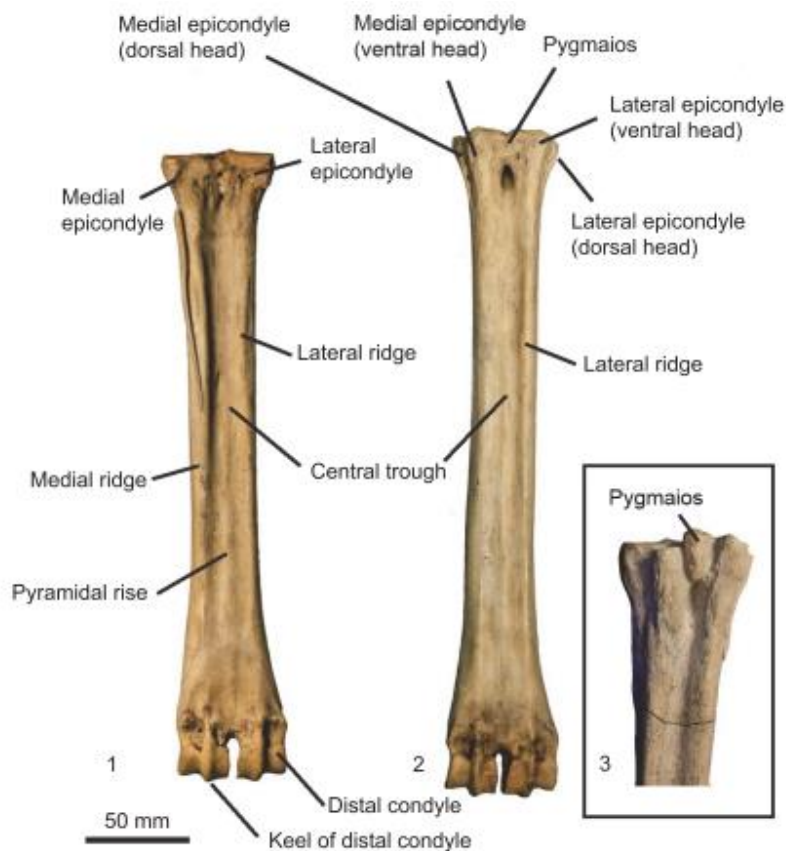


Figure 15: Morphology of giraffid metapodials: (1) metacarpal palmar view; (2) metatarsal dorsal view; (3) pygmaios (recovered from Rios *et al.* 2016)



Figure 16: Morphology of giraffid proximal metatarsal (left) and metacarpal (right): (NC) os naviculocuboideum facet; (CIL) os cuneiforme intermediolaterale facet (CM) os cuneiforme mediale facet (HA) os hamatum facet; (TC) os trapezoideocapitatum facet; (S) synovial fossa (adopted from Rios et al. 2016)

For the measurements of the postcranial bones, the system of measurements by von der Driesch (1976) was used (Figs 17-19).

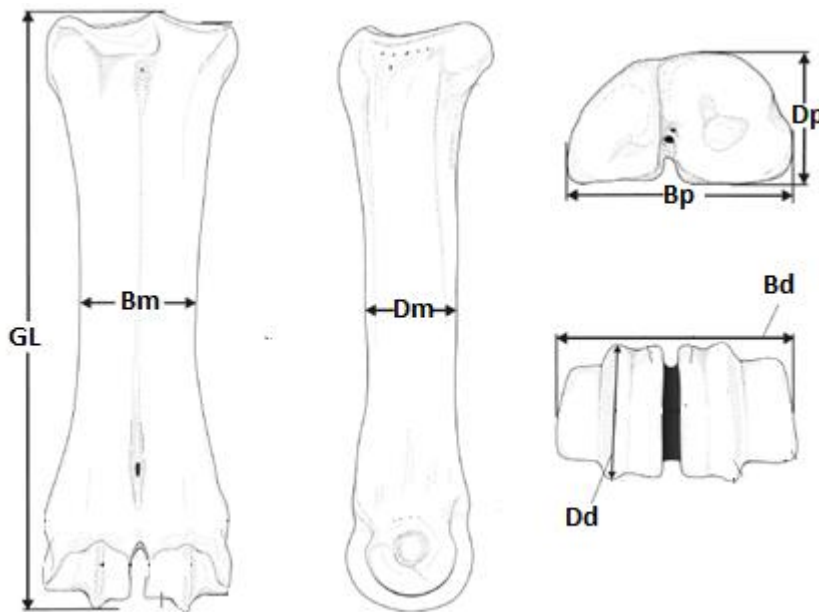


Figure 17: System of metapodial measurements based on von der Driesch (1976): (GL) Greatest Length; (Bm) Breadth of the middle shaft; (Dm) Depth of the middle shaft; (Bp) Greatest Breadth of the proximal end; (Dp) Greatest Depth of the proximal end; (Bd) Greatest Breadth of the distal end; (Dd) Greatest Depth of the distal end. The same system of measurements was used for all the long bones (modified from Maniakas & Kostopoulos 2017)

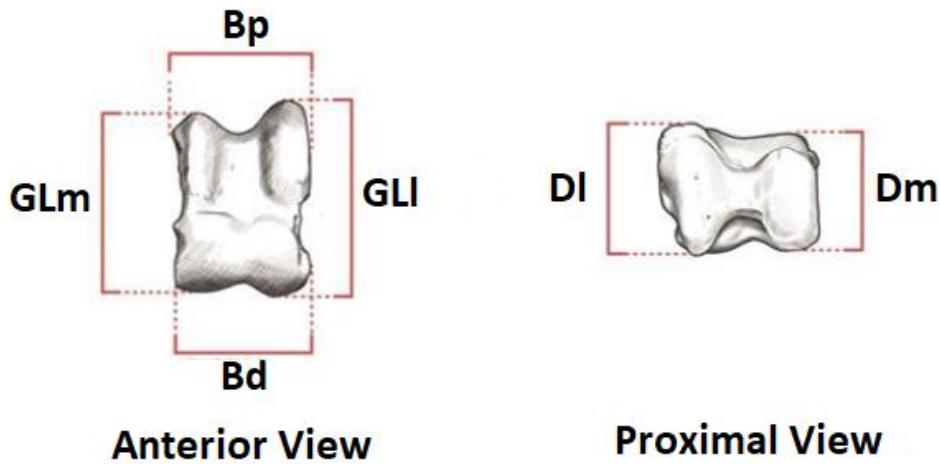


Figure 18: System of astragalus measurements based on von der Driesch (1976): (Dm) Greatest Depth of the medial half; (GLm) Greatest Length of the medial half; (GLl) Greatest Length of the lateral half; (DI) Greatest Depth of the lateral half; (Bp) Greatest Breadth of the proximal end; (Bd) Greatest Breadth of the distal end (modified from Rios 2018)

Plantar View

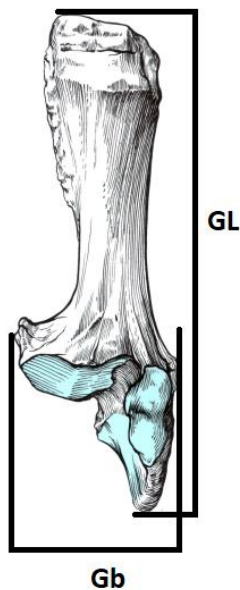


Figure 19: System of calcaneus measurements based on von der Driesch (1976): (GL) Greatest Length; (Gb) Greatest Breadth (modified from Pales & Garcia 1981)

2.2 Studied and Comparative Material

All the studied material comes from the collections of the Laboratory of Geology & Palaeontology of the AUTH and takes part of the Museum of Geology-Palaeontology-Palaeoanthropology of AUTH collections.

Fossils' photos from the following museums were used, as comparative material for the morphology of dental and skull specimens: AeMNH, AMNH, AMPG, AUTH, CMNH, EU, MCML, MNHN, MSU, MTA, NHMW, NMENH, NMNSU (curtesy D.S. Kostopoulos).

The morphology of the studied postcranial bones was compared with *Palaeotragus rouenii* postcranials, from the sites Perivolaki and Nikiti-2. That comparative material also belongs to the collections of the Museum of Geology-Palaeontology-Palaeoanthropology of the Aristotle University of Thessaloniki.

Measurements by Godina (1979) (from CRGEM, NMENH, NMNSU, OSU, PIN, RSGU and SIZK), Iliopoulos (2003) (from AMPG, AMNH, NHML and several authors) and Kostopoulos (personal measurements from the AMNH, MGML, MNHN, MMTT, NMENH and HUM) were used for metric comparisons.

2.3 Sites

The fossil giraffid material studied in this work comes from four fossiliferous localities of Northern Greece (Fig. 13).

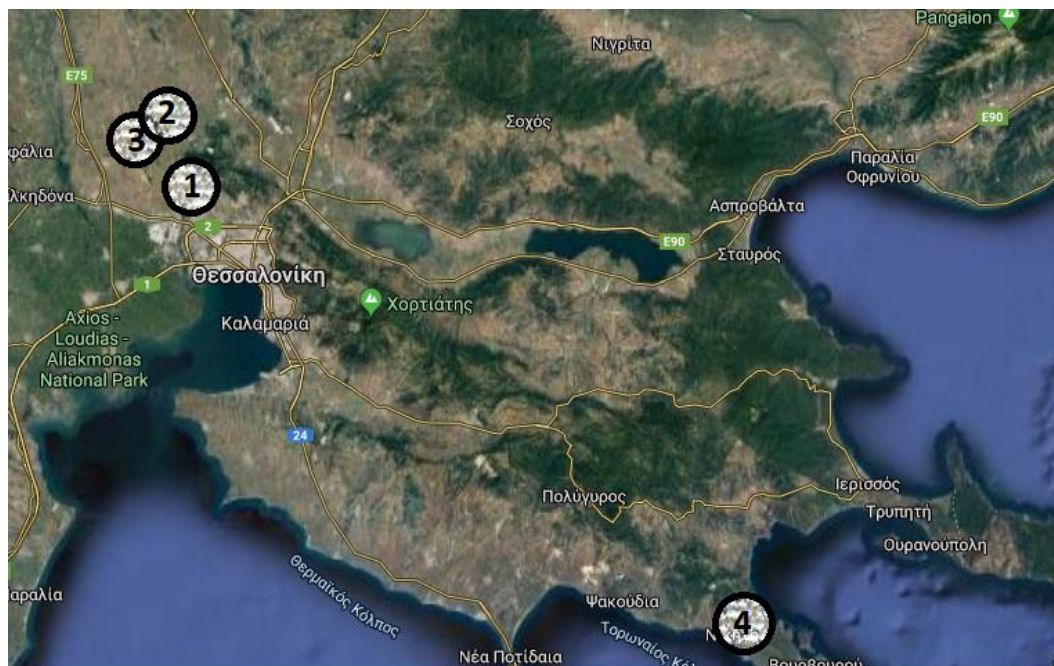
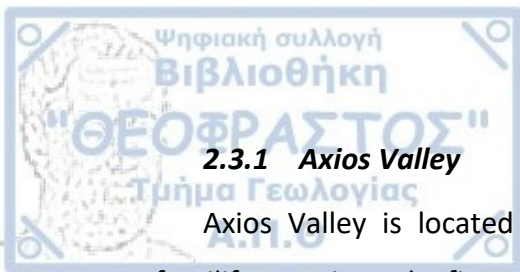


Figure 13: The four examined fossiliferous localities of Northern Greece. (1) Pentalophos; (2) Xirochori; (3) Ravin de la Pluie; (4) Nikiti (Photo recovered from Google Maps)



2.3.1 Axios Valley

Axios Valley is located northwestern of Thessaloniki and contains numerous fossiliferous sites. The first excavation in Axios Valley took place in 1915 by the French geologist C. Arambourg. From 1972 until 2012 the Laboratory of Geology & Palaeontology of the AUTH, in collaboration with the universities of Paris and of Poitiers (PIs: I. Melentis and then G.D. Koufos for the Greek part and L. de Bonis and then G. Merceron for the French one) conducted long lasting systematic excavations in the area, unearthing thousands of mammal fossils from more than 10 fossil sites, the most important ones being: Xirochori (XIR), Pentalophos (PNT), Ravin de la Pluie (RPI), Ravin de Zouaves-1 (RZI), Ravin de Zouaves-5 (RZO), Prochoma (PXM), Vathylakkos (VLO, VTK, VAT) and Ditiko-1, 2, 3 (DTK, DIT, DKO) respectively. The sites and their faunas cover the whole Late Miocene (Table 2); their stratigraphic context is given in Figure 14.

Palaeotragus material from the sites PNT, XIR and RPI is examined in the present master thesis. All those sites are included in Nea Messimvria formation, consisting of alternations of gravels, sands, red clays, and conglomerates, which are dated to the first part of the Upper Miocene, bearing a characteristically Vallesian fauna. Specifically, the fauna from PNT is dated as late Early Vallesian (MN 9), while XIR, and RPI are dated as Late Vallesian (MN 10) (Koufos 1990, Konidaris 2013). The faunas of PNT, RPI and XIR are shown in Tables 2, 3 and 4 respectively.

Continental stages	MN Zones	Lithostratigraphy	Fossiliferous locations
Pliocene			
Turolian	13	Ditiko Formation Yellowish - grey sand, Marl, Gravels, Sandy Marls, White - Yellow Limestones	Ditiko-1, 2, 3 (DTK, DIT, DKO)
	12		
	11	Vathylakkos Formation White - Yellow Alternated Beds of Marl, Sand, Gravel and Sandy Marl	Vathylakkos (VLO, VTK, VAT) Prochoma (PXM) Ravin de Zouaves-5 (RZO)
Vallesian	10		Ravin de Zouaves-1 (RZI) Pavin de la Pluie (RPI) Xirochori (XIR)
	9	Nea Messimvria Formation Sands, Gravels, Red - Brown Clays	Pentalophos (PNT)

Figure 14: Stratigraphic setting of Upper Miocene fossil sites from Axios Valley (modified from Koufos 1990)

Table 2: The faunal composition of PNT (modified from Koufos 2006, Konidaris 2013). Species marked in bold are included in the present study

Artiodactyla		Perissodactyla	
<i>Palaeogiraffa macedoniae</i> ?Palaeotragus coelophrys <i>Ouzocerus pentalophosi</i> <i>Helladorcas geraadsi</i> ? <i>Gazella</i> sp. <i>Protoryx</i> sp.		<i>Hipparion</i> cf. <i>sebastopolitanum</i> <i>Hipparion macedonicum</i> <i>Ancylotherium hellenicum</i> <i>Chilotherium kiliasi</i> <i>Acerorhinus</i> cf. <i>zernovi</i> "Diceros" <i>neumayri</i>	
Tubulidentata	Proboscidea	Carnivora	
<i>Orycteropus pottieri</i>	<i>Choerolophodon anaticus</i>	<i>Dinocrocuta gigantea</i> <i>Protictitherium</i> cf. <i>crassum</i>	

Table 3: The faunal composition of RPI (modified from Koufos 2006, Konidaris 2013). Species marked in bold are included in the present study

Artiodactyla		Carnivora		Perissodactyla	
<i>Palaeogiraffa major</i> Palaeotragus cf. coelophrys <i>Palaeotragus</i> cf. <i>rouenii</i> <i>Bohlinia</i> cf. <i>attica</i> <i>Mesebriacerus melentisi</i> <i>Samotragus praecursor</i> <i>Postrepsiceros vallesiensis</i> <i>Palaeoryx</i> sp.		<i>Metailurus parvulus</i> <i>Adcrocuta eximia</i> <i>Protictitherium thessalonikensis</i> <i>Protictitherium</i> aff. <i>intermedium</i> <i>Hyaenictis</i> sp. <i>Eomellivora wimani</i>		<i>Hipparion sebastopolitanum</i> <i>Hipparion macedonicum</i> Rhinocerotidae indet.	
Eulipothyphla	Rodentia	Primates		Proboscidea	
<i>Palerinaceus</i> sp.	<i>Speromphilinus</i> sp. <i>Progonomys cathalai</i>	<i>Ouranopithecus macedoniensis</i>		<i>Deinotherium giganteum</i> <i>Choerolophodon pentelici</i>	

Table 4: The faunal composition of XIR (modified from Koufos 2006, Konidaris 2013)

Artiodactyla	Proboscidea	Perissodactyla
<i>Palaeogiraffa pamiri</i> <i>Ouzoceus</i> sp. <i>Samotragus praecursor</i> ? <i>Palaeoryx</i> sp.	<i>Choerolophodon pentelici</i>	<i>Hipparion</i> sp., "Dicerops" <i>neumayri</i>
Carnivora	Primates	
<i>Adcrocuta eximia</i> , <i>Protictitherium crissum</i> , <i>Dinocrocuta</i> sp.	<i>Ouranopithecus macedoniensis</i>	

2.3.2 Nikiti

Nikiti fossiliferous assemblage is located at Sithonia, Chalkidiki, very close to the village of Nikiti. Excavations have been carried out in Nikiti from 1990 to 2005 (Koufos *et al.* 1991), when fossils discovered due to the opening of the road Nikiti – Agios Nikolaos (Koufos *et al.* 1991). The local stratigraphy (Fig. 15) includes two Formations: Nikiti Formation, consisting of intercalations of pebbles covered by red-brown sands, sandstones and finally red beds, and Nikolaos Formation consisting of marls, marly limestones, clays, sands and sandstones.

Nikiti fossil sites are located into the upper part of the homonymous Formation, within the red beds (Koufos *et al.* 1991). Two fossil sites have been discovered: Nikiti-1 (NKT) bearing a Late Vallesian fauna (latest MN10) and Nikiti-2 (NIK) bearing an Early Turolian (MN 11) fauna (Kostopoulos & Koufos 1999, Koufos 2000, Vlachou & Koufos 2002). *Palaeotragus* material from NKT is studied in this work. The fauna of NKT is shown in Table 5.

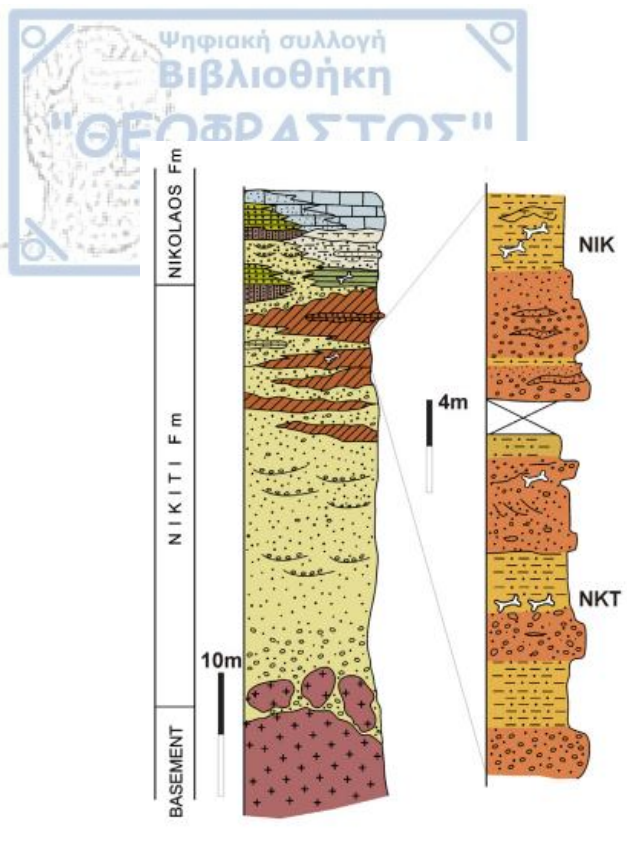


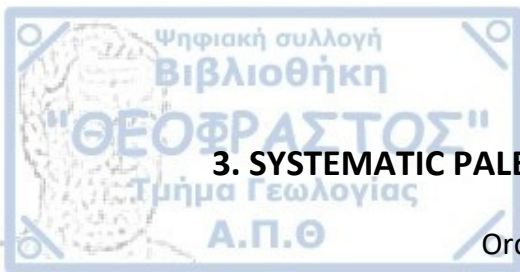
Figure 15: Stratigraphic column of Nikiti Formation indicating the position of the fossil sites NKT and NIK (recovered from Koufos 2016)

Table 5: The faunal composition of NKT (Koufos et al. 2016). Species marked in bold are included in the present study

Artiodactyla	Perissodactyla
<i>Helladotherium duvernoyi</i> <i>Bohlinia nikitiae</i> <i>Bohlinia attica</i> <i>Palaeotragus</i> sp. <i>Postrepsiceros syridisi</i> <i>Hispanodorcas</i> cf. <i>orientalis</i> <i>Microstonyx major</i> <i>Miotragocerus</i> nov. sp.	<i>Hipparion</i> aff. <i>giganteum</i> <i>Hipparion macedonicum</i> <i>"Diceros" neumayri</i> <i>Dihoplus pikermiensis</i>
Primates	Carnivora
<i>Ouranopithecus macedoniensis</i>	Hyaenidae indet.

2.4 Statistical Analyses and Illustrations

The PAST software (Hammer *et al.* 2001) was used for the statistical analyses. The program Inkscape was used for the dental and metapodial illustrations provided. The program Adobe Photoshop was used for the processing of the studied material from NKT, PNT, RPI and XIR.



3. SYSTEMATIC PALEONTOLOGY

Order: ARTIODACTYLA, Owen 1848

Family: Giraffidae Gray, 1821

(Subfamily: Palaeotraginae Pilgrim, 1911)

Genus: *Palaeotragus* Gaudry, 1861

Type Species: *Palaeotragus rouenii* Gaudry, 1861 from Pikermi, Greece

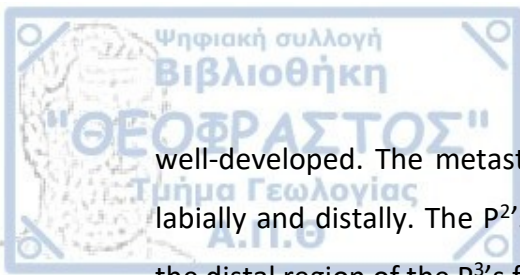
3. 1. Description

3.1.1. Site: Nikiti-1 (NKT)

Material – A skull with two complete tooththrows (NKT-172); a left humerus distal articulation (NKT-161); three left radii (NKT-156, NKT-159, NKT-169); a right radius (NKT-155); a proximal part of radius (NKT-167); two right metacarpals (NKT-137, NKT-141); a left metacarpal (NKT-131); two proximal parts of left metacarpals (NKT-26, NKT-67); a right tibia (NKT-271); two distal parts of tibia (NKT-150, NKT-154); two left astragali (NKT-163, NKT-266); a right astragalus (NKT-267); two right calcanei (NKT-153, NKT-268); four left metatarsals (NKT-133, NKT-136, NKT-139, NKT-160); two right metatarsals (NKT-138, NKT-144); a distal part of a right metatarsal (NKT-151); three proximal parts of right metatarsals (NKT-132, NKT-140, NKT-168). The material is illustrated in Plates 1-8.

Description - The skull (Pl. 1) is moderately deformed, and laterally compressed. It preserves both tooththrows but in the left one the molars are in bad conservation status. The mesial margin of the orbit reaches the level of M³. The length from the mesial edge of the orbit to the mesial root of P² is 154 mm. A pair of supraorbital ossicones is present, both broken near the base. It can be assumed that the ossicones are placed relatively centrally, although the skull is deformed. The basal anteroposterior diameter of the ossicones is 43.4 mm, while the transverse diameter is ~32 mm.

The labial side of the left molars is damaged. The tooththrows are not very worn. The P² and P³ are circular lingually. Labially the parastyle and the paracone ribs are



well-developed. The metastyle is not well-developed, so those teeth are flattened labially and distally. The P²'s and P³'s fossettes are wide and U-shaped. However, in the distal region of the P³'s fossette there is a hypoconal fold. In contrast to P² and P³, the P⁴ has a more pronounced metastyle. It is a more squared tooth than the P² and P³, as it is less convex lingually. Moreover, in the disto-lingual part of P⁴'s base there is a style that reaches almost to the half of the crown's height. Finally, its fossette is wide and simple.

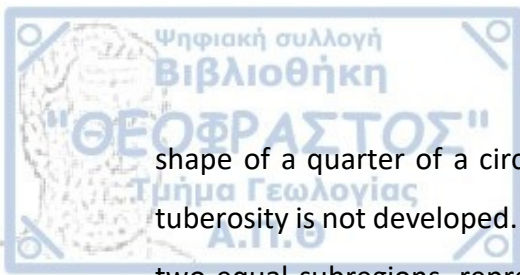
The molars, especially M² and M³, are slightly worn and have well-developed parastyle, paracone rib, mesostyle and metastyle. Metacone's labial rib is almost flat. In M¹ and M² there is a weak labial cingulum. Finally, there is a labial style in the basis of the metacone in M³. Lingually, the protocone and the hypocone are almost equally prominent and of similar shape on the M¹ and M². In M³ the protocone is more prominent than the hypocone. As a result, the mesial and distal lobes are of equal size at M¹ and M², while the mesial lobe is larger in M³. The distal protocone and mesial hypocone flanges converge in the middle of the tooth. The hypocone flange tends to connect with the metastyle distally. In fact, in M³, which is less worn than the other two molars, the hypocone flange and the metastyle are connected. Mesially, the hypocone flange disrupts the mesial fossette and meets the postparacrista. As a result, the size of the mesial fossette is limited, and the distal area of the protocone flange reaches almost at the middle of the tooth. Mesially, the protocone flange is connected to the parastyle. Both fossettes are U-shaped. Only in the M² a very weak hypoconal fold is observed. Dental measurements are given in Table 6.

Table 6: Dental measurements of the toothrows of the NKT skull (in mm). L: Length, W: Width

Measurements	Code	
	NKT-172 left	NKT-172 right
LPM	141.41	146.1
LP	62.35	63.49
LM	85.1	84.9
LP ²	22.4	21.61
WP ²	18.93	18.91
LP ³	20.79	21.2
WP ³	23.5	21.18
LP ⁴	20.66	20.14
WP ⁴	27.26	24.72
LM ¹	25.59	29.46
WaM ¹		27.8
WpM ¹		26.3
LM ²	29.87	30.22
WaM ²	33.29	28.14
WpM ²		28.25
LM ³	27.66	30.58
WaM ³	141.41	31.63
WpM ³	62.35	27.68

The only available measurements for the distal fragment of the humerus from NKT (Pl. 2) were the breadth and the depth of its distal end (85.4 mm and 40.94 mm respectively). Its size is intermediate between *P. rouenii* and *P. coelophrys*. It has the same breadth with a *P. microdon* specimen described by Bohlin (1926). On NKT's specimen, the olecranon fossa is deep, wide and U-shaped. Other features of the humerus are not evident due to specimen's conservation status.

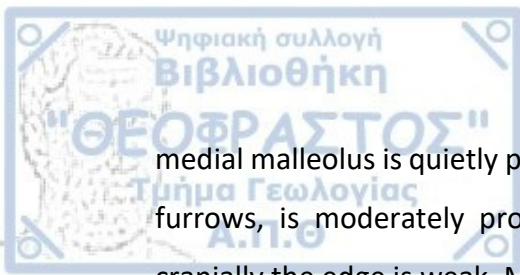
The radii (Pl. 3) are all elongated. They are relatively slender, being much slenderer than those of *P. coelophrys* and slightly more robust than those of the *P. rouenii*. A general difference in between the NKT's specimens is that two of them are fairly curved, while the other two are straight. The cross section of the bones is crescent shaped throughout bone's length, as the bone is rounded cranially and straight caudally. The two epiphyses' areas are both much wider than the shaft, since they both tilt medially and laterally. In the specimen NKT-159 the olecranon is evident but broken. It seems to greatly tilt laterally and distally. Traces of olecranon are preserved in specimens NKT-155 and NKT-169 too. In the proximal articular surface, the medial region is much larger than the lateral and it is either rectangular or it has a



shape of a quarter of a circle, while the lateral region is quadrangular. The medial tuberosity is not developed. A tilted narrow crest divides the distal articular surface in two equal subregions, representing the articular surfaces for the scaphoideum and semilunare. They are both round and slightly concave. The semilunare surface is interrupted by a convex protrusion distally. In four of the examined radii a V-shaped formation at the cranial part of the distal epiphysis indicates the presence of the extensor carpi radialis muscle. Measurements are given in Table 7.

The three best preserved metacarpals (Pl. 4) vary in length, however the robusticity indices are similar and show that the metacarpals are as slender as but shorter than in *P. rouenii*. The lateral and medial epicondyles are asymmetrical. The lateral epicondyle has half the size of the medial, and it is of square or rectangular shape. The medial epicondyle is circular dorsally and has an overall shape of a half-circle or of the $\frac{1}{4}$ of a circle. There is a fossa in the middle of the two epicondyles. That fossa seems to continue in the medial epicondyle. The medial and lateral epicondyles continue to the medial and lateral ridges respectively. The ridges are similar in width and morphology. They are both rounded near the proximal end and they become slenderer and sharper in the shaft area. The central trough is very deep near the proximal end of the bone but becomes shallower and flatter towards the distal end. The trough's width is variable. However, it can be said that the longer the bone, the wider is the trough. The pyramidal rise is absent in most of the specimens. Only in NKT-137 seems to be a slight protrusion that could be attributed to the pyramidal rise, however it is not prominent at all. The keels of the distal epicondyles are more prominent palmary, and they also extend onto the distal end of the palmar side of the shaft. Measurements are given in Table 8.

Three tibia specimens have been found in NKT (Pl. 5). Proximally, the angle of the sulcus muscularis is obtuse, relatively to *Bos* and *Cervus*. The tuberosity is not clearly evident, but it does not seem to be pronounced. The tibial crest, as in all ruminants, is laterally tilted. The lateral condyle is somewhat damaged laterally and cranially. In the distal tibia fragment NKT-154 the cross section of the distal shaft is rectangular. In the other two specimens this is not obvious, probably due to taphonomic processes. The distal articular surface has a broad rectangular shape, and the articular surface for the

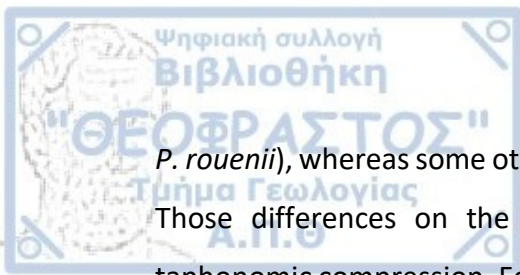


medial malleolus is quietly prominent. The cochlear crest, that separates the cochlear furrows, is moderately prominent; it creates caudally a very strong edge, while cranially the edge is weak. Measurements are given in Table 9.

As for the astragali (Pl. 6), the size of the NKTs specimens is intermediate between the group of small *Palaeotragus* and the group of the bulky *Palaeotragus*. NKT's specimens are rectangular in shape, as the lateral and medial lengths are of almost equal size and they are not thick medially. The proximal and the distal edges are of similar width. The lateral and medial crests are equally thick, with the lateral pointing posteriorly, and the medial slightly tilting medially. Proximally, the intertrochlear groove is shallow. The lateral side of the astragali is somewhat concave, forming a greater depression distally. The dorsal side is smooth. The intertrochlear groove begins in the distal edge of the astragali and leads to a plantar triangular-shaped cavity. That cavity is prominent on NKT-266 and NKT-163, while it is weaker on NKT-267. Finally, the two lateral crests and the two medial crests are both separated by an equally shallow furrow. Measurements are given in Table 10.

Two right calcanei were collected (Pl. 7). Their size falls into *P. rouenii* range. The calcaneus NKT-153 is bigger, having a more robust corpus than NKT-268. However, NKT-268 head seems to be stronger relatively to the corpus, than the NKT-153. Both the dorsal and plantar crests are parallel to the bone axis. The calcaneal tuberosity is prominent, however it is weathered in both of the specimens. In NKT-268 a medial crest separates the calcaneal tuberosity from the rest of the calcaneal corpus. The sustentaculum tali is somewhat damaged in NKT-153, while it is robust in the other specimen. The proximal-plantar articular surface for the astragalus consists of two concave surfaces, with the plantar one being almost double in size than the dorsal. Medially, there is another articular surface for the astragalus, which is fairly deep and concave. The articular surface for the scaphocuboideum is plantarly located and somewhat damaged in both the specimens. Dorsally, there is a well-developed, articular facet for the malleolus. Measurements are given in Table 11.

The metatarsals (Pl. 8) demonstrate a variation in both the total length and the robusticity indices, as some specimens are rather slender (with slenderness similar to



P. rouenii), whereas some others are extremely robust (similar to *P. coelophrys* group). Those differences on the robustness should be attributed to the metatarsals' taphonomic compression. For example, the extreme robustness of the specimen NKT-133 has been clearly exaggerated by taphonomic processes. The two proximal epicondyles demonstrate some differences. First of all, the lateral epicondyle is smaller and subdivided in two regions, the dorsal and the plantar heads. In contrast, in the medial proximal epicondyle this separation is not evident. Those epicondyles' heads represent the articular surfaces for the tarsal bones. The articular surface for the naviculocuboideum bone is the largest, the articular surface for the os cuneiforme intermediolaterale has almost half the size of the first and finally the articular surface for the os cuneiforme mediale is by far the smallest. The medial epicondyle has a trapezoid shape. The lateral dorsal head is more circular. The shape of the lateral plantar head is intermediate in shape. The pygmaios is strongly reduced to absent. The central trough varies in the studied specimens. However, it is significantly shallow and it disappears towards the distal end of the bone. In most of the specimens it disappears at about the middle of the shaft. The width of the trough also varies and it seems to follow the total bone width. The proximal, plantar fossa is present, weak and communicates with the central trough in the specimen NKT-139 whereas it is absent in the specimen NKT-133, NKT-136 and NKT-169. The bad conservation status of the other specimens does not allow to identify the presence of that fossa. In contrast to the metacarpals, a dorsal trough is evident; it is deeper at the distal end of the bone, becomes shallower upwards and disappears at the proximal end. The distal end of the metatarsals is similar to the distal end of the metacarpals. Postcranial measurements are provided in Tables 7-12.

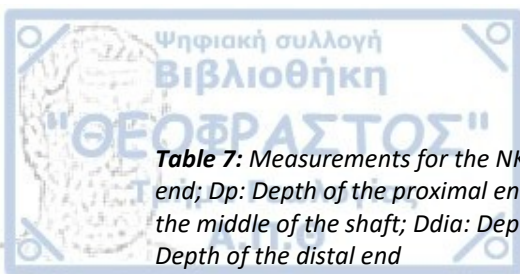


Table 7: Measurements for the NKT radii (in mm). GL: Greatest Length; Bp: Breadth of the proximal end; Dp: Depth of the proximal end; Bpart: Breadth of the proximal articular surface; Bdia: Breadth in the middle of the shaft; Ddia: Depth In the middle of the shaft; Bd: Breadth of the distal end; Dd: Depth of the distal end

Measurements	Code				
	NKT-159	NKT-167	NKT-156	NKT-155	NKT-169
R-GL	449		462	476	470
R-Bp	82.42	88.05	81.24	82.82	71.45
R-Dp	53.25	46.82	44.64	49	40.74
R-Bpart			67.95	73.83	
R-Bdia	48.18	48.25	51.47	49.61	51.25
R-Ddia	36.03	35.02	41.64	33.26	30.77
R-Bd	75.51		75.66	80.59	73.95
R-Dd	55.17		54.47	51.78	42.6

Table 8: Measurements for the NKT metacarpals (in mm). GL: Greatest Length; Bp: Breadth of the proximal end; Dp: Depth of the proximal end; Bdia: Breadth in the middle of the shaft; Ddia: Depth In the middle of the shaft; Bd: Breadth of the distal end; Dd: Depth of the distal end

Measurements	Code				
	NKT-141	NKT-137	NKT-131	NKT-67	NKT-26
Mc-GL	409	378	380		
Mc-Bp	64.68	57.89	64.6	70.37	61.15
Mc-Dp	40.25	32.71	46.55	39.63	41.28
Mc-Bdia	35.8	31.68	32.79	42.3	
Mc-Ddia	31.44	31.21	30.74	30.79	
Mc-Bd	63.41	60.26	61.65		
Mc-Dd	38.19	35.56	37.16		

Table 9: Measurements for the NKT tibiae (in mm). GL: Greatest Length; Bp: Breadth of the proximal end; Dp: Depth of the proximal end; Bdia: Breadth in the middle of the shaft; Ddia: Depth In the middle of the shaft; Bd: Breadth of the distal end; Dd: Depth of the distal end

Measurements	Code		
	NKT-271	NKT-150	NKT-154
T-GL	451		
T-Bp	82.57		
T-Dp	82.07		
T-Bdia	50.4	45.49	47.78
T-Ddia	35.53	36.98	39.6
T-Bd	81.6	67.53	68.9
T-Dd	55.79	54.73	45.77

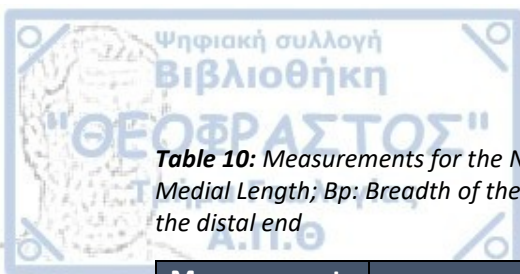


Table 10: Measurements for the NKT astragali (in mm). GLI: Greatest Lateral Length; GLm: Greatest Medial Length; Bp: Breadth of the proximal end; DI: Lateral Depth; Dm: Medial Depth; Bd: Breadth of the distal end

Measurements	Code		
	NKT-267	NKT-63	NKT-166
A-GLI	78.58	77.83	78.64
A-GLm	70.75	72.57	67.41
A-Bp	49.29	52.01	50.17
A-DI	45.4	43.42	49.2
A-Dm	47.25	46.36	51.3
A-Bd	47.03	50.96	50

Table 11: Measurements for the NKT calcanei (in mm). GL: Greatest Length, GB: Greatest Breadth, GAP: Greatest Anteroposterior diameter

Measurements	Code	
	NKT-268	NKT-153
C-GL	136.61	147.35
C-GB	45.76	55

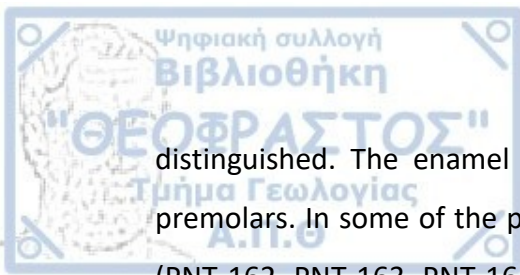
Table 12: Measurements for the NKT metatarsals (in mm). GL: Greatest Length; Bp: Breadth of the proximal end; Dp: Depth of the proximal end; Bdia: Breadth in the middle of the shaft; Ddia: Depth in the middle of the shaft; Bd: Breadth of the distal end; Dd: Depth of the distal end

Measurements	Code									
	NKT-136	NKT-160	NKT-139	NKT-133	NKT-144	NKT-138	NKT-168	NKT-151	NKT-140	NKT-132
Mt-GL	414	409	386	412	415	436				
Mt-Bp	58.86	60.85	52.45	62.76	59.5	59.46	56.44		58.42	54.81
Mt-Dp	57.83	49.49	54.62	53.06	45.71		50.44		44.82	
Mt-Bdia	34.22	41.25	33.65	49.6	33.35	31.94	38.48	40.73	40.98	32.8
Mt-Ddia	33.58	34.93	29.68	28.75	33.05	30.21	36.3	31.35	34	35.18
Mt-Bd		64.8	57.84	60.56	57.89			61.19		
Mt-Dd		38.49	35.3	40.47	35.68	33.92		37.81		

3.1.2 Site: Pentalophos (PNT)

Material – Right maxilla with P²-M³ (PNT-113); part of left maxilla with M²-M³ (PNT-165); an upper right P² (PNT-161); upper right P²-P³ (PNT-162); upper right P²-P³; upper left P³ (PNT-164); part of right mandible with M₁-M₃ (PNT-328F); part of right mandible with dP₂-M₁ (PNT-121F); distal part of left humerus; proximal parts of a right and a left metatarsal (PNT-114F, PNT-119F). The material is illustrated in Plates 9-15.

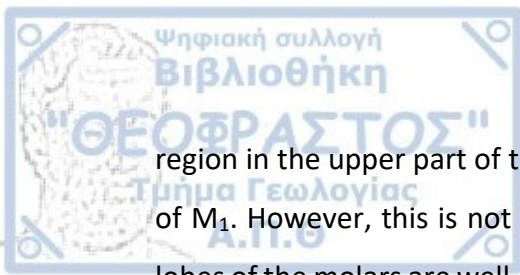
Description – All the premolars' labial ribs and styles (parastyle, paracone, metastyle) are well developed (Pl. 9-11). The hypocone is not well developed, but it can be



distinguished. The enamel is finely rugosed especially on the lingual side of the premolars. In some of the premolars a well-developed lingual cingulum can be seen (PNT-162, PNT-163, PNT-164). In the available P^2 and P^3 the parastyle and paracone ribs are close to each other and the enamel is folded in the area of parastyle towards the paracone. Moreover, these teeth are lingually rounded and they delineate an almost half circle from lingual to labial side. P^2 and P^3 are inflated at the basis. The P^2 of the PNT-113 toothrow has a prominent style disto-labially, that reaches almost to the 1/3 of the crown's height. In the single available P^4 , the paracone is more centrally placed, however it is slightly folded towards the parastyle. In addition, the tooth is not rounded lingually, but triangularly shaped. The fossettes of the P^2 are distorted, so there are not a lot of things that can be said, except that they are wide. The fossettes of the P^3 and P^4 are also wide. They show a hypoconal fold distally.

The molars are typically giraffid (Pl. 9, 10). The most prominent labial features are the parastyle, the paracone rib and the mesostyle. The metastyle is weakly developed in M^1 - M^2 and equally developed to the parastyle in M^3 . Lingually, the protocone is more prominent than the hypocone, especially in the M^3 . The mesial lobe is wider and squared shaped. The distal lobe is narrower and more round. The fossettes converge in the center of the tooth but they never fuse. The hypocone flange reaches almost at the labial side of the molar, stopping just before the mesostyle mesially and the metastyle distally. The protocone flange, reaches almost at the parastyle mesially. Distally, it reaches almost at the center of the tooth, meaning that it rests away from the mesostyle. The enamel is finely rugosed in all the teeth. The molars of PNT-165 have a lingual cingulum, which is stronger in the mesial lobe than in the distal. Even if the PNT-165 molars are a little less worn than those of PNT-113, the basic features are the same. Finally, the molars of the right maxilla specimen (PNT-113) have a fine cement cover, mostly labially. Measurements of upper teeth are given in Table 13.

The right mandible (PNT-328F; Pl. 12) preserves only the molars. The most prominent lingual characteristic is the metastylid, and then the metaconid. The entoconid is clear, but in contrast with the metastylid and the metaconid, it is not well-developed. In the distal, lingual side of the M_1 and M_2 the entoconid is clear but not prominent. The entoconid of the M_2 is completely separated from the hypocone



region in the upper part of the crown. The same applies probably for the entoconulid of M_1 . However, this is not certain as the tooth is more worn than the M_2 . The two lobes of the molars are well-distinguished. The praentocristid penetrates in the mesial fossette, separating the labial and lingual side of the mesial lobe. Protoconid and hypoconid are almost equally developed. M_1 bears an ectostylid. In M_2 the ectostylid is less prominent, and absent in M_3 . Finally, the hypoconulid is pointed labially and parallel to the protoconid and hypoconid. Lingually, the third lobe of the M_3 is separated from the second one by a shallow, yet clear, furrow. The teeth preserve a fine cement cover. Cingulum appears strong on M_1 , but weak on M_2 . M_3 has no cingulum. The mandibular height at the M_1 - M_2 level is 48.9 mm, while it is 53.6 mm at M_3 's distal lobe level. Measurements are given in Table 14.

The right mandible with the deciduous dentition (Pl. 13) consists of the series of milk premolars and M_1 . The dP_2 is of primitive morphology. The paraconid and anteparaconid (=parastylid) are barely distinguished from each other lingually and mesially. The protoconid is the strongest element of the tooth and it is placed medially. Distally, the entoconid and the hypoconulid are distinguished in the upper part of the crown, whereas they fuse in the lower. The hypoconid is prominent, placed more labially. The dP_3 is a micrography of a lower ruminant adult premolar. Firstly, paraconid and anteparaconid are pointed lingually and they are well distinguished in the upper part of the crown, whereas they fuse each other toward the base of the crown. The metaconid and protoconid are the most prominent features (especially the protoconid). They fuse distally and they are folded and oriented mesially. The mesosinusid is lingually open. The distal and mesial part of the dP_3 are clearly separated, in the area of the metaconid and protoconid fusion. The distal region consists of the hypoconid, hypoconulid and entoconid. The hypoconulid is equally developed with the protoconid. Hypoconulid and entocristid are distinguished in the upper part of the crown but they fuse below. The metasinusid is clear but weaker than the mesosinusid. The dP_4 has the morphology of a three-lobe molar. There are two prominent ectostylids. The mesial lobe is distorted, although it seems that its ribs and stylids are weaker. In the two distal lobes the labial cones are equally developed. The lingual ribs and stylids are weaker too, as they are in the mesial lobe. The distal flange

of the third labial cone reach the lingual side of the tooth. The distal flange of the second labial cone is also well-developed and it is placed next to the metastylid; it is the feature that separates the second from the third lobe. Finally, M_1 's morphology agrees with the morphology of M_1 from the adult toothrow described earlier; the metaconid, metastylid, entoconid and entoconulid ribs are developed in some point in the upper half of the crown. There is no cement neither cingulum. Dental measurements are provided in Table 15. Morphological features of the very few preserved postcranials (Pl. 14-15) are provided directly on the comparison chapter; measurements are given in Table 16.

Table 13: Measurements of the PNT upper teeth (in mm). L: Length, W: Width

Measurements	Code					
	PNT-113	PNT-165	PNT-152	PNT-163	PNT-161	PNT-164
LPM	138.45					
LP	59.5					
LM	82.14					
LP ²	17.42		20.06	19.32	19.02	
WP ²	19.54		18.73	19.54	19.17	
LP ³	20.21		20.53	20.8		21.4
WP ³	21.2		21.65	24.37		24.1
LP ⁴	20.47					
WP ⁴	26.05					
LM ¹	26.8					
WaM ¹	28.13					
WpM ¹	27.62					
LM ²	30.1	28.6				
WaM ²	31.06	28.15				
WpM ²	26.8	26.23				
LM ³	29.36	31.64				
WaM ³	18.1	30.26				
WpM ³	24.18	26.74				



Table 14: Dental measurements of the mandible from PNT (in mm). L: Length, W: Width

Measurements	Code
	PNT-328F
LM	97
LM ₁	28.18
WaM ₁	18.55
WpM ₁	21.45
LM ₂	28.05
WaM ₂	22.31
WpM ₂	23.5
LM ₃	38.08
WaM ₃	21.37
WpM ₃	21.96
W3M ₃	16.7

Table 15: Dental measurements of the mandible with the deciduous teeth from PNT (in mm). L: Length, W: Width

Measurements	Code
	PNT-121F
LdP	69.79
LdP ₂	15.82
WdP ₂	8.38
LdP ₃	22.98
WdP ₃	9.71
LdP ₄	31.03
WadP ₄	11.34
WmdP ₄	16.23
Wpdp ₄	16.14
LM ₁	28.88
WaM ₁	20.12
WpM ₁	20.06

Table 16: Measurements for the PNT metatarsals (in mm). Bp: Breadth of the proximal end; Dp: Depth of the proximal end; Bdia: Breadth in the middle of the shaft; Ddia: Depth in the middle of the shaft

Measurements	Code	
	PNT-119F	PNT-114F
Mc-Bp	62.98	60.39
Mc-Dp	60.75	57.58
Mc-Bdia	37.02	40.66
Mc-Ddia	37.2	32.81



3.1.3 Site: *Ravin de la Pluie* (RPI)

Material – A ‘hornless’ skull with a highly worn toothrow (RPI-91B); part of right mandible, with highly worn M₁-M₃ (RPL-104F) An isolated upper molar (M¹ or M²) (RPL-315n). The material is illustrated in plates 16-17.

Description – Although the skull is deformed (Pl. 16) it is evident that lacks ossicones, and it demonstrates a flattened frontal region probably representing a female individual. The parietal region is strongly compressed. The postorbital region is elongated. The mesial border of the orbit reaches almost at the level of the center of M³. In the right side of the skull the auditory canal is evident and has the shape of the ¼ of a circle. The length from the mesial margin of the orbit to the mesial root of P² is 153.79. The height of the orbit is 58.91 mm, while the horizontal (caudo-rostral) diameter is 59.19 mm. Finally, the width of the region of the frontal bone behind the orbits is 95.36 mm.

The toothrow of the skull RPI-91B is strongly worn. The premolars’ width is similar to that of the molars (especially the width of P⁴). P² and P³ are lingually circular. Labially, the paracone, parastyle and metacone ribs are all well-developed. The premolar fossettes demonstrate a slight hypoconal fold. P⁴ is more laterally flattened than P² and P³ and it is more acute lingually than the other premolars, which are circular. It also demonstrates strong parastyle, paracone rib and metastyle. The molars’ labial ribs are not well-developed, especially when compared to PNT or NKT molars likely due to advanced wear stage and damages during and after fossilization. Finally, little quantity of cement is observed labially.

The mandible RPL-104F (Pl. 17) preserves only the molars. The mandibular height is 48,9 mm at the level of M₁-M₂ and 53.6 at level of the distal lobe of the M₃. The lingual ribs seem to be very weak though the dentition is in very advanced wear stage. Labially, M₁’s lobes are pointed centrally, M₂’s lobes are slightly pointed centrally, while M₃’s lobes are more distally pointed. The M₃’s distal lobe is pointed completely distally. The distal lobe of M₃ is separated lingually only by a slight groove, although the separation is clear. Cingulum and cement are absent. Dental measurements provided in Tables 17-18.

Table 17: Dental measurements from the tooththrows of the RPI skull (in mm). L: Length, W: Width

Measurements	Code	
	RPI-91 left	RPI-91 right
LPM	152.25	147.4
LP	68.68	62.81
LM	94.07	85.41
LP ²	18.82	22.88
WP ²	20.44	20.62
LP ³	21.61	21.25
WP ³	23.67	22.61
LP ⁴	21.14	19.21
WP ⁴	26.04	26.64
LM ¹	24.82	23.96
WaM ¹	26.85	27.42
WpM ¹	26.28	26.85
LM ²	28.5	30.51
WaM ²	29.21	28.7
WpM ²	27.81	27.38
LM ³	28.63	28.47
WaM ³	28.18	26.41
WpM ³	24.59	22.41

Table 18: Dental measurements from the tooththrows of the RPI mandible (in mm). L: Length, W: Width

Measurements	Code
	RPI-104
LM	89.59
LM ₁	24.92
WaM ₁	17.09
WpM ₁	17.38
LM ₂	25.8
WaM ₂	18.3
WpM ₂	19.24
LM ₃	39.15
WaM ₃	18.89
WpM ₃	19.91
W3M ₃	10.97

3.1.4 Site: Xirochori (XIR)

Material – Part of right mandible with M₂-M₃ (XIR-24)

Description – The morphology of XIR M₂ and M₃ (Pl. 18) is almost identical to that of RPI, although the teeth from XIR are less worn. As a result, a very strong metaconid is lingually observed. The lingual ribs and stylids are not well-developed. The only prominent element is that of the metastylid. The second and third lobe of the M₃ are

distinguished by a very shallow groove, as in RPI. Labially, the protoconid and hypoconid are both fairly sharper in M_2 than in M_3 . All the lobes are pointed distally. One difference between XIR and RPI teeth is that the third lobe of M_3 is pointed more distally in RPI. A weak entoconid is observed in M_2 . A strong entoconid is observed between the first and the second lobe of M_3 , while a weaker one between the second and the third lobe. Neither cingulum nor cement is observed. Dental measurements are provided in Table 20.

Table 20: Measurements of the XIR lower teeth (in mm). L: Length, W: Width

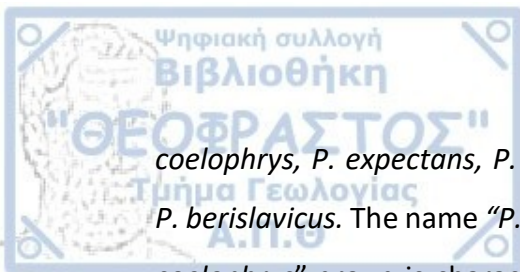
Measurements	Code
	XIR-24
LM ₂	26.93
WaM ₂	19.55
WpM ₃	19.04
LM ₃	40.33
WaM ₃	20.06
WpM ₃	20.00
W3M ₃	11.95

3.2. Comparison

3.2.1 The taxonomy of Late Miocene Eurasian *Palaeotragus*

Assessing relationships inside Late Miocene *Palaeotragus* representatives is a difficult task. A variety of species were described in the late 19th and early 20th centuries, in a time when the communication among different scholars was difficult. Since then, just a few comprehensive studies have been published, in order to understand *Palaeotragus* systematics and phylogeny (e.g. Godina 1979, Geraads 1986), although *Palaeotragus* is the most common giraffid genus in the Late Miocene of Eurasia.

Generally, *Palaeotragus* species are distinguished by means of size in two groups (Geraads 1974, Geraads 1986, Iliopoulos 2003, Kostopoulos & Saraç 2005, Kostopoulos 2009). The first group contains the small-sized *Palaeotragus rouenii*, *P. microdon* and *P. pavlowae*. For that group the name "*P. rouenii*" group is generally used. Those species are characterized by their small size and their long, slender metapodials. The second group contains the large sized species *Palaeotragus*



coelophrys, *P. expectans*, *P. borissiaki*, *P. hoffstetteri*, *P. moldavicus*, *P. asiaticus* and *P. berislavicus*. The name “*P. coelophrys*” group is usually suggested for that group. “*P. coelophrys*” group is characterized by the relatively larger size and the existence of shorter and more robust metapodials than the “*P. rouenii*” group.

Another bulky *Palaeotragus* is *P. quadricornis*, from the Turolian of Samos. It is claimed to be distinguished by having a second pair of ossicones, although it is not certain whether this pair really existed at all or if it is a misinterpretation based on the swollen supraorbital frontals due to extended frontal sinuses (Kostopoulos 2009). As for *Palaeotragus quadricornis*, Bosscha-Erdbrink (1977), Geraads (1986) and Gentry & Heizmann (1996) regard it as synonym with *P. coelophrys*, while Geraads (1978) and Hamilton (1978) consider it as a valid species mainly because of the supposed presence of two pairs of ossicones. *Palaeotragus quadricornis*, also belongs to “*P. coelophrys*” group.

Inside the “*P. rouenii*” group the validity of *P. pavlowae* is doubtful, because of its scarce specimens. On the other hand, a distinction between *P. rouenii* and *P. microdon* is considered solid, due to a number of morphological differences (Hamilton 1978, Kostopoulos & Saraç 2005). The taxonomy of the “*P. rouenii*” group will not be further discussed.

As for the “*P. coelophrys*” group, earlier works by Geraads (1974, 1986), do not detect any differences among its members. He considers all these taxa as synonyms, proposing that they should be referred to as *P. coelophrys*, although he recently recognized the need of a deeper revision (Geraads 2013).

On the other hand, Godina (1979) has a different point view. Firstly, he considers features, different than the species size, as more important. In his study three subgenera are proposed: *Palaeotragus (Palaeotragus)*, which contains *P. rouenii* and *P. pavlowae*, *Palaeotragus (Yuorlovia)*, which contains *P. coelophrys*, *P. microdon*, *P. asiaticus* and *P. hoffstetteri*, and finally *Palaeotragus (Achtiaria)*, which contains *P. expectans*, *P. borissiaki*, *P. moldavicus* and *P. berislavicus*. *Palaeotragus (Achtiaria)* representatives demonstrate a short cranial face, their diastema is shorter than their tooththrow and the inner wall of their P₃ is not continuous. According to Godina (1979)



those features differentiate them from *Palaeotragus (Yuorlovia)* representatives. Finally, *Palaeotragus (Palaeotragus)* subgenus is characterized by smaller size, the front skull is elongated and the diastema length exceeds that of the dentition. The continuous internal wall of P_3 is either present or absent.

Godina's (1979) taxonomic point of view is quite doubtful. Firstly, most of the species' type material does not contain the anatomical elements on which Godina was based for attributing relationships/distinctions. Original description of several of these species used different features. Additionally, the material scarcity of some of the species does not allow the characterization of the proposed features as valid. For example, while Godina (1979) repeatedly used features of the mandible to assess relationships, for some of the proposed species only one mandibular specimen was known at that time per species, while for some others there were not even complete mandibular specimens preserved (Tab. 21). Thus, it is impossible to know if those features differentiate really between reported species, or if they are just a reflection of intraspecific variability. Furthermore, while Godina (1979) uses the morphology of the P_3 as a diagnostic feature, he also mentions that its morphology varies even within the same species. Hence, that feature cannot be considered as valid. Lastly, the morphology of the ossicones is used by Godina (1979) to distinguish some of the bulky *Palaeotragus* species. That character is also doubtful; not all species are known by their ossicones (Tab. 21). E.g., no ossicones specimens are known for *P. coelophrys*. The type localities with the name of the authors and the original designations of the Late Miocene Eurasian *Palaeotragus* are given in Table 21.

Table 21: Late Miocene Eurasian *Palaeotragus*. Information about the type material of *P. microdon* could not be recalled. No holotype was cited for *P. hoffstetteri* by Ozansoy (1965).

Species	Authorship	Type locality	Original designation	Type material	Other Refs
<i>P. rouenii</i>	Gaudry 1861	Pikermi, Greece	<i>Palaeotragus rouenii</i>	Incomplete male skull	Akkasdagi, Corakyerler, Esmé Akçaköy, Kavakdere, Kemiklitepe (1,2), Sinap (Turkey) Belka, Grebeniki, Novo-Elizavetovka (Ukraine) Chobruchi, Cimislia, Taraclia (Moldova) Hadjimovo-1, Kalimanci 2, (Bulgaria) Dytiko 2, Kerassia, Kryopigi, Mytilinii 1A, 1B, 4, Perivolaki (Greece)
<i>P. pavlowae</i>	Pavlov 1913	Grebeniki, Ukraine	<i>Camelopardalis parva</i>	Lower part of the facial part of the skull with teeth	Kemiklitepe (A-B, D) Turkey
<i>P. microdon</i>	Koken 1885	Shansi, China	<i>Camelopardalis microdon</i>	-	Chongxin, Hezheng-Dashengou, Ho-qu-114, Huoxian-anlecut, Jilong, Jungar-Yaogou, Lantian-42, Lantian-44, Lantian-Shuijiazui, Lantian-shuijiazui-s4, Pao-Te-Lok.108, Pao-Te-Lok.109, Pao-Te-Lok.30, Pao-Te-Lok.49, Qingyang-Lok.115, Qingyang-Lok.116, Songshan-Loc.3, Yangjiashan (China)
<i>P. coelophrys</i>	Rodler & Weithofer 1890	Maragheh, Iran	<i>Alcicephalus coelophrys</i>	Incomplete female skull	Ravin de la Pluie, Samos (Greece) Injana (Iraq), Karatchik Dagh (Syria), Garkin, Kink & Matmutgazi, Sinap 1 (Turkey) Eldari1 (Georgia) Sevastopol, Berislav (Ukraine), Pao-Le-Tok, Songshan-Loc, Wu-Hsiang-Loc (China)
<i>P. asiaticus</i>	Godina 1975	Ortok, Kyrgyzstan	<i>Palaeotragus (Yvarlovia) asiaticus</i>	Part of upper jaw with P2-M3	Kalmakpaj, Gusinyy Perehyot, Pavlodar, Karabulak Svita (Kazakhstan), Pristashkent district (Uzbekistan)
<i>P. expectans</i>	Borissiak 1914	Sevastopol, Ukraine	<i>Achtiaria expectans</i>	Skull (Lectotype)	Varnitsa (Moldova) Zhehtokamenka (Ukraine)
<i>P. berislavicus</i>	Korotkevitch 1957	Berislav, Ukraine	<i>Palaeotragus (Achtiaria) berislavicus</i>	Mandible	-
<i>P. moldavicus</i>	Godina 1979	Starye Bogeny, Moldova	<i>Palaeotragus (Achtiaria) moldavicus</i>	Part of mandible with P4-M3	Raspopeny (Moldova)
<i>P. hoffstetteri</i>	Ozansoy 1965	Sinap, Turkey	<i>Palaeotragus hoffstetteri</i>	-	-
<i>P. borissiakii</i>	Alexejew 1930	Eldari, Georgia	<i>Achtiaria borissiakii</i>	Part of mandible with P2-M3 (Lectotype)	-
<i>P. quadricornis</i>	Bohlin 1926	Samos, Greece	<i>Palaeotragus quadricornis</i>	Skull	-

The validity of previous assumptions is tested here through a set of biometrical comparisons combined with morphological features. The specimens from NKT, PNT and RPI are also included. When the sizes of the toothrows were examined, a clear trend was observed (Figs 16-17). The Late Miocene Eurasian *Palaeotragus* are indeed distinguished in two different size groups; the first one contains *Palaeotragus rouenii*, *Palaeotragus microdon* and *Palaeotragus pavlowae* [in contrast to Godina's (1979) point of view] which share small-sized toothrow. The second one contains

Palaeotragus coelophrys, *Palaeotragus hoffstetteri*, *Palaeotragus moldavicus*, *Palaeotragus expectans*, *Palaeotragus borissiaki*, *Palaeotragus berislavicus*, *Palaeotragus asiaticus* and *Palaeotragus quadricornis*. Hence, the distinction of the two size groups (the “*P. rouenii*” and “*P. coelophrys*” groups) seems to be reasonable. Inside “*P. coelophrys*” group, however, the species *Palaeotragus expectans* and *P. borissiaki* have the largest tooththrows, while the other species have smaller dentition. Nevertheless, the material of *Palaeotragus expectans* and *P. borissiaki* is so scarce (Tab. 21), that a distinction based on the tooththrow size is quietly doubtful; the observed differences could just reflect intraspecific variation.

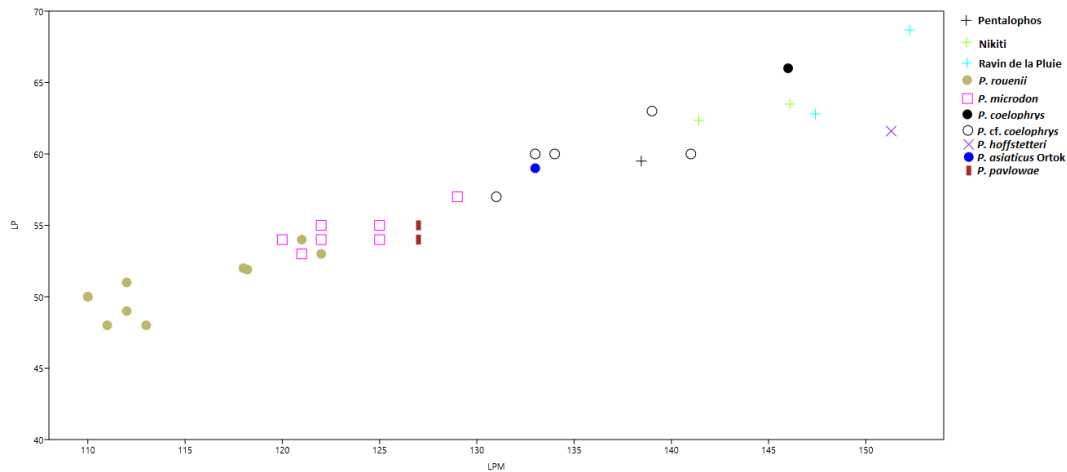


Figure 16: Scatter plot with measurements of upper tooththrows of several *Palaeotragus* species. (LPM) Total tooththrow length; (LM) Molar row length.

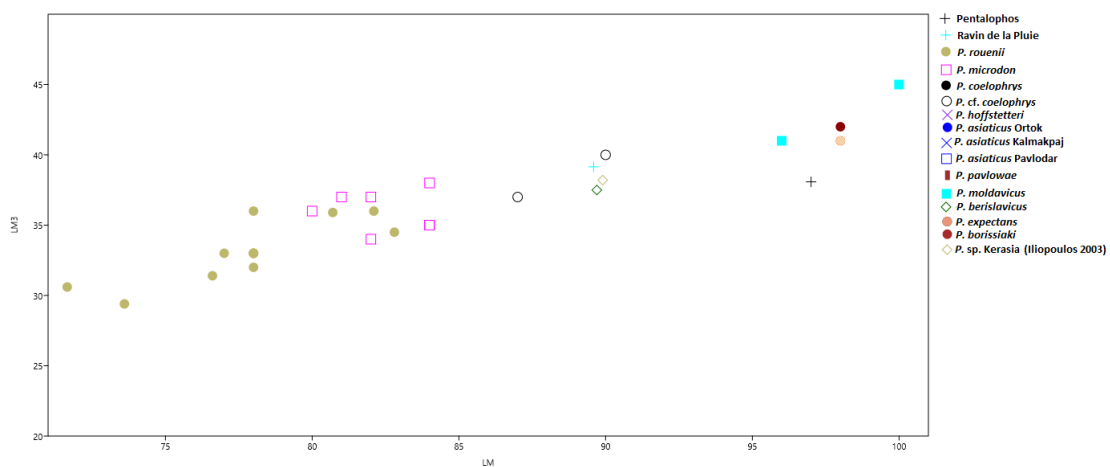


Figure 17: Scatter plot with measurements of lower tooththrows of several *Palaeotragus* species. (LM) Molar row length; (LM3) Lower M₃ length.

On the other hand, when the postcranial material was examined a different pattern was revealed. While the representatives of "*P. rouenii*" group are clustered together, large sized taxa of "*P. coelophrys*" group are subdivided in two subgroups. The first one includes the species *Palaeotragus coelophrys*, *P. expectans*, *P. borissiaki*, *P. hoffstetteri* and *P. moldavicus* which share the feature of larger postcranial bones and of shorter, more robust metapodials. The variations inside that group doesn't seem to be important, firstly because of the scarcity of the material and secondly because overlapping is observed among different species. The second group includes the species of *Palaeotragus asiaticus* and *P. berislavicus* with smaller postcranial bones, and longer, slenderer metapodials (Figs 18-21). It could be said that *Palaeotragus asiaticus* and *Palaeotragus berislavicus* are intermediate *Palaeotragus* species, on account of their size and proportions. In fact, *P. asiaticus* was inducted in "*P. rouenii*" group on account of its metatarsals' dimensions (Fig. 21).

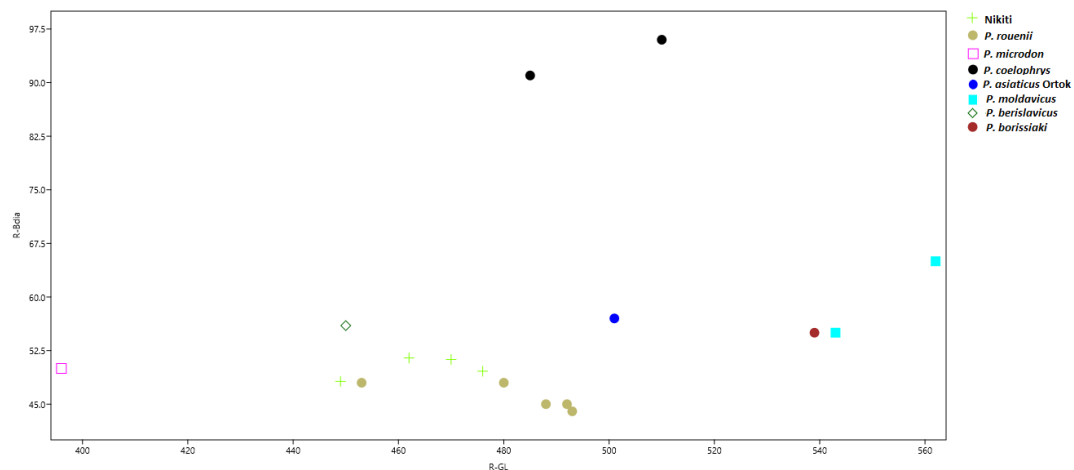


Figure 18: Scatter plot of radii measurements of several *Palaeotragus* species. (R-GL) Radius greatest length; (R-Bdia) Breadth in the middle of the radii shaft.

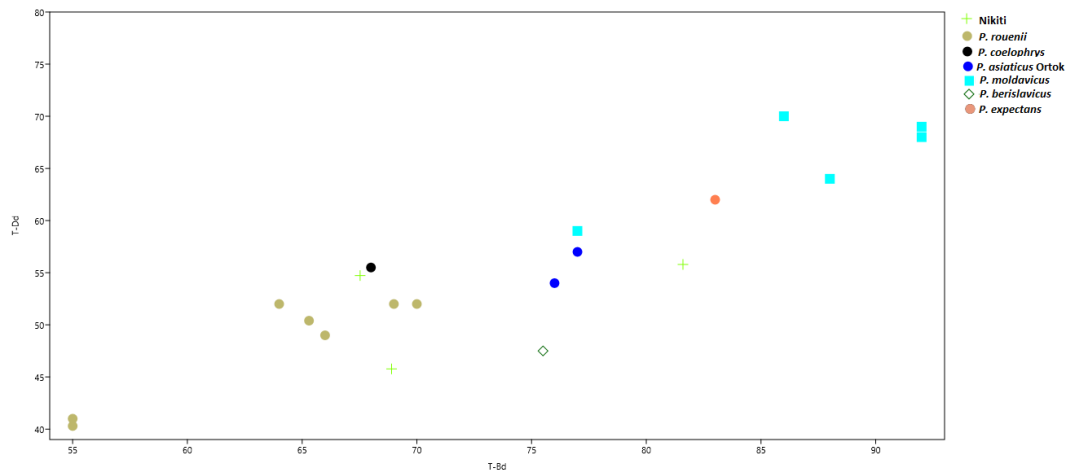


Figure 19: Scatter plot of tibiae measurements of several Palaeotragus species. (T-Bd) Breadth of tibiae distal part; (T-Dd) Depth of tibiae distal part.

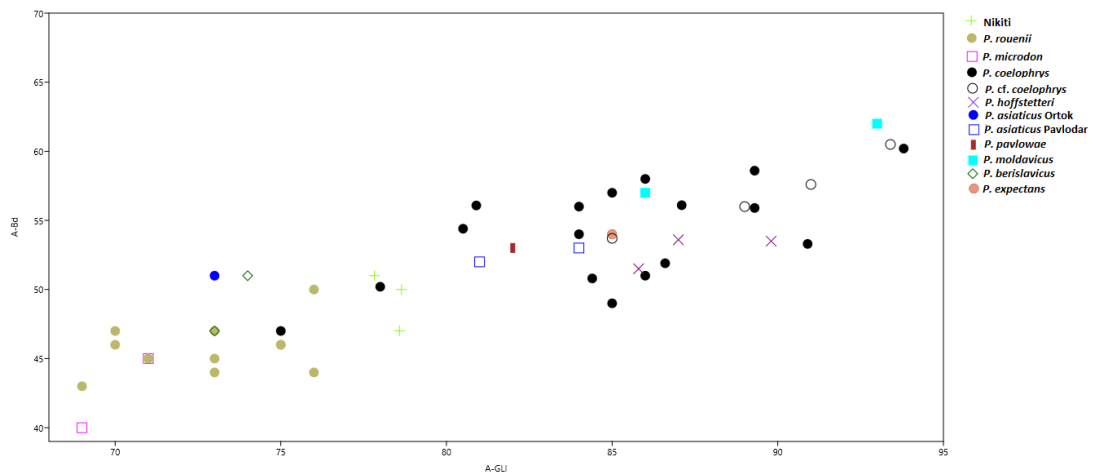


Figure 20: Scatter plot of astragali measurements of several Palaeotragus species. (A-GLI) Astragalus greatest lateral length; (A-Bd) Breadth of astragali distal part.

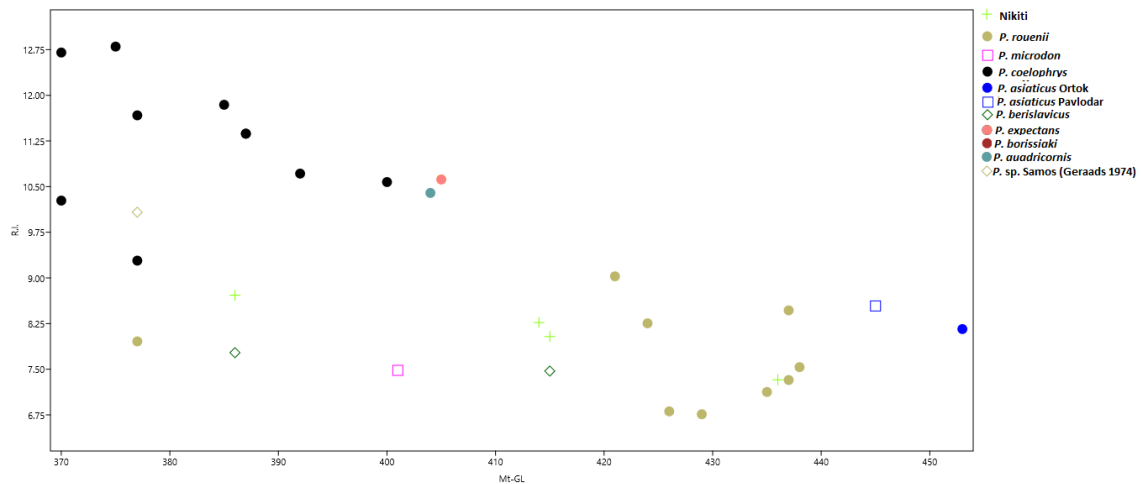


Figure 21: Scatter plot of metatarsal measurements of several Palaeotragus species. (Mt-GL) Metatarsals' greatest length; (R.I.) Robusticity Index. The R.I. is given by the following formula:

$$R.I. = \frac{\text{Depth in the middle of the metatarsals shaft}}{\text{Metatarsals' greatest length}} \times 100$$

The validity of *P. asiaticus* cannot be tested decisively. As registered, *P. asiaticus* demonstrates rather slender and long metatarsals that cannot be distinguished by those of *P. rouenii* and a dentition that falls in the lower range of "*P. coelophrys*" group. However, no metatarsals have been collected from the type locality (Ortok, Kyrgyzstan). The Ortok material contains two upper dentitions that fit in "*P. coelophrys*" group (Fig. 16), some isolated upper and lower teeth that are intermediate in size -with some approaching better to "*P. coelophrys*" group, while others being close to the upper range of "*P. rouenii*" group (Figs 22-24)- a "*P. rouenii*" group astragalus (Fig. 20), an intermediate radius, close to "*P. rouenii*" group (Fig. 18) and two intermediate tibiae (Fig. 19). Another locality where *P. asiaticus* has been found is Pavlodar. A "*P. rouenii*" group metatarsal (Fig. 21), two "*P. coelophrys*" group astragali (Fig. 20) and some lower isolated teeth, intermediate in size but closer to "*P. coelophrys*" group (Fig. 24) have been described from there. A "*P. rouenii*" metatarsal (Fig. 21) and a "*P. coelophrys*" lower dentition (length 141mm) have been described from Kalmakpaj, Kazakhstan. Finally, a "*P. rouenii*" metatarsal has been described from Pristashkent district, Uzbekistan (Fig. 21). We think that the described material attributed to *P. asiaticus* is too scarce for any reliable conclusion; it could reflect the co-existence of a *P. rouenii* and a *P. coelophrys* population in areas such as Pavlodar

and Kalmakpaj and a population of smaller *P. coelophrys* or other taxon in Ortok. Therefore, more research is needed in order to classify that material.

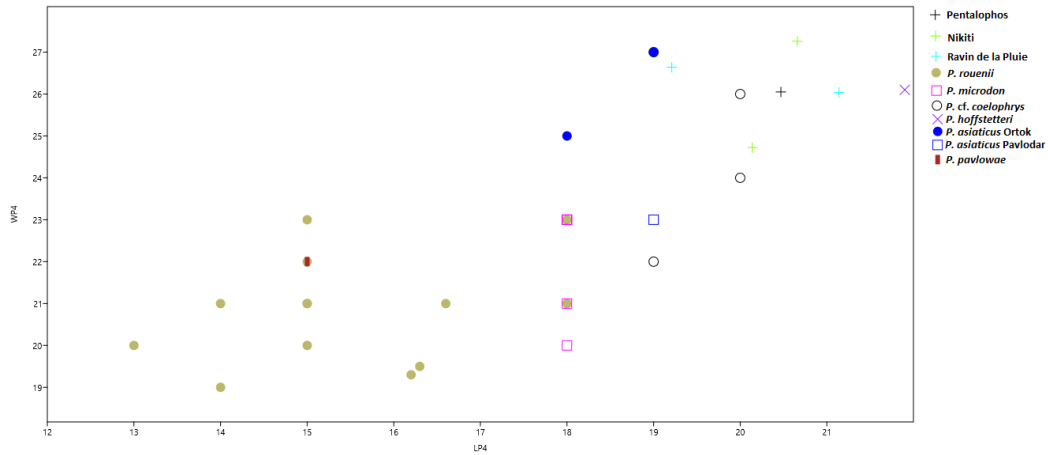


Figure 22: Dimensions of P^4 of several Palaeotragus species. (LP4) Length of P^4 ; (WP4) Width of P^4 .

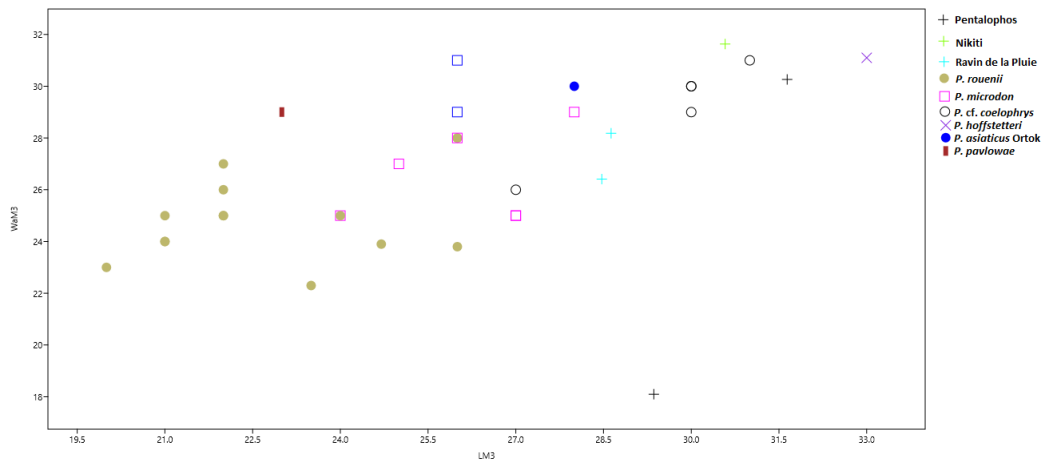


Figure 23: Dimensions of M^3 of several Palaeotragus species. (LM3) Length of M^3 ; (WM3) Width of M^3 .

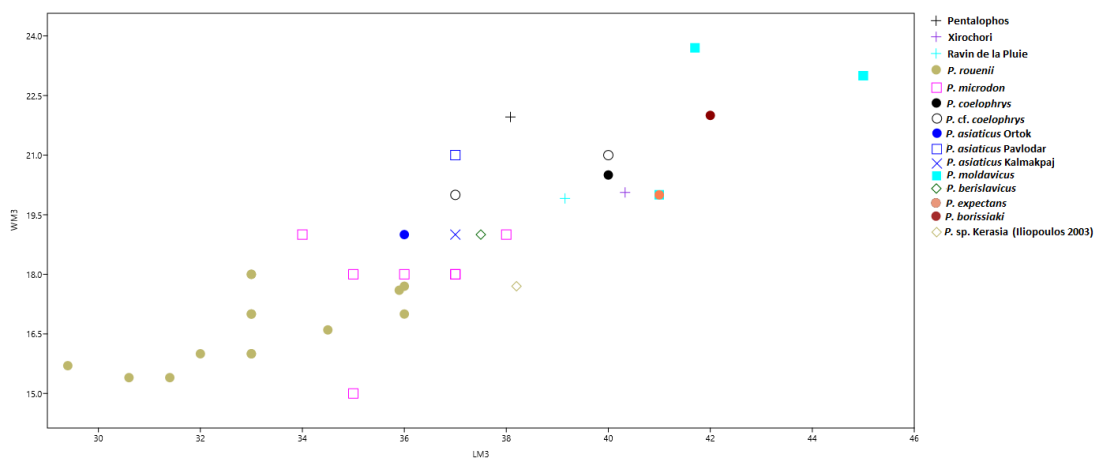
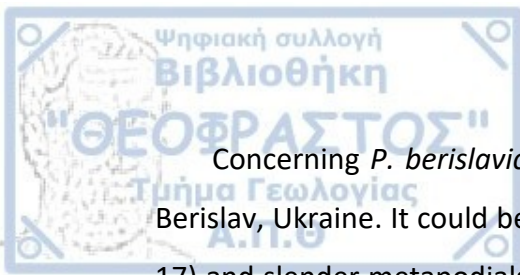


Figure 24: Dimensions of M_3 of several Palaeotragus species. (LM3) Length of M_3 ; (WM3) Width of M_3 .

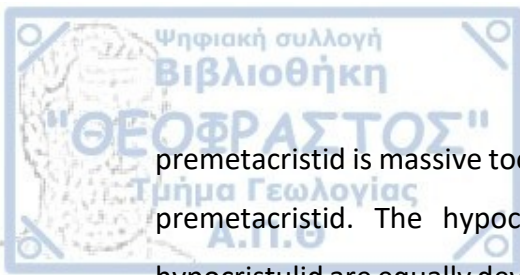


Concerning *P. berislavicus*, all its but scarce specimens come from a single site Berislav, Ukraine. It could be described as a palaeotragine with a large dentition (Fig. 17) and slender metapodials, intermediate in length between “*P. rouenii*” group and “*P. coelophrys*” group (Fig. 21). Other *P. berislavicus* postcranial elements fit in the “*P. rouenii*” group. Specifically, that is revealed by data for the dimensions of radii and astragali (Figs 18, 20). It could be assumed that there is a higher possibility that *P. berislavicus* is a valid species, as it fulfils the homogeneity criterion at least.

A comprehensive examination of illustrations of the dental morphology of numerous Late Miocene Eurasian *Palaeotragus* species did not reveal any important difference. The main reason is that dental features of the type species *Palaeotragus rouenii* show a remarkable variability. For example, the upper premolars present a number of morphotypes; having either wide, simple fossettes or narrow, W-shaped fossettes; P⁴s with one lingual style (similar to that of NKT), others with two or none, and semi-circular shaped or square in occlusal view. As for the upper molars, these are quietly conservative inside Giraffidae in general. Their morphology cannot be distinguished among different genera (*Palaeotragus* upper molars compared to that of today's *Okapia johnstoni* and *Giraffa camelopardalis*). The same goes for the lower molars.

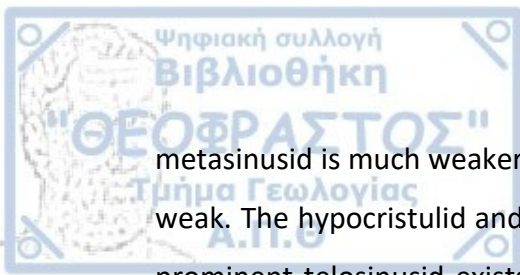
The lower premolars show some variation (Figs 25-26). They have been used as a source of taxonomic information for palaeotragines in the past (Hamilton 1978, Godina 1979), so they are examined more carefully in the present study. On account of P₄, the degree of the P₄ molarization varies, although it seems to vary inside the same species [e.g., different *P. coelophrys* specimens from Maragheh (MNHN MAR-669, MAR-528)]. The same goes for the proportions of the two lobes of the molarized P₄s [e.g. P₄'s lobes from different specimens of *P. rouenii* from Pikermi have different relative size (MNHN PIK-1671, PIK-1675)]. The aforementioned differences are demonstrated in Figure 25.

As for the P₃, the variability of its morphology is remarkable. In *P. rouenii* mandible MNHN PIK-1671 from Pikermi, the paracristid and anteparacristid of P₃ are not distinguished. The metaconid is massive, while the protoconid is weak. The



premetacristid is massive too. The postmetacristid is underdeveloped relatively to the premetacristid. The hypoconid is prominent. Distally, the entocristid and the hypocristulid are equally developed. The mesosinusid, metasinusid and telosinusid are very weak. A *P. rouenii* P₃ from Cimisia (Godina 1979) has a completely different morphology. In contrast to the PIK-1671 P₃ the paracristid and anteparacristid are clearly distinguished, although they are not well developed. The metaconid is massive, although the premetacristid and postmetacristid are separated by a deep groove. The premetacristid is much more developed than the postmetacristid. The hypocristulid and entocristid are not fused and they tend to fuse distally with the postmetacristid, while they are much longer and weaker than those of MNHN PIK-1671. The telosinusid is almost absent, whereas the metasinusid and mesosinusid are prominent. In the *P. rouenii* mandible AeMNH MTLB226 the paracristid and anteparacristid are separated by a very slight groove, resembling that of *P. rouenii* from Cimisia. The premetacristid and postmetacristid are completely absent, as well as the transverse cristid. As a result, the metaconid is the only prominent lingual feature. The protoconid is well-developed. The mesosinusid is also well-developed. The metasinusid and telosinusid are prominent too, although they are less developed than the mesosinusid. The hypocristulid and entocristid are distinguished, as in Cimisia's P₃ but much shorter. Finally, in another *P. rouenii* P₃ from Samos (in the mandible PIM-293) a different morphology is observed. It resembles more that of Pikermi, as the paracristid and anteparacristid are fused. The mesosinusid is very well-developed, in contrast to MNHN PIK-1671. The metaconid is not so massive and the premetacristid is absent. The postmetacristid is weak (relatively to *P. rouenii* from Pikermi). The metasinusid and telosinusid are very weak too, although they are prominent. The entocristid and hypocristulid resemble that of Pikermi.

As for *P. coelophrys* P₃, the P₃ from the Maragheh mandible MNHN MAR-669 shows a more primitive morphology. The metaconid is much more prominent than the protoconid, which is very weak. The transverse cristid is also massive. The premetacristid exists here and it is distinguished by a groove from the metaconid. Paracristid and anteparacristid are fused, and they almost fuse mesially with the premetacristid. Thus, the mesosinusid is closed lingually and it is prominent. The



metasinusid is much weaker than in the other Maragheh specimen. The hypoconid is weak. The hypocristulid and entocristid are equally developed, and between them a prominent telosinusid exists. A P_3 from a *Palaeotragus* cf. *coelophrys* from China is completely different than the two aforementioned, as it is molarized (AMNH-26363). Finally, a P_3 from a large *Palaeotragus* from Samos (in the mandible CMNH CM-370), is completely different than all the aforementioned. Mesially, the paracristid and anteparacristid are not fused to each other. The metaconid is weak. Instead, there is a groove that separates the premetacristid and postmetacristid. The hypoconid and protoconid are well developed, while the entocristid and hypocristid are fused together. The mesosinusid is large. The metasinusid is prominent, yet weak. The telosinusid is absent. Two P_3 s of *Palaeotragus expectans* from Varnitsa resemble the first described morphotype from Maragheh P_3 . A *P. microdon* P_3 is somewhat molarized (in the mandible AMNH-26360).

To summarize, neither the morphology of P_3 is a reliable character, due to its variability. Illustrations of P_3 's morphology are provided in Figure 26.

Concluding, for the "*P. coelophrys*" group, *P. coelophrys*, *P. expectans*, *P. borissiaki*, *P. hoffstetteri*, *P. quadricornis* and *P. moldavicus* do not seem to differ, based on the material examined in the present study. Hence, all these species are considered synonyms. More research is needed to support the validity of *P. asiaticus*. *P. berislavicus* seems to be a valid species, although further investigation is needed, as well.

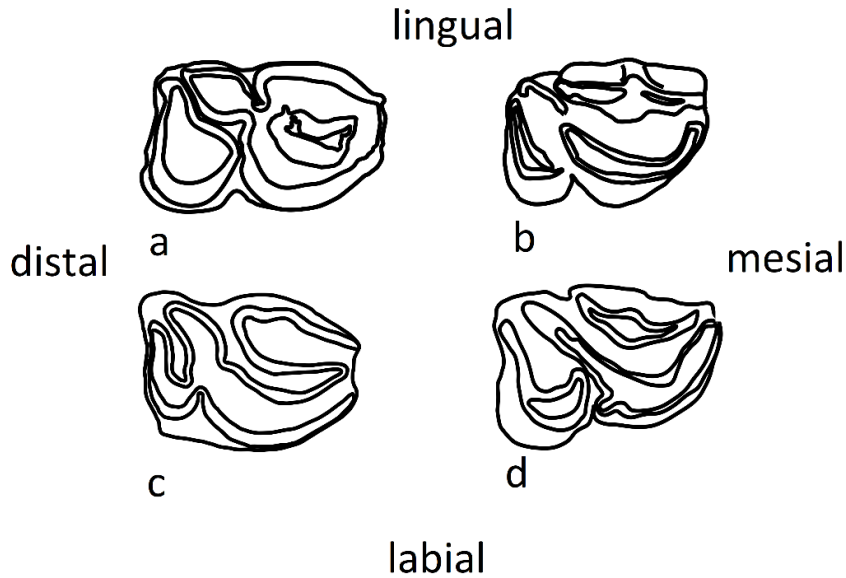


Figure 25: P_4 morphology of various *Palaeotragus* species. (a) *P. rouenii* P_4 from Pikermi (PIK-1671); (b) *P. rouenii* P_4 from Pikermi (PIK-1675); (c) *P. coelophrys* P_4 from Maragheh (MAR-528); (d) *P. coelophrys* P_4 from Maragheh (MAR-669).

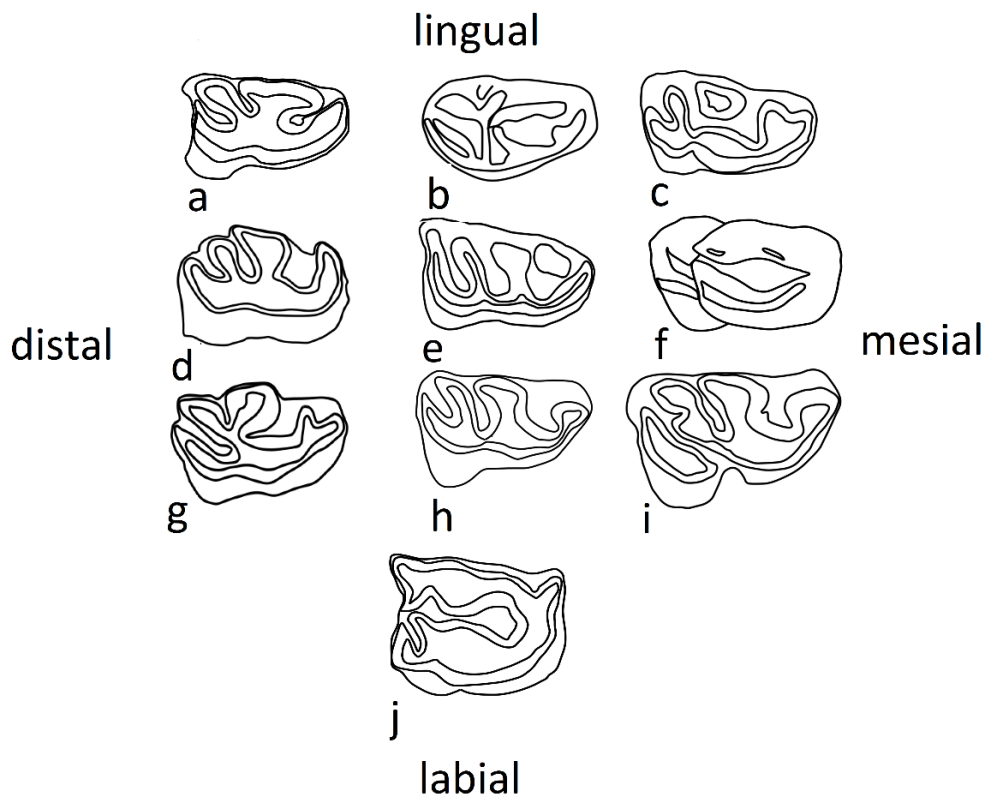


Figure 26: P_3 morphology of various *Palaeotragus* species. (a) *P. rouenii* P_3 from Pikermi (PIK-1671); (b) *P. rouenii* P_3 from Cimislia (Godina 1979); (c) *P. rouenii* P_3 from Samos (MTLB226); (d) *P. rouenii* P_3 from Samos (PIM293); (e) *P. coelophrys* P_3 from Maragheh (MAR-669); (f) *P. cf. coelophrys* P_3 from Shansi (AMNH-26363); (g) *P. quadricornis* P_3 from Samos (CM-370); (h) first *P. expectans* P_3 from Varnitsa; (i) second *P. expectans* P_3 from Varnitsa; (j) *P. microdon* P_3 from Kansu (AMNH-26360).

3.2.2. Comparison of the Greek Vallesian large Palaeotragus

3.2.2.1 Nikiti-1 (NKT)

The case of NKT's material is interesting. Firstly, the skull and teeth are of large size and clearly belong to "*Palaeotragus coelophrys*" group (Figs 16-17). On the other hand, NKT postcranial material is proportionally closer to "*Palaeotragus rouenii*" group (except the specimens NKT-133 and NKT-160 which are considerably compressed, giving the impression of a more robust bone) creating a subgroup, with slightly shorter metapodials than those of other large *Palaeotragus* representatives (Figs 21, 27). Other exceptions are the specimens NKT-138 and NKT-139. NKT-138 is a damaged specimen that groups together with *P. rouenii*, as it is fairly long and slender, while the NKT-139 is slender but it is relatively shorter, having a length that approaches that of *P. coelophrys* group. Based on the metatarsals, it could be assumed that NKT material could be attributed to a population which is closer to *P. rouenii*, although it is distinct (Fig. 21). The two specimens (NKT-138 and NKT-139) could just reflect the diversity inside that population. Metacarpals from NKT are scarcer than the metatarsals, although it seems that they follow the same rule, being similar in slenderness with those of *P. rouenii* but shorter (Fig. 27). That feature, of slender metapodials, but shorter than in *P. rouenii*, is shared with *P. berislavicus*.

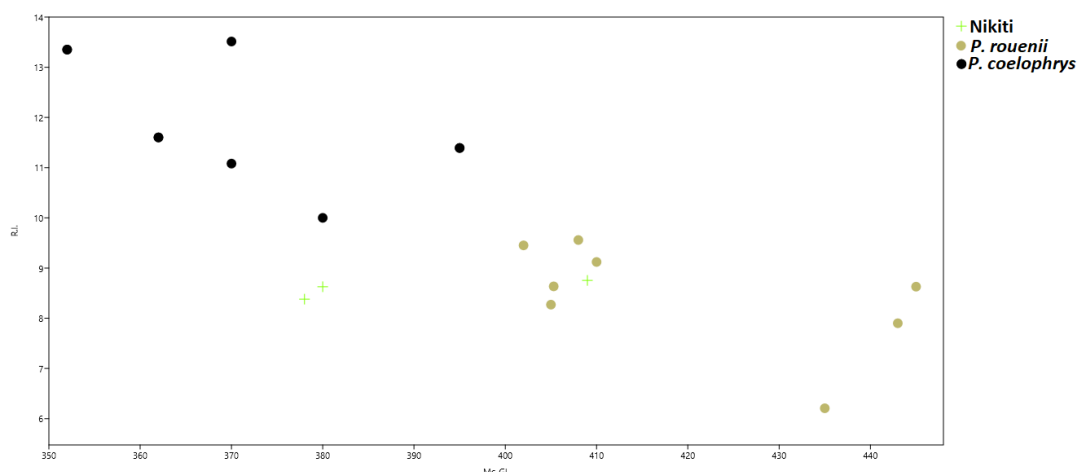


Figure 27: Scatter plot of metacarpal proportions of several Palaeotragus species. (Mc-GL) Metacarpals' greatest length; (R.I.) Robusticity index.

Concerning the morphology of the metacarpals, there are numerous differences between NKT-taxon and *P. rouenii* (Fig. 28). Proximally, the bone protrusion which separates the medial and lateral epicondyles is much more intense in *P. rouenii* than in NKT. Moreover, the medial epicondyle is of trapezoid shape and the lateral epicondyle is of square shape in *P. rouenii*, while they are of half-circle shape in NKT. As a result, the proximal articular surface has a trapezoid shape in *P. rouenii* and a half-circle shape in NKT specimens. Dorsally, the shaft is parallel to the bone axis medially, while the axis of the bone and the shaft are angled laterally in *P. rouenii*. That feature is very prominent proximally and it could be said that the cross section of the shaft has a shape of a right triangle. The same feature exists in NKT's metacarpals too, although it is much less prominent, and as a result, the cross section of the shaft is more rectangularly shaped. Palmar, the central trough extends throughout the whole bone in *P. rouenii* reaching at the trochlear, although it is considerably shallower distally than proximally. On the contrary, in the NKT metacarpals, the central trough seems to disappear at about the 1/3 of the bone distally. Thus, the distal and palmar side of the bone is completely flat in NKT. Distally the lateral condyle, seems to extend slightly more laterally in *P. rouenii* than in the NKT metacarpal. Finally, distally and dorsally, the shaft is somewhat more curved in *P. rouenii*, while in NKT's metacarpals is more flattened.

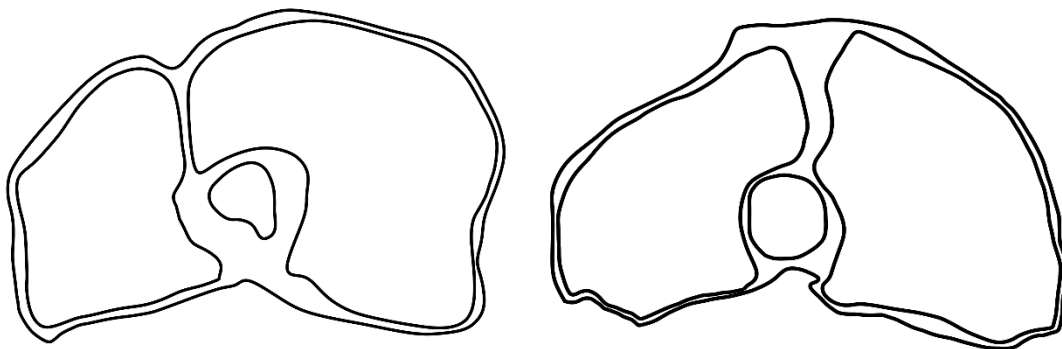


Figure 28: Comparison of proximal metacarpals epiphyses. Left: *Palaeotragus rouenii* from NIK; Right: *Palaeotragus* from NKT.

Concerning the metatarsals, proximally there are numerous differences among NKT-form and *P. rouenii* (Fig. 29). At first, medially the proximal articular surface is

continuous in *P. rouenii*, while in NKT it is separated by a groove in the point between the two heads. Hence, the two heads of the medial epicondyle are more prominently separated in NKT. The shape of the dorsal head of the lateral epicondyle is half-circular in both NKT and *P. rouenii*, but in NKT is much more elongated. Moreover, in NKT that head is placed at a more obtuse angle to the axis of the proximal articular surface. In contrast, in *P. rouenii*, it is placed parallel to the proximal articular surface axis. As a result, the lateral epicondyle is of equal or of greater width to the medial epicondyle in NKT than in *P. rouenii*. In the medial epicondyle, the highest point dorsally is more medially placed in *P. rouenii*. The plantar head of the medial epicondyle is extended fairly plantarly in *P. rouenii* and it tilts laterally, while in NKT it is not so extended plantarly and it tilts medially. Those two heads are separated by a slight medial groove that is much better developed in *P. rouenii* than in NKT. Finally, the pygmaios is prominent in *P. rouenii* but absent in NKT. That difference is probably due to the bad conservation status of the most NKT specimens. Plantarly only a few things can be said, as the central trough seems to variate a lot between NKT specimens in terms of depth and width. Finally, the distal part, relatively to the shaft, is wider in NKT than in *P. rouenii*.

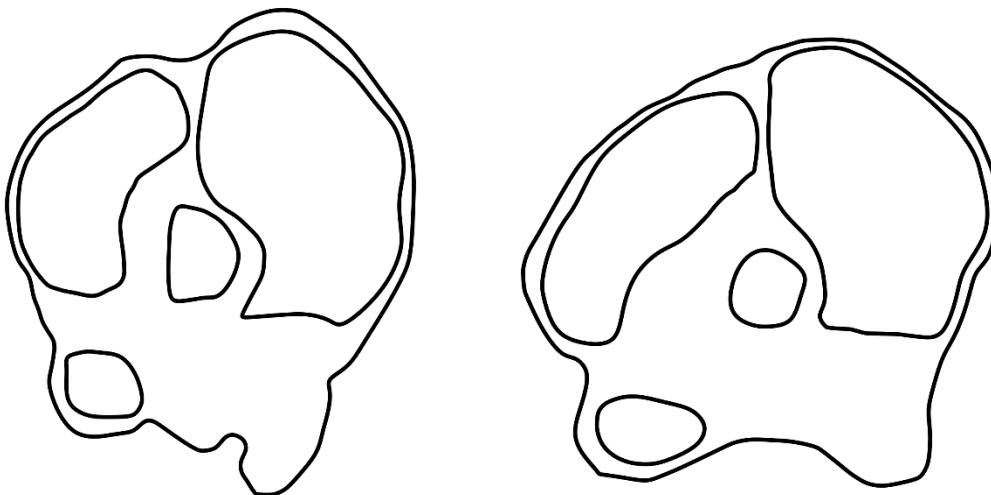


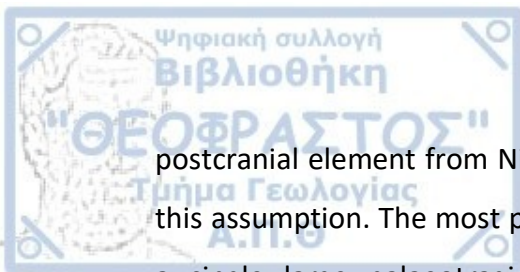
Figure 29: Comparison of proximal metatarsals epiphyses. Left: *Palaeotragus rouenii* from PER; Right: *Palaeotragus* from NKT.

When it comes to the radii, NKT's specimens fall into the lower range of *P. rouenii* radii length (Fig. 18). In contrast to *P. rouenii*, NKT radii have a broader distal part. In that feature they agree with *P. berislavicus* and *P. asiaticus* (Fig. 18), although there is only one radius specimen available in the literature for each of these two taxa. Unfortunately, literature for the cranial-caudal diameter of radius is very limited. However, from some scarce measurements (Geraads 1974), it seems that *P. rouenii* had a significantly slenderer radius than NKT, at least proximally. In fact, the cranial-caudal diameter of NKT's radius is closer to that reported for *P. coelophrys*. However, when NKT specimens are compared with some *P. rouenii* specimens from the sites Perivolaki and Nikiti-2, they did not seem to be more robust proximally. The radius curvature is a feature which also varies among NKT, as well as among *P. rouenii*. Shafts' cross section is of similar crescent shape. Distally and cranially, the V-shaped formation for the adhesion of extensor carpi radialis muscle is equally prominent in NKT and *P. rouenii*. The distal articular surface is also very similar in NKT and *P. rouenii*.

Concerning the astragali, the NKT astragali are intermediate in size between those of "*P. rouenii*" group and the "*P. coelophrys*" group, while the astragali of *P. berislavicus* is smaller than the NKT ones and cannot be separated from the "*P. rouenii*" group (Fig. 20). Moreover, the astragalus of *P. rouenii* from Perivolaki (PER) is more elongated than the NKT astragali, having a more rectangular shape (more squarish in NKT).

The tibia data are rarer. According to the only full specimen of tibia available from NKT, its length falls inside the *P. rouenii* range. However, it seems that NKT palaeotragines had broader distal tibia parts than *P. rouenii*. This is another feature that they share with *P. berislavicus* and *P. asiaticus* (Figs 17-21).

Two assumptions can be done about NKT's taxon. The first one could be that in Nikiti two populations of *Palaeotragus* were present: a population of *P. rouenii* represented exclusively by postcranials and with slightly shorter postcranial bones than typically, and a population of *P. coelophrys* represented by a partial cranium (NKT-172). The case of coexistence of different *Palaeotragus* species in Greece is confirmed (Iliopoulos 2003, Kostopoulos 2009). However, the absence of any



postcranial element from Nikiti that could be grouped with *P. coelophrys* challenges this assumption. The most probable and parsimonious hypothesis is that in NKT site, a single large palaeotragine population existed, characterized by intermediate proportions between *P. coelophrys* and *P. rouenii*. That population is diagnosed by slender metapodials, which are shorter than those of “*P. rouenii*” group and skulls with dimensions similar to those of “*P. coelophrys*” group. Morphological differences between metapodials of Nikiti and *P. rouenii* also favor this hypothesis. On the other hand, metric features are close to those of *P. berislavicus* (with the exception of the astragali) (Fig. 17).

To sum up, the NKT taxon is a distinct form than both *P. rouenii* and *P. coelophrys*. Moreover, even if *P. asiaticus* is a valid species, it differs from the NKT’s taxon on account of the dimensions of the metapodials (*P. asiaticus* reported metapodials appear identical to those of *P. rouenii*). Considering that *P. berislavicus* is probably a valid species and that it shares a number of similarities with the NKT form, a classification as *Palaeotragus* aff. *berislavicus* is proposed for the NKT taxon, with all reservations.

3.2.2.2 Pentalophos (PNT)

The dental specimens from PNT are large in size and do clearly fit to “*Palaeotragus coelophrys*” group (Figs 16-17, 22-24). Comparing the PNT teeth with those of the type *Palaeotragus coelophrys* from Maragheh, in both the PNT and Maragheh premolars, a slight hypoconal fold is observed. The P² from Maragheh seems to have a somewhat prominent lingual rib in the hypocone area that it is absent from the P²s of PNT. In the only available P⁴ from PNT, the paracone is more centrally placed, than it is in the P⁴ from Maragheh. PNT’s P⁴ fossette is somewhat better developed mesially and lingually, than the fossette of P⁴ from Maragheh. Finally, the PNT P⁴ is clearly more triangularly shaped than that of Maragheh.

The distal part of the PNT humerus (Pl. 14) approaches in size *P. rouenii*’s humerus. Its olecranon fossa is filled with sediment, however it is probably deep, wide

and U-shaped. The medial epicondyle is flat and it is not expanding medially, while the lateral epicondyle is projecting laterally and a round concave cavity is laterally present.

PNT's metatarsals (Pl. 15) are somewhat different from those of NKT. They statistically seem to approach better to "*P. coelophrys*" group, as they are considerably robust proximally (Fig. 30). Unfortunately, it is impossible to know their full length as they are fragmented. The morphology of the proximal articular surface of PNT looks more like the NKT's than the *P. rouenii*'s. Medially, a bone protrusion separates the plantar and dorsal heads in contrast to the light medial groove of both *P. rouenii* and NKT. The plantar head does not seem to tilt neither medially nor laterally in PNT, in contrast to *P. rouenii* and NKT. The lateral dorsal head is more robust in PNT than in both *P. rouenii* and NKT, and it is placed parallel to the proximal articular surface's axis as in *P. rouenii*. The plantar and dorsal heads of the lateral epicondyle are separated by a groove in PNT, as they do in NKT. Finally, the pygmaios is present but less prominent than it is in *P. rouenii*.

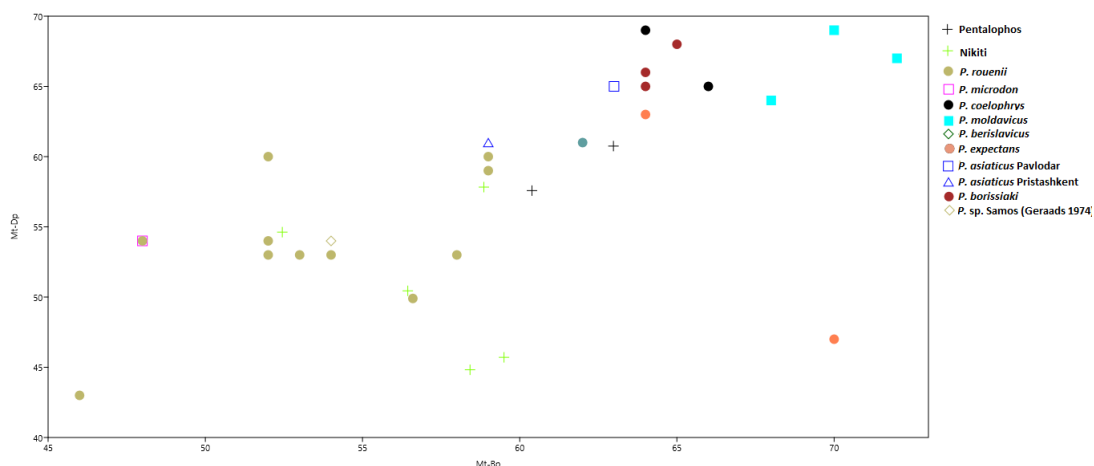


Figure 30: Scatter plot of metatarsal proximal proportions on several Palaeotragus species. (Mt-Bp) Breadth of metatarsals' proximal part; (Mt-Dp) Depth of metatarsals' proximal part.

To sum up, there are very few postcranial elements from PNT site, although it could be hypothesized that PNT held a population different to that of NKT, as the available material (both the dental and postcranial) from PNT seems to fit better *P. coelophrys*. The co-occurrence of *P. coelophrys* dental and postcranial material allow for a classification as *Palaeotragus coelophrys*.

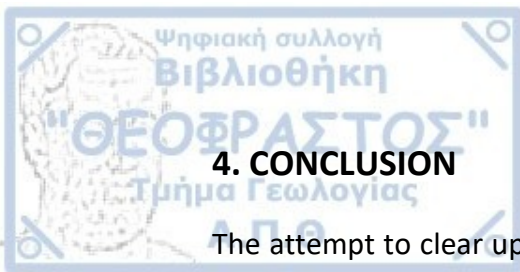


3.2.2.3 Ravin de la Pluie (RPI)

RPI skull has been studied in the past (Geraads 1978). It was then classified as *Palaeotragus cf. coelophrys*. First of all, the morphological examination of the teeth, does not provide us with something valuable. A difference among the RPI teeth and that of *P. coelophrys* type from Maragheh is that the RPI premolars are larger in comparison to molars and that they are more rectangular shaped. However, this impression may be given due to the advanced RPI teeth wear. Not a lot can be said for the comparison of the RPI teeth labial ribs with those of the Maragheh teeth, again due to the extended wear. According to our observations and measurements (Figs 16-19), the size of the skull and the size of the other RPI specimens fit indeed to *P. coelophrys*. In fact, RPI's skull has one of the largest described tooththrows. However, the absence of any postcranial material from that site does not allow for RPI's classification as *P. coelophrys*, as in the cases of NKT and PNT. Hence, we just confirm Geraads (1978) classification of that material as *Palaeotragus cf. coelophrys*.

3.2.2.4 Xirochori (XIR)

The size of the mandibular teeth (M_2 - M_3) from Xirochori approaches the lower range of "*Palaeotragus coelophrys*" group (Fig. 24). However, it cannot be excluded that these teeth belong to either a "*P. rouenii*" group individual or a *P. aff. berislavicus* individual, as overlap is observed, to some extent, among different groups. Hence, the material is classified as *Palaeotragus sp.*



4. CONCLUSION

The attempt to clear up the Late Miocene Eurasian *Palaeotragus* taxonomy was based exclusively in metric features, as the morphology of *Palaeotragus* lower and upper premolars demonstrates high variability, and the morphology of the upper and lower molars is quietly conservative. It should not be excluded that other bones could provide morphological phylogenetic information.

The dental metric comparisons revealed the existence of three different groups: one of small-sized palaeotragines with long-slender metapodials ("*P. rouenii*" group) and one of large-sized animals with short-robust metapodials ("*P. coelophrys*" group). "*P. coelophrys*" group was examined more carefully, as all of our fossils belong to a large-sized *Palaeotragus*. *Palaeotragus coelophrys*, *P. expectans*, *P. borissiaki*, *P. moldavicus*, *P. hoffstetteri* and likely *P. quadricornis* cannot be distinguished on account of metric features and present data available. Thus, they are considered here as synonyms under *P. coelophrys*. On the other hand, *P. asiaticus* and *P. berislavicus* are clearly distinguished on account of their dimensions. The available material of *P. asiaticus* is scarce and fragmentary. As a result, its validity cannot be decisively tested here. All of *P. berislavicus* material comes from a single site (Berislav). It reveals a *Palaeotragus* with intermediate size between *P. rouenii* and *P. coelophrys*, demonstrating a relatively large skull and slender metapodials, intermediate in length between those of *P. rouenii* and *P. coelophrys*.

The NKT *Palaeotragus* represents a unique population that shares a lot of similarities in dimensions with *P. berislavicus*. Therefore, it is referred to as *Palaeotragus* aff. *berislavicus*.

Several dental specimens and metatarsal fragments were described from PNT. Both cranial and postcranials agree with a *Palaeotragus coelophrys* assignment. Hence the PNT material is referred to as *Palaeotragus coelophrys*, although it is scarce. The *Palaeotragus* skull from RPI is classified here as *Palaeotragus* cf. *coelophrys*, in agreement with previous identification by Geraads (1978). A mandible preserving the molars and an isolated upper molar, are inside "*P. coelophrys*" group size range and they are attributed to *Palaeotragus* cf. *coelophrys* too. The single mandible from



Xirochori is relatively large-sized, but insufficient to allow for a proper classification. Therefore, the Xirochori *Palaeotragus* is referred to as *Palaeotragus* sp.

In this study, we had the opportunity to test the Eurasian Late Miocene *Palaeotragus* taxonomy, although this attempt was incomplete. In order to properly clarify the taxonomy inside the most common giraffid genus of Eurasia's Late Miocene, *Palaeotragus*, a much more comprehensive analysis of all the collected *Palaeotragus* material is needed. That analysis should contain the examination of several dental, cranial and postcranial features. The postcranial morphology has never been thoroughly studied. We propose that it could possibly reveal features with diagnostic importance; as it has been already mentioned the metapodials from NKT have morphological features that they are always different from those of *P. rouenii*. The metric comparisons that were carried out at the present study, should also be used in order to assess relationships inside *Palaeotragus*. Finally, future excavations seem necessary in order more fossil material to be available and any assumptions about the *Palaeotragus* taxonomy to be more solid. In particular, the discovery of several well-preserved cranial specimens could offer much in terms of understanding the phylogenetic relationships inside the genus *Palaeotragus*.

Aftab, K., Khan, M.A., Babar, M.A., Ahmad, Z. & Akhtar, M. 2016. *Giraffa* (Giraffidae, Mammalia) from the lower Siwaliks of Pakistan. *The Journal of Animal & Plant Sciences*, 26(3):833-841.

Alexeiev, A. 1930. Die obersarmatische Fauna von Eldar. *Travaux du Musée Géologique près l'Académie des Sciences de l'URSS*, 8:167-204. (In Russian with German abstract).

Arambourg, C. 1959. Vertébrés continentaux du Miocène supérieur de l'Afrique du Nord. *Publications du service de la Carte Géologique de l'Algérie (Nouvelle série). Palaeontologie, Memoirs Algiers*, 4:1-159.

Athanassiou, A. 2014. New giraffid (Artiodactyla) material from the Lower Pleistocene locality of Sésklo (SE Thessaly, Greece): Evidence for an extension of the genus *Palaeotragus* into the Pleistocene. *Zitteliana B*, 32:71-89.

Bishop, W. W. & Pickford, M.H.L. 1975. Geology, fauna and palaeoenvironments of the Ngogora Formation, Kenya, Rift Valley. *Nature*, 254:185-192.

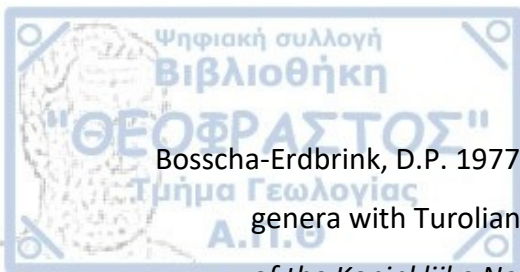
Bohlin, B. 1926. Die Familie Giraffidae. In: Ting, V.K. & Wong, W.H. (ed.) *Palaeontologia Sinica*, Series C, Volume 4. Beijing 1926.

Bonis, L.D., Koufos, G.D. & Sen, S. 1997. A giraffid from the Middle Miocene of the island of Chios, Greece. *Palaeontology*, 40:121-134.

Bonis, L.D. & Koufos, G.D. 1999. The Miocene large mammal succession in Greece. p. 205-237. In: Agustí, J., Rook, L. & Andrews, P. (ed.) *Hominoid Evolution and climatic change in Europe, vol. I, The evolution of the Neogene terrestrial ecosystems in Europe*. Cambridge University Press, New York, USA.

Bonis, L.D. & Bouvrain, G. 2003. Nouveaux Giraffidae du Miocène supérieur de Macédoine (Grèce). p. 5-16. In: Petculescu, A. & Stiuca E. (ed.) *Advances in Vertebrate Paleontology "Hen to Panta"*. Romanian Academy, Bucharest.

Borissiak, A. 1914. Mammifères fossiles de Sébastopol II. *Mémoires du comité Géologique, Nouvelle série, Livraison 137*, Paris, France.



Bosscha-Erdbrink, D.P. 1977. On the distribution in time and space of three giraffid genera with Turolian representatives at Maragheh in N.W. Iran. *Proceedings of the Koninklijke Nederlandse Akademie van Wetenschappen B*, 80 (5):337-355.

Brünnich, M. Th. 1772. M. T. Brünnichii Zoologiae fundamenta, Grunde i Dyreloeren. *Hafnioe et Lipsioe*, 253.

Ciric, A. & Thenius E. 1959. Über das Vorkommen von *Giraffokeryx* (Giraffidae) im europäischen Miozän. *Anzeiger der Akademie Wissenschaften mathematisch und naturwissenschaftliche Klasse, Wien*, 9:153-162.

Colbert, E.H. 1936. *Palaeotragus* from the Tun Gur formation of Mongolia. *American Museum Novitates*, 874.

Colbert, E.H. 1938. The relationships of the Okapi. *Journal of Mammalogy*, 19:47-64.

Crusafont-Pairó, M. 1952. *Los Jirafidos fosiles de España*. PhD Thesis, Barcelona, Diputation provincial de Barcelona, Spain.

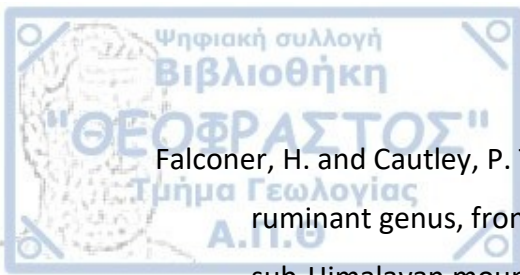
Crusafont-Pairó, M. 1979. Les Girafidés des gisements du Bled Douarah (W. de Gafsa, Tunisie). *Notes du Service géologique*, 44:7-75.

Danowitz, M., Vasilyev, A., Kortlandt, V. & Solounias, N. 2015a. Fossil evidence and stages of elongation of the *Giraffa camelopardalis* neck. *Royal Society Open Science*, 2(10).

Danowitz, M., Domalski, R. & Solounias N. 2015b. The cervical anatomy of *Samotherium*, an intermediate-necked giraffid. *Royal Society Open Science*, 2(11).

Dietrich, W. O. 1941. Die Säugetier paläontologischen Ergebnisse der Kohl-Larsen'schen Expedition, 1937-1939 in nördlichen Deutsch-Ostafrika. *Zentralblatt für Mineralogie, Geologie und Palaontologie*, 1941B:217-223

Duvernoy, M. 1854. Sur des ossements de Mammifères fossiles découverts à Pikermi, village près d'Athènes, au pied du mont Pentélique. *Comptes Rendus hebdomadaires des séances de l'Académie des Sciences de Paris*, 38:252–257.



Falconer, H. and Cautley, P. T. 1836. On the *Sivatherium giganteum*, a new fossil ruminant genus, from the valley of the Markanda, in the Sivalik branch of the sub-Himalayan mountains. *Asiatic Resolutions*, 19:1-24.

Forsyth-Major, C.J. 1888. Sur un gisement d'ossements fossiles dans l'île de Samos contemporains de l'âge de Pikermi. *Compte Rendus Hebdomadaire, Séances de la Société Géologique de France*, 107:1178-1181.

Fortelius, M., Eronen, J. Liu, L., Pushkina, D., Tesakov, A., Vislobokova, I. & Zhang, Z. 2006. Late Miocene and Pliocene large land mammals and climatic changes in Eurasia. *Palaeogeography, Palaeoclimatology, Palaeoecology*, 238:219-227.

Gaudry, A. 1860, Resultats des fouilles executees en Grece sous les auspices de l'Academie. *Comptes Rendus de l'Academie des Science, Paris*, 51:802-804.

Gaudry, A. 1861, Note sur la Girafe et l' *Helladotherium* trouvees a Pikermi (Grece). *Bulletin Societe Geologique de France, Ser. 2*, 18: 587-598.

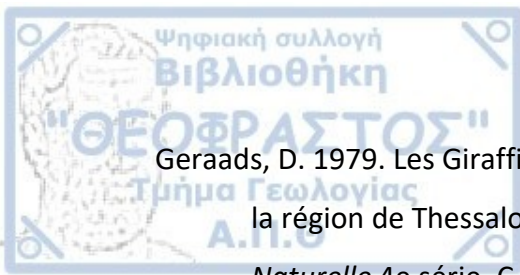
Gaudry, A. & Lartet, E. 1856. Résultats des recherches paléontologiques entreprises dans l'Attique sous les auspices de l'Académie. *Comptes rendus hebdomadaires des séances de l'Académie des Sciences*, 43:271-274.

Gentry, A.W. & Heizmann, E.P.J. 1996. Miocene Ruminants of the central and eastern Tethys and Paratethys, p. 378-391. In Bernor, R.L., Fahlbusch, V., and Mittmann, H.W. (ed.), *The Evolution of Western Eurasian Neogene Mammal Faunas*. Columbia University Press, New York, USA.

Gentry, A.W., Rössner, G.E. & Heizmann, E.P.J. 1999. Suborder Ruminantia, p. 225-253. In Rössner, G.E. & Heissig, K. (ed.), *The Miocene Land Mammals of Europe*. Verlag Dr. Friedrich Pfeil, Munich, Germany.

Geraads, D. 1974. *Les Giraffidés du Miocène Supérieur de la région de Thessalonique (Grèce)*. Unpublished PhD Thesis, University of Paris, France.

Geraads, D. 1978. Les Palaeotraginae (Giraffidae, Mammalia) du Miocène Supérieur de la région de Thessalonique (Grèce). *Géologie Méditerranéenne*, 5(2):269-276.



Geraads, D. 1979. Les Giraffinae (Artiodactyla, Mammalia) du Miocène Supérieur de la région de Thessalonique (Grèce). *Bulletin du Muséum National d'Histoire Naturelle* 4e série, C 4:377-389.

Geraads, D. 1986. Remarques sur la systématique et la phylogénie des Giraffidae (Artiodactyla, Mammalia). *Geobios*, 19(4):465-477.

Geraads, D. 1989. Un nouveau giraffidé du Miocène supérieur de Macédoine (Grèce). *Bulletin du Muséum national d'Histoire naturelle* 4e série, C 11:189-199.

Geraads, D. 1998. Le gisement de vertébrés pliocènes de Çalta, Ankara, Turquie. 9. Cervidae et Giraffidae. *Geodiversitas*, 20(3): 455-465.

Geraads, D. 2013. Large Mammals from the Late Miocene of Çorakyerler, Çankırı, Turkey. *Acta Zoologica Bulgarica*, 65(3):381-390.

Geraads, D., Reed, K. & Bobe, R. 2013. Pliocene Giraffidae (Mammalia) from the Hadar Formation of Hadar and Ledi-Geraru, Lower Awash, Ethiopia. *Journal of Vertebrate Paleontology*, 32(2):470-481.

Godina, A.Y. 1975. *Palaeotragus* from Neogene deposits of Mongolia and Middle Asia, p. 67-76. In Academia Nauk USSR (ed.), *The fossilized fauna and flora of Mongolia – Transactions of unified Soviet-Mongolian Palaeontology, Vol 2.* (In Russian).

Godina, A.Y. 1979. History of Fossil Giraffes of the Genus *Palaeotragus*. *Trudy. Paleontological Institute Akademia Nauk USSR*, Vol. 177. (In Russian).

Godina, A.Y. 2002. On the Taxonomy and Evolution of *Samotherium* (Giraffidae, Artiodactyla). *Paleontological Journal*, 36(4):395-402.

Godina, A.Y. & Bajgusheva V.S. 1985. A new *Palaeotragus* species from the Late Pliocene of the peri-Azov region. *Paleontologicheskii Zhurnal* 1985(3):84–89. (in Russian).

Gray, J.E. 1821. On the natural arrangement of vertebrate animals. *London Medical Repository*, 15:296-310.



Haile-Selassie, Y. 2009. Giraffidae, p. 389-396. In Haile-Selassie, Y. & WoldeGabriel, G. (ed.), *Ardipithecus kadabba: Late Miocene evidence from the Middle Awash, Ethiopia*. University of California Press, London, England.

Hamilton, W.R. 1973. The Lower Miocene Ruminants of Gebel Zelten, Libya. *Bulletin of the British Museum (Natural History) Geology*, 21(3);73-150.

Hamilton, W.R. 1978. Fossil giraffes from the Miocene of Africa and a revision of the phylogeny of the Giraffoidea. *Philosophical Transactions of the Royal Society of London B: Biological Sciences*, 283(996):165-229.

Hammer, Ø., Harper, D.A.T. & Ryan, P.D. 2001. PAST: Palaeontological statistics software package for education and data analysis. *Palaeontologia Electronica* 4.1.4A:9p.

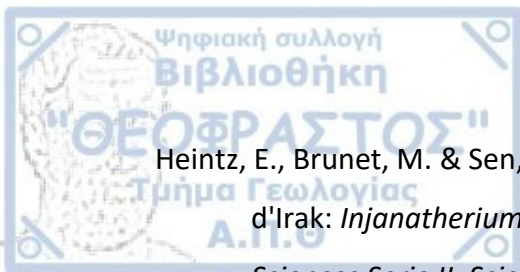
Harris, J., Solounias, N. & Geraads, D. 2010. Giraffoidea, p. 797-811. In Werdelin, L. & Sanders, W.J. (ed.), *Cenozoic Mammals of Africa*. University of California Press, Berkley, USA.

Hassanin, A. & Douzery, E. J. P. 2003. Molecular and morphological phylogenies of Ruminantia and the alternative position of the Moschidae. *Systematic Biology*, 52:206-228.

Hassanin, A., Delsuc, F., Ropiquet, A., Hammer, C., van Vuuren, B. J., Matthee, C., Ruiz-Garcia, M., Catzeflis, F., Areskoug, V., Nguyen, T.T. & Couloux, A. 2012. Pattern and timing of diversification of Cetartiodactyla (Mammalia, Laurasiatheria), as revealed by a comprehensive analysis of mitochondrial genomes. *Comptes Rendus Biologies*, 335:32-50.

Haughton, S.H. 1922. A note on some fossils from the Vaal River gravels. *Transactions of the Geological Society of South Africa*, 24:11-16.

Heintz, E. 1976. Les Giraffidae (Artiodactyla, Mammalia) du Miocène de Beni Mellal, Marocco. *Géologie Méditerranéenne*, 3:91-104.



Heintz, E., Brunet, M. & Sen, S. 1981. Un nouveau giraffide du Miocene superieur d'Irak: *Injanatherium hazimi* n. g., n. sp. *Comptes Rendus de l'Académie des Sciences Serie II, Sciences de la Vie*, 292:423-426.

Hou, S., Danowitz, M., Sammis, J. & Solounias, N. 2014. Dead ossicones and other characters describing Palaeotraginae (Giraffidae; Mammalia) based on new material from Gansu, Central China. *Zitteliana*, B(32): 91-98.

Iliopoulos, G. 2003. *The Giraffidae (Mammalia, Artiodactyla) and the Study of the Histology and Chemistry of Fossil Mammal Bone from the Late Miocene of Kerassia (Euboea Island, Greece)*. Unpublished PhD Thesis, University of Leicester, UK.

Irwin, D.M., Kocher, T.D. & Wilson, A.C. 1991. Evolution of the cytochrome *b* gene of mammals. *Journal of Molecular Evolution*, 32:128-144.

Janis, C.M. & Scott, K.M. 1987. The interrelationships of higher ruminant families: with special emphasis on the members of the Cervoidea. *American Museum Novitates*, 2893:1-85.

Kappelman, J., Dunham, A., Feshea, M., Lunkka, J.-P., Ekart, D., Mcdowell, F., Ryan, T. & Swisher III, C.C. 2003. Chronology of the Sinap Formation. In: Bernor, R., Kappelman, J., Sen, S. & Fortelius, M. (ed.), *Monograph on the Sinap Formation, Anatolia, Turkey*. Columbia University Press, New York, USA.

Killgus, H. 1922. Die unterpliocaenen chinesischen Säugetierreste der Tafel'schen Sammlung zu Tübingen. *Paleontologie Z*, 5.

Koken, E. 1885. Über fossile Säugethiere aus China. *Palaeontologische Abhandlungen*, 3:31-113.

Konidaris, G.E. 2013. *Palaeontological and biostratigraphical of the Neogene Proboscidea from Greece*. PhD Thesis, Aristotle University of Thessaloniki, Greece (In Greek).



Korotkevich, E. L. 1957. Giraffes in Hipparion fauna of Berislav. *Trudy. Zoological Institute Academia Nauk USSR*, Vol. 14:129-140 (In Ukrainian with Russian abstract).

Kostopoulos, D.S. 1996. *The Plio-Pleistocene Artiodactyls of Macedonia (N. Greece). Systematics, Palaeoecology, Biochronology, Biostratigraphy*. Unpublished PhD Thesis, Aristotle University of Thessaloniki, Greece (In Greek with English summary).

Kostopoulos, D.S. 2009. The Late Miocene mammal faunas of the Mytilinii Basin, Samos Island, Greece: new collection: 13. Giraffidae, p. 299-343. In Koufos G.D. and Nagel D. (ed.), *The Late Miocene Mammal Faunas of Samos*. Beiträge zur Paläontologie, 31, Vienna, Austria.

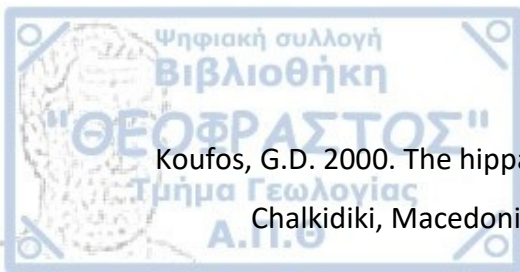
Kostopoulos, D.S., Koliadimou, K.K. & Koufos, G.D. 1996. The giraffids (Mammalia, Artiodactyla) from the Late Miocene mammalian localities of Nikiti (Macedonia, Greece). *Palaeontographica Abteilung A*, 239(1-3):61-88.

Kostopoulos, D.S. & Koufos, G.D. 1999. The Bovidae (mammalia, artiodactyla) of the "Nikiti-2" [NIK] faunal assemblage (Chalkidiki peninsula, N. Greece). *Annales de Paléontologie*, 85(3):193-218.

Kostopoulos D.S. & Athanassiou A. 2005. In the shadow of bovids: suids, cervids and giraffids from the Plio-Pleistocene of Greece. *Quaternaire hors-série*, 2:179-190.

Kostopoulos, D.S. & Saraç, G. 2005. Giraffidae (Mammalia, Artiodactyla) from the Late Miocene of Akkaşdağı, Turkey, p. 735-745. In Sen, S. (ed.), *Geology, Mammals and Environments at Akkaşdağı, Late Miocene of Central Anatolia*. Geodiversitas 27.

Koufos, G.D. 1990. The hipparions of the Lower Axios valley (Macedonia, Greece). Implications about the Neogene biostratigraphy and the evolution of the *Hipparion*, p. 321-338. In Lindsay, E.H., Fahlbush, V. & Mein P. (ed.), *European Neogene Mammal Chronology*, Plenum Press, NATO ASI.



Koufos, G.D. 2000. The hipparions of the Vallesian (Late Miocene) locality Nikiti 1 Chalkidiki, Macedonia, Greece. *Revue de Paléobiologie*, 19(1):47-77.

Koufos, G.D. 2003. Late Miocene mammal events and biostratigraphy in the Eastern Mediterranean, p. 343-372. In Reumer, J.W.F. & Wessels, W. (ed.), *Distribution and migration of tertiary mammals in Eurasia. A volume in honour of Hans de Bruijn*, DEINSEA 10.

Koufos, G.D. 2006. The Neogene mammal localities of Greece: Faunas, chronology and biostratigraphy. *Hellenic Journal of Geosciences*, 41:183-214.

Koufos, G.D. 2016. History, stratigraphy and fossiliferous sites, p. 3-10. In Koufos, G.D. & Kostopoulos, D.S. (ed.), *Palaeontology of the upper Miocene vertebrate localities of Nikiti (Chalkidiki Peninsula, Macedonia, Greece)*, *Geobios*, 49(1-2):3-10.

Koufos, G.D., Syrides, G. Koliadimou, K.K. & Kostopoulos, D.S. 1991. Un nouveau gisement de vertébrés avec hominoïde dans le Miocène supérieur de Macédoine (Grèce). *Comptes Rendus de l'Academie des Science, Paris*, 313:691-696.

Koufos, G.D., Kostopoulos, D.S., Vlachou, T.D. & Konidaris, G.E. 2016. Revision of the Nikiti 1 (NKT) fauna with description of new material. *Geobios*, 49(1-2): 11-22.

Lankester, R. 1902. On *Okapia*, a new genus of Giraffidae from Central Africa. *Transactions of zoological Society of London*, 16(6).

Lazaridis, G. 2015. *Study of the Late Miocene vertebrate locality of Kryopigi and other localities of Kassandra Peninsula, Chalkidiki (Greece). Systematics, Taphonomy, Paleoecology, Biochronology*. PhD Thesis, Scientific Annals of the School of Geology, Aristotle University, Thessaloniki, Greece. (In Greek)

Linnaeus, C. 1758. *Systema Naturae*.

Lunkka, P.J., Fortelius, M., Kappelman, J. & Sen, S., (1999) Chronology and mammal faunas of the Miocene Sinap Formation, Turkey, p. 238-264 in: Agustí, J., Rook, L. & Andrews, P. (ed.), *Hominoid Evolution and climatic change in*



Europe, vol. I, *The evolution of the Neogene terrestrial ecosystems in Europe*, Cambridge University Press, New York, USA.

Lydekker, R. 1886. On the fossil Mammalia of Maragha, in North-Western Persia.

Quarterly Journal of the Geological Society, 42(1–4):173–176.

Maniakas, I. & Kostopoulos, D.S. 2017, Morphometric-palaeoecological discrimination between *Bison* populations of the western Palaearctic.

Geobios, 50:155-171.

Marra, C.N., Solounias, N., Carone, G. & Rook, L. 2011. Palaeogeographic significance of the giraffid remains (Mammalia, Arctiodactyla) from Cessaniti (Late Miocene, Southern Italy). *Geobios*, 44:189-197.

Matthew, W.D. 1929. Critical observations upon Siwalik Mammals. *Bulletin of American Museum of Natural History*, 56:437-560.

Mitchell, G. & Skinner, J.D. 2003. On the origin, evolution and phylogeny of giraffes *Giraffa camelopardalis*. *Transactions of the Royal Society of South Africa*, 58:51-73.

Nakaya, H., Pickford, M. Yasui, K. & Nakano, Y. 1987. Additional large mammalian fauna from the Namurungule Formation, Samburu Hillhs, Northern Kenya. *African Study Monographs. Supplementary Issue*, 5:79-129

Owen, R. 1848. On the archetype and homologies of the vertebrate skeleton. *Richard and John E. Taylor*, London, UK.

Ozansoy, F. 1965. Etudes des gisements continentaux et des mammifères du Cénozoïque de Turquie. *Au Siège de la Société Géologique*, 102:1-92.

Pales, L. & Garcia, M.A. 1981. Atlas ostéologique pour servir á l'identification des Mammifères du Quaternaire, II: Herbivores. *Edition du centre national de la recherche scientifique*. Paris, France.

Paraskevaïdis I. 1940. Eine obermiocene Fauna von Chios. *Neues Jahrbuch fur Mineralogie Geologie und Palaontologie*, 83:363–442.



Pavlovic, M.B. 1969. Miozän-Säugetiere des Toplica-Beckens. *Annales Géologiques de la Péninsule des Balkans*, 34:269-394 (In Serbo-Croatian with German Abstract).

Pavlow, M. 1913. Mammifères tertiaires de la Nouvelle Russie. *1re partie. Nouveaux Mémoires de la Société impériale des Naturalistes de Moscou*, 17(3).

Pilgrim, G.E. 1910. Notices of new mammalian genera and species from the Tertiaries of India. *Records of the Geological Survey of India*, 40:63-71.

Pilgrim, G.E. 1911. The Fossil Giraffidae of India. *Memoirs of the Geological Survey of India*, 4:1-29.

Pomel, A. 1892. Sur le *Libytherium maurusium*, grand Ruminant du terrain pliocène plaisancien d'Algérie - *Comptes Rendus de l'Académie des Sciences, Paris*, 115:100-102.

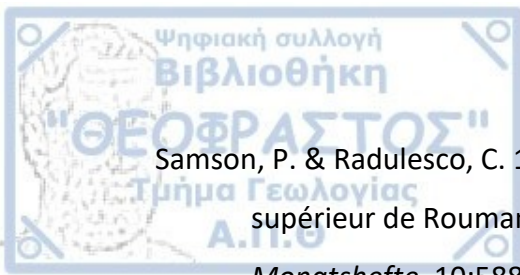
Ríos, M. 2018. Is the Astragalar Index a Valid Character for the Study of Giraffid Phylogeny? *International Journal of Paleobiology & Paleontology*, 1(1).

Ríos, M., Danowitz, M. & Solounias, N. 2016. First comprehensive morphological analysis on the metapodials of Giraffidae. *Palaeontologia Electronica* 19.3.50A: 1-39.

Ríos, M., Sánchez, I.M. & Morales, J. 2017. A new giraffid (Mammalia, Ruminantia, Pecora) from the Late Miocene of Spain, and the evolution of the sivathere-samothere lineage. *PlosOne*, 12(11).

Robinson, P. & Black, C.C. 1974. Vertebrate faunas from the Neogene of Tunisia. *Annual Geological Survey of Egypt*, 4:309–332

Rodler A. & Weithofer K.A. 1890. Die Wiederkäuer der Fauna von Maragha. *Denkschriften der Kaiserlichen Akademie der Wissenschaften Wien*, 57:753-772.



Samson, P. & Radulesco, C. 1966. Sur la présence des Girafidés dans le Villafranchien supérieur de Roumanie. *Neues Jahrbuch für Geologie und Paläontologie, Monatshefte*, 10:588-594.

Schmid, E. 1972. Atlas of Animal Bones for Prehistorians, Archaeologists and Quaternary Geologists. *Elsevier Publishing Company*, Amsterdam, The Netherlands.

Schmidt-Kittler, N., De Bruijn, H. & Doukas, C. (1995) The vertebrate locality Maramena (Macedonia, Greece) at the Turolian-Ruscinian boundary. *Münchener Geowissenschaftliche Abhandlungen A*, 28:9-18.

Sclater, P.L. 1901. On an apparently new species of Zebra from the Semliki Forest. *Proceedings of zoological Society of London*, 1.

Sen, S. 1977. La faune de Ronguers pliocènes de Çalta (Ankara, Turquie). *Bulletin du Muséum National d'Histoire Naturelle 3e série*, 465:89-171.

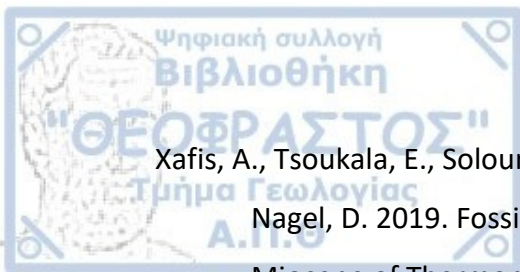
Solounias, N. 2007. Family Giraffidae, p. 257-277. In Prothero, D.R. & Foss, S.E. (ed.), *The Evolution of Artiodactyls*. Johns Hopkins University Press. Baltimore, USA.

Van der Made, J. & Morales J. 2011. *Mitilanotherium inexpectatum* (Giraffidae, Mammalia) from Huélago (Lower Pleistocene; Guadix-Baza basin, Granada, Spain) — observations on a peculiar biogeographic pattern. *Estudios Geológicos*, 67(2):613–627.

Vislobokova, I. (1997) Eocene –Early Miocene Ruminants in Asia. *Actes du Congres BiochroM 1997*, 21: 215-223.

Vlachou, T. & Koufos, G.D. 2002. The hipparions (Mammalia, Perissodactyla) from the Turolian locality "Nikiti-2" (NIK), Macedonia, N. Greece. *Annales de Paléontologie*, 88(4):215-263.

Von der Driesch, A. 1976. A guide to the measurement of animal bones from archaeological sites. *Peabody Museum Bulletins, Harvard University*, Cambridge, USA.



Xafis, A., Tsoukala, E., Solounias, N., Mandic, O., Harzhauser, M., Grímsson, F. & Nagel, D. 2019. Fossil Giraffidae (Mammalia, Artiodactyla) from the Late-Miocene of Thermopigi (Macedonia, Greece). *Palaeontologia Electronica*, 22(3.68):1-38.



PLATES



Plate 1

Palaeotragus aff. *berislavicus*

Nikiti skull (NKT-172)

- a) Right view
- b) Left view
- c) Occlusal view

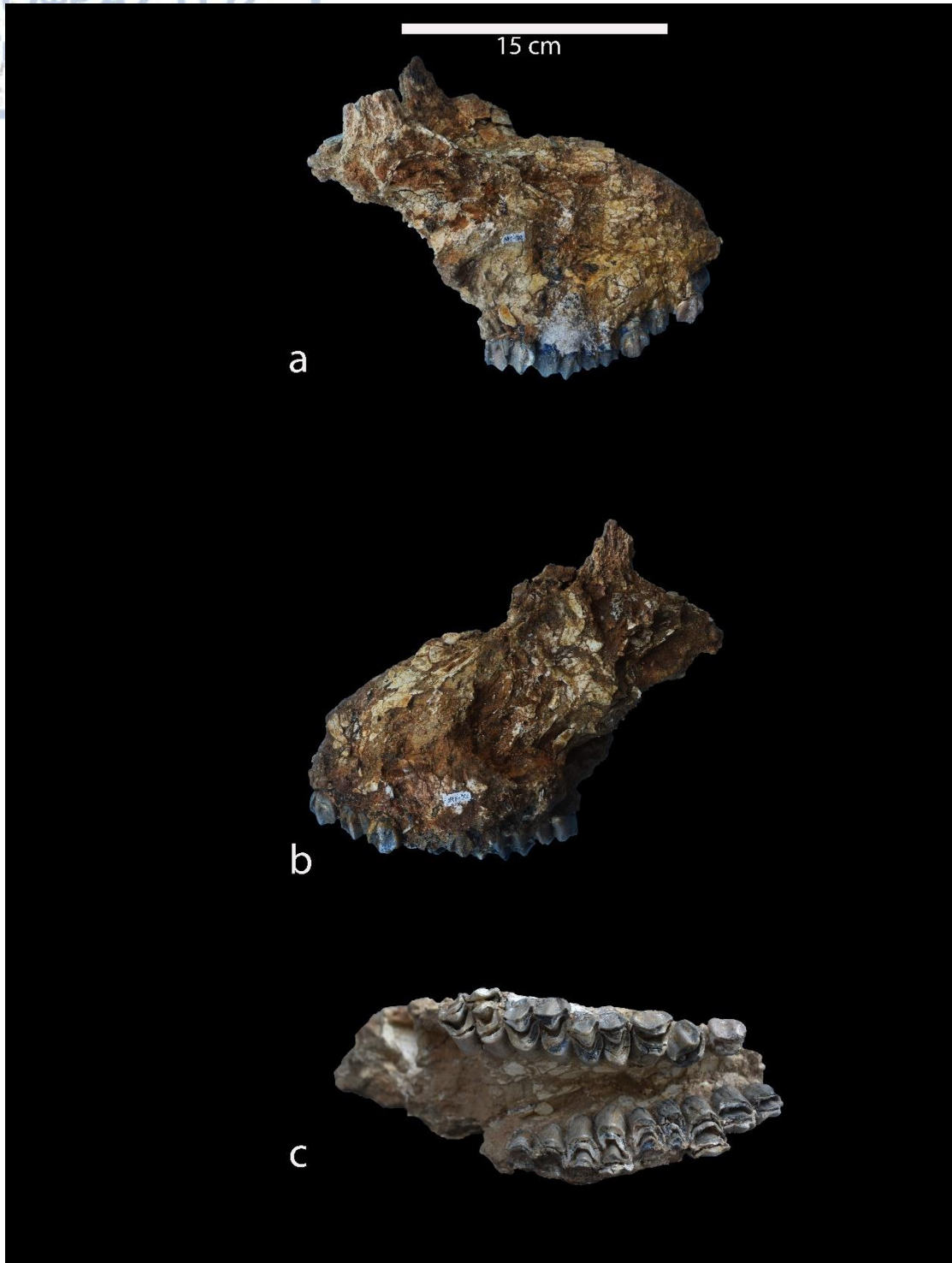




Plate 2

Palaeotragus aff. *berislavicus*

Nikiti Humerus (NKT-161)

- a) Cranial view
- b) Caudal view

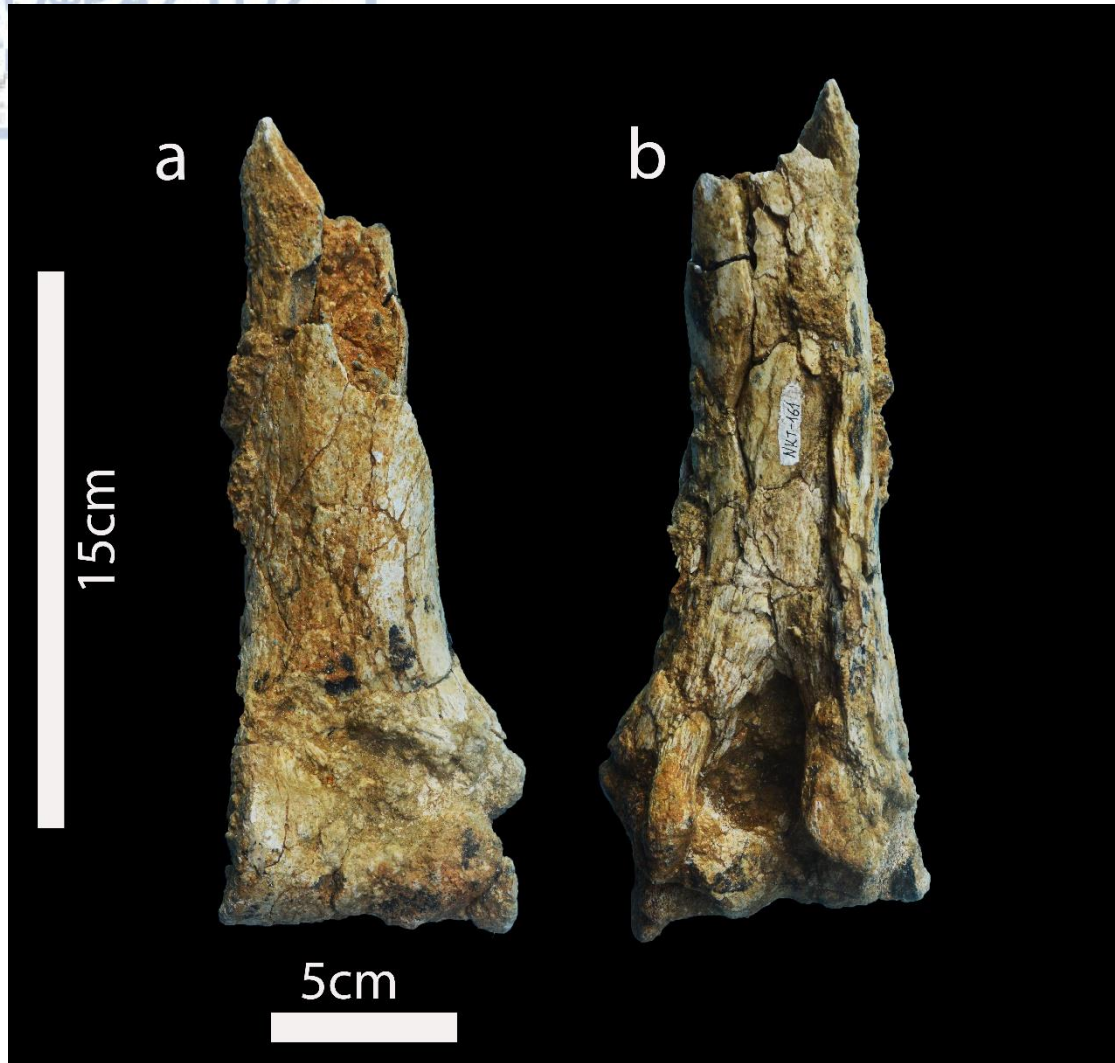




Plate 3

Palaeotragus aff. *berislavicus*

Nikiti Radii

- a) NKT-156
 - i) Proximal view
 - ii) Cranial view
 - iii) Distal view
 - iv) Caudal view
- b) NKT-155
 - i) Proximal view
 - ii) Cranial view
 - iii) Distal view
 - iv) Caudal view
- c) NKT-169
 - i) Cranial View
 - ii) Distal View
 - iii) Caudal View
- d) NKT-159
 - i) Cranial View
 - ii) Caudal View

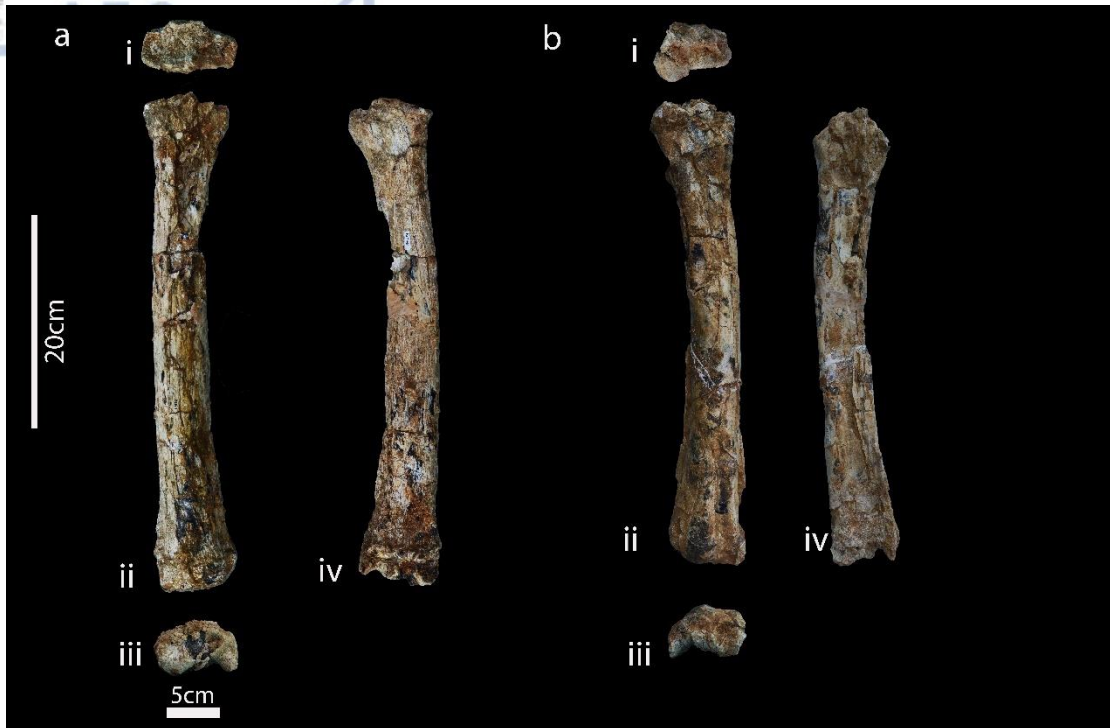




Plate 4

Palaeotragus aff. *berislavicus*

Nikiti Metacarpals

a) NKT-137

- i) Proximal view
- ii) Dorsal view
- iii) Distal view
- iv) Palmar view

b) NKT-131

- i) Proximal view
- ii) Dorsal view
- iii) Distal view
- iv) Palmar view

c) NKT-141

- i) Proximal view
- ii) Dorsal view
- iii) Distal view





Plate 5

Palaeotragus aff. berislavicus

Nikiti Tibia (NKT-271)

- a) Proximal view
- b) Cranial view
- c) Distal view
- d) Caudal view





Plate 6

Palaeotragus aff. *berislavicus*

Nikiti Astragali

a) NKT-267

- i) Anterior view
- ii) Posterior view
- iii) Medial view
- iv) Lateral view

b) NKT-163

- i) Anterior view
- ii) Posterior view
- iii) Medial view
- iv) Lateral view

c) NKT-266

- i) Anterior view
- ii) Posterior view
- iii) Medial view
- iv) Lateral view

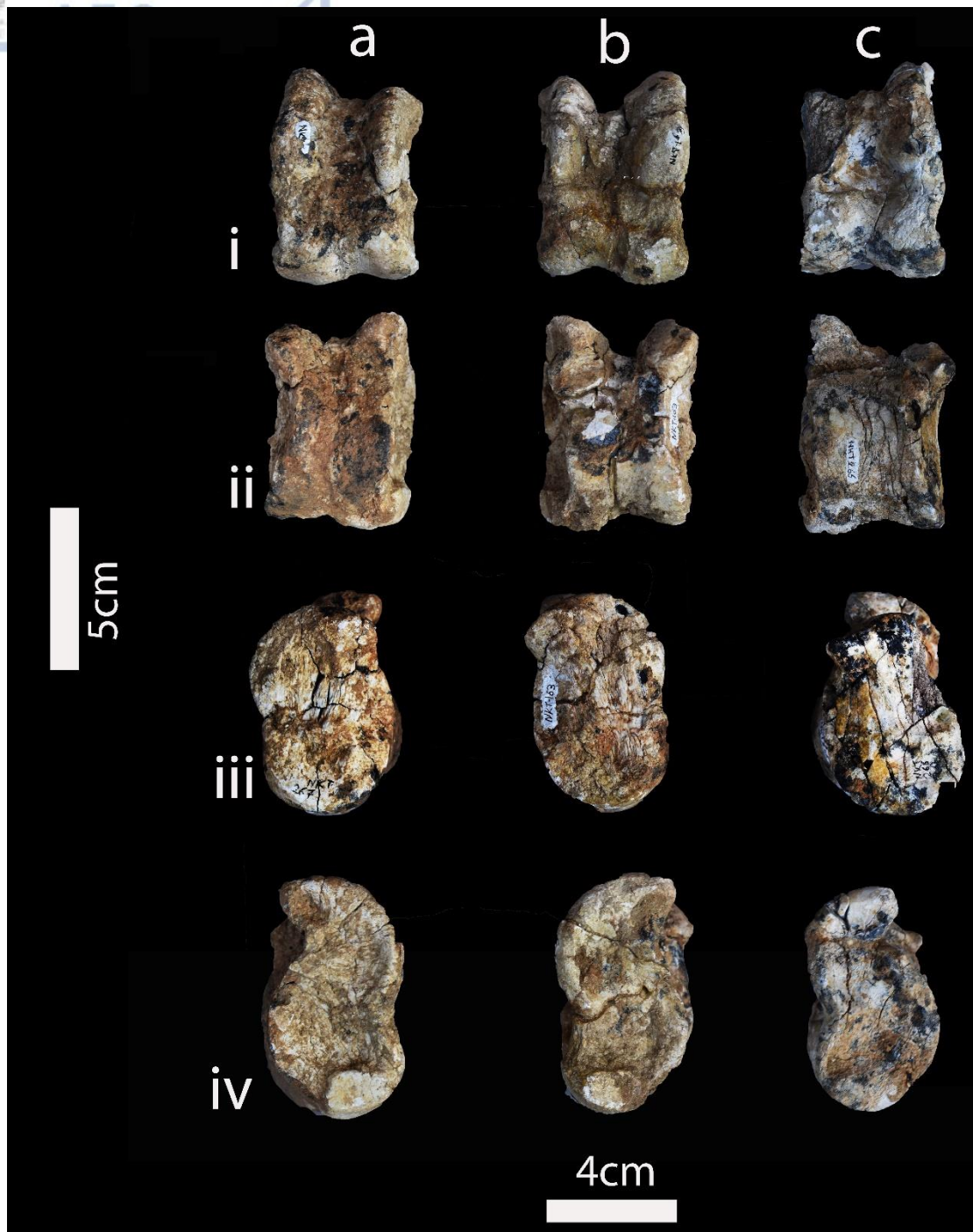




Plate 7

Palaeotragus aff. *berislavicus*

Nikiti Calcanei

a) NKT-153

- i) Plantar view
- ii) Dorsal view
- iii) Medial view
- iv) Lateral view

b) NKT-268

- i) Plantar view
- ii) Dorsal view
- iii) Medial view
- iv) Lateral view

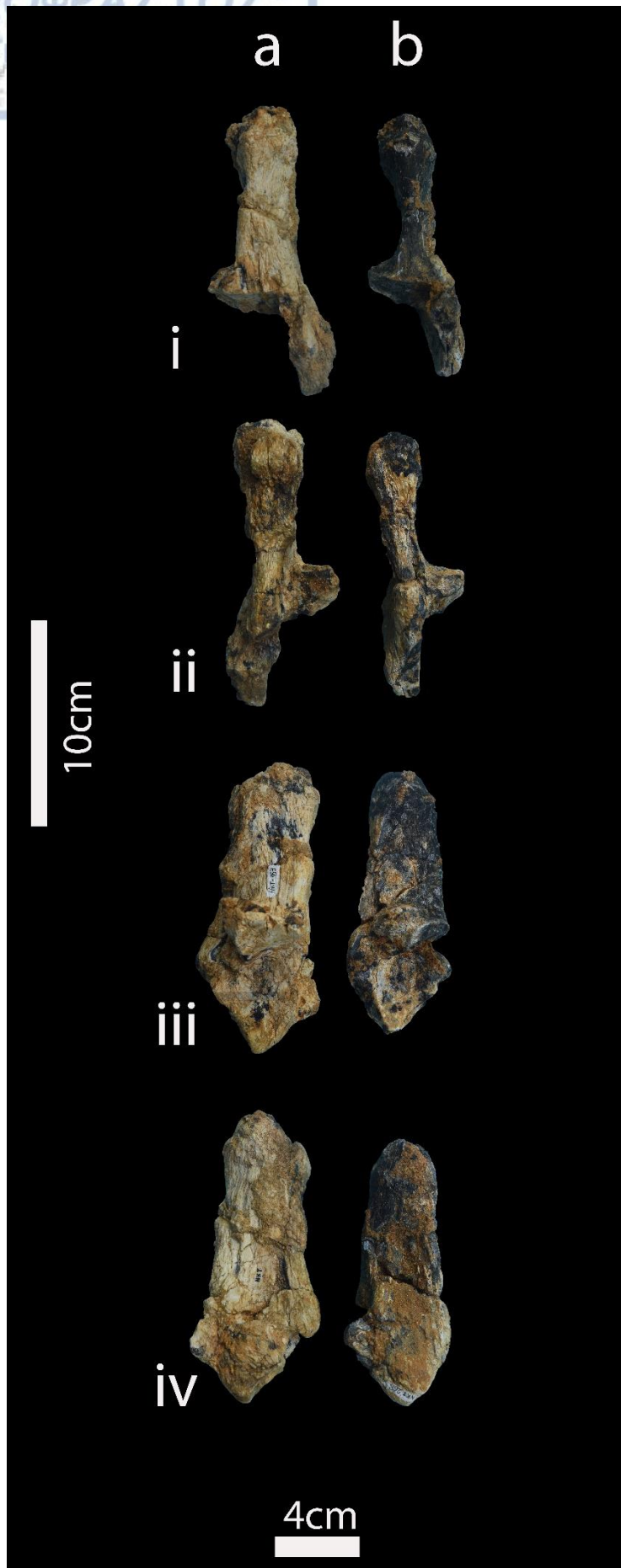




Plate 8

Palaeotragus aff. *berislavicus*

Nikiti Metatarsals

a) NKT-136

- i) Proximal view
- ii) Dorsal view
- iii) Distal view
- iv) Plantar view

b) NKT-160

- i) Dorsal view
- ii) Distal view

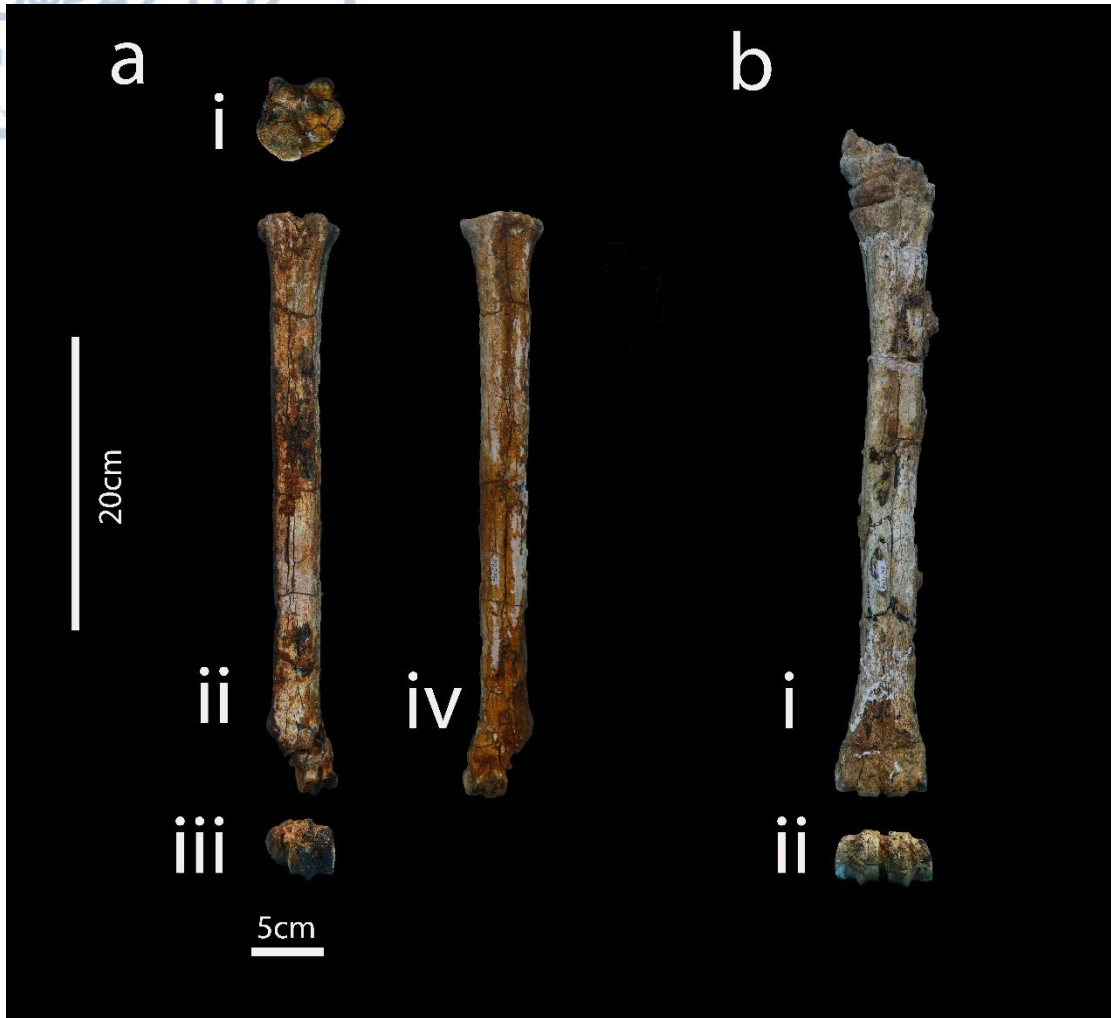




Plate 9

Palaeotragus coelophrys

Pentalophos Toothrow with P²-M³ (PNT-113f)

- a) Occlusal view
- b) Lingual view
- c) Labial view

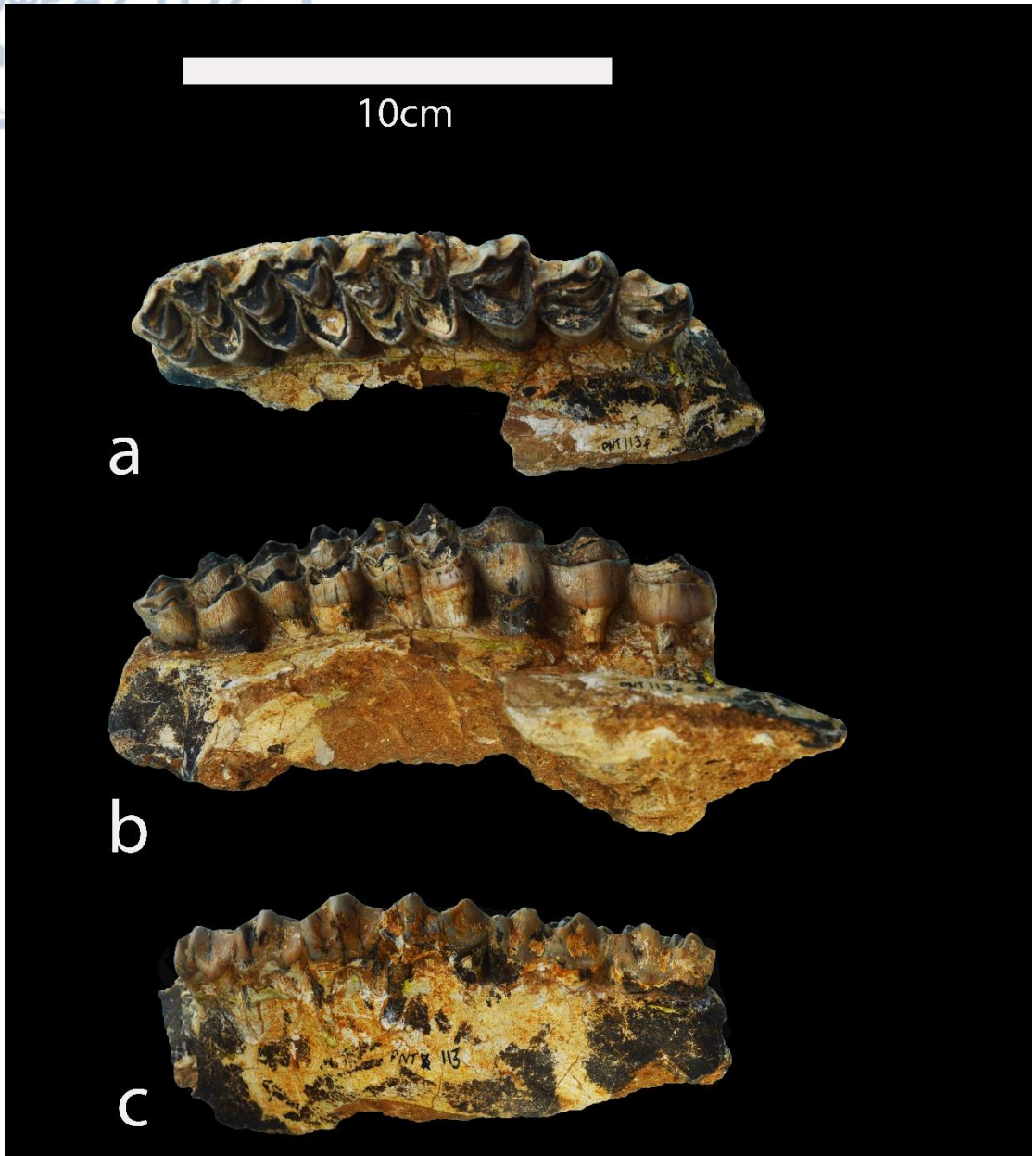




Plate 10

Palaeotragus coelophrys

Pentalophos Isolated Teeth i: PNT-165 (M²-M³)

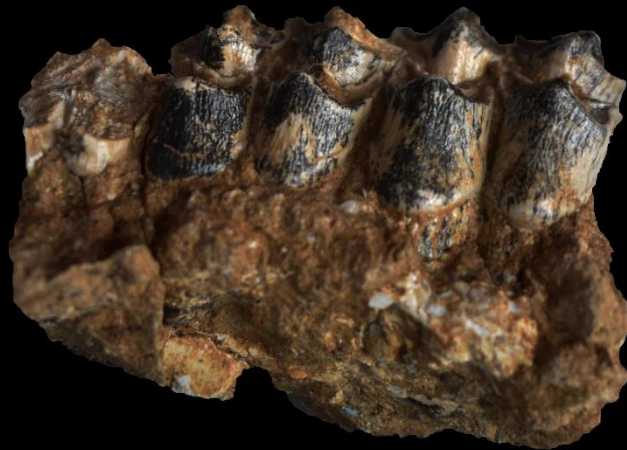
- a) Occlusal view
- b) Lingual view
- c) Labial view

5cm

a



b



c



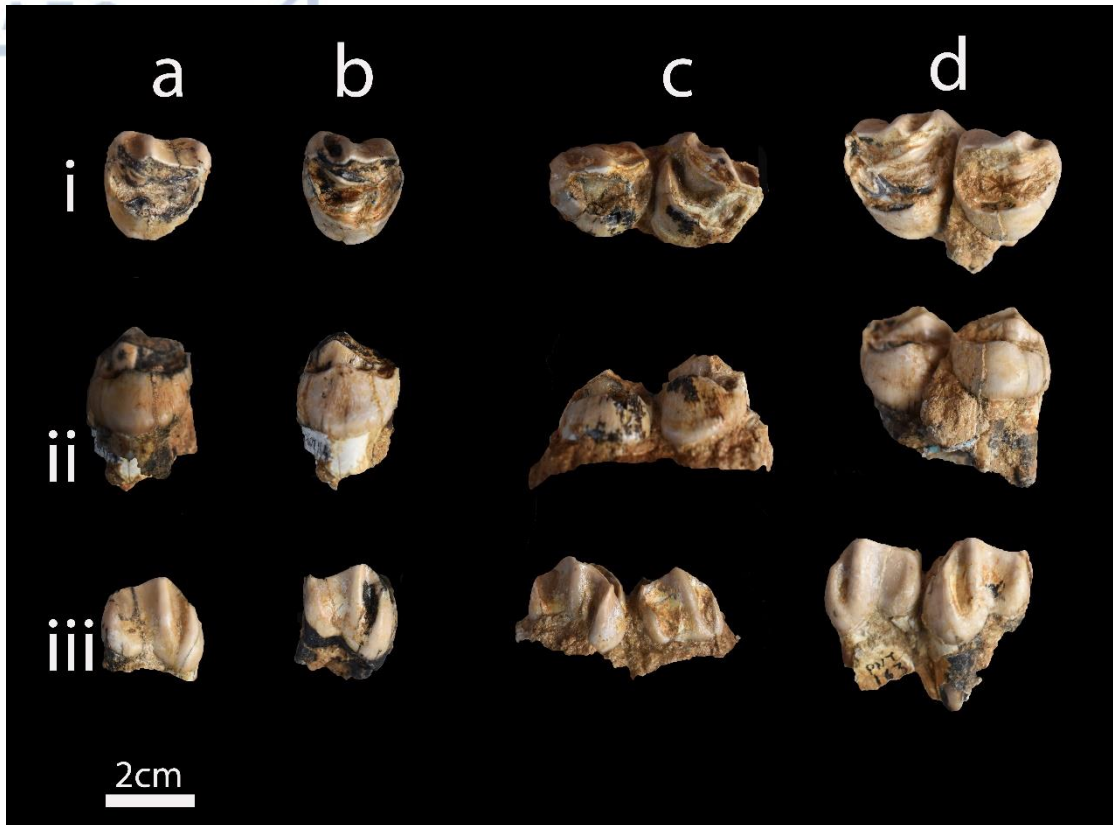


Plate 11

Palaeotragus coelophrys

Pentalophos Isolated Teeth ii

- a) PNT-161 (P^2)
 - i) Occlusal view
 - ii) Lingual view
 - iii) Labial view
- b) PNT-164 (P^3)
 - i) Occlusal view
 - ii) Lingual view
 - iii) Labial view
- c) PNT-162 (P^2 - P^3)
 - i) Occlusal view
 - ii) Lingual view
 - iii) Labial view
- d) PNT-163 (P^2 - P^3)
 - i) Occlusal view
 - ii) Lingual view
 - iii) Labial view





Palaeotragus coelophrys

Pentalophos Mandible with M₁-M₃ (PNT-328f)

- a) Occlusal view
- b) Lingual view
- c) Labial view

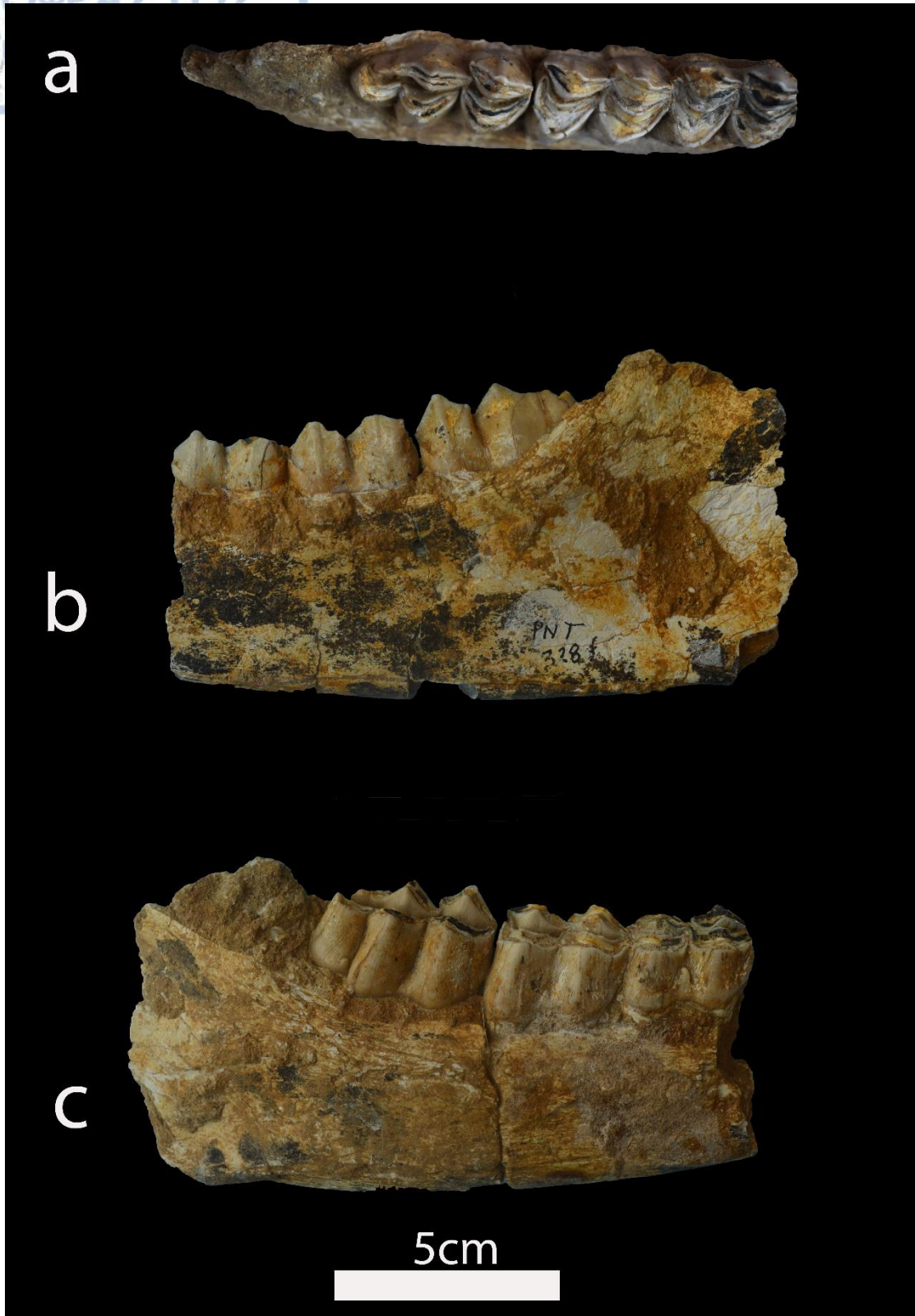




Plate 13

Palaeotragus coelophrys

Pentalophos Deciduous Mandible with dP_2-M_1

(PNT-121f)

- a) Occlusal view
- b) Lingual view
- c) Labial view

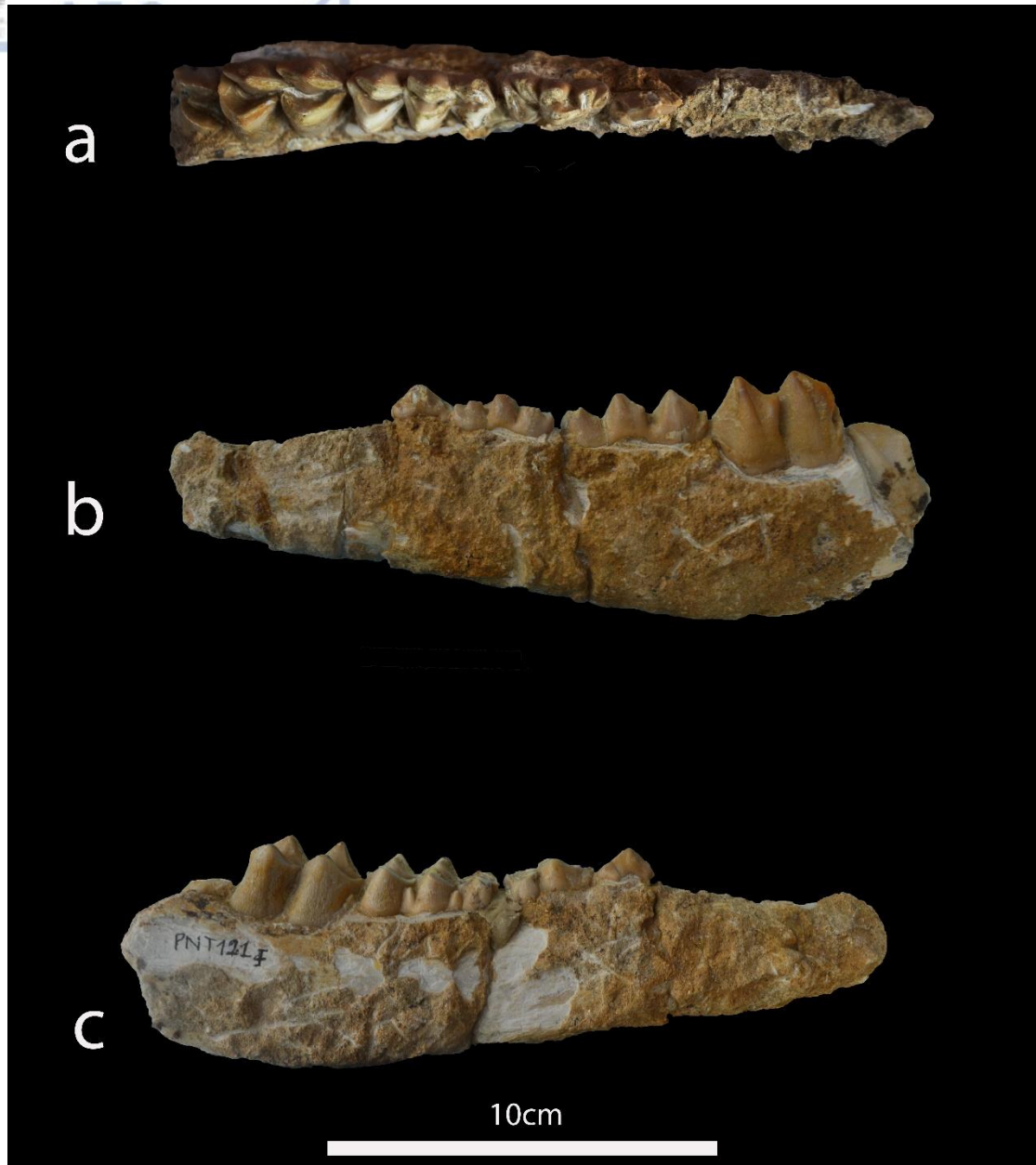




Plate 14

Palaeotragus coelophrys

Pentalophos Humerus (PNT-155)

- a) Cranial view
- b) Caudal view
- c) Right view
- d) Left view

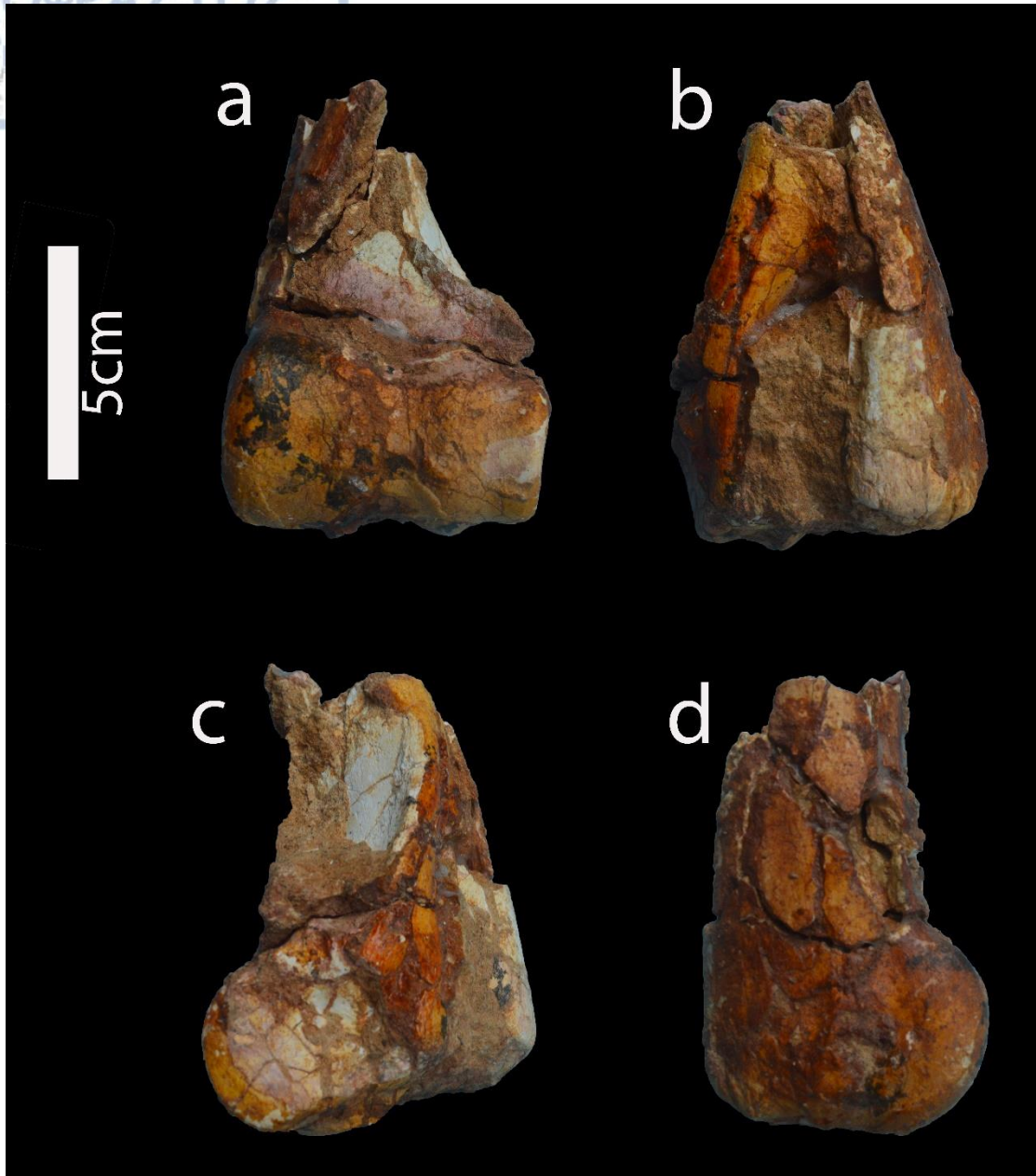




Plate 15

Palaeotragus coelophrys

Pentalophos Metatarsals

a) PNT-114f

i) Proximal view

ii) Dorsal view

iii) Plantar view

b) PNT-119f

i) Proximal view

ii) Dorsal view

iii) Plantar view





Plate 16

Palaeotragus cf. coelophrys

Ravin de la Pluie Skull (RPI-91)

- a) Left view
- b) Right view
- c) Occlusal view

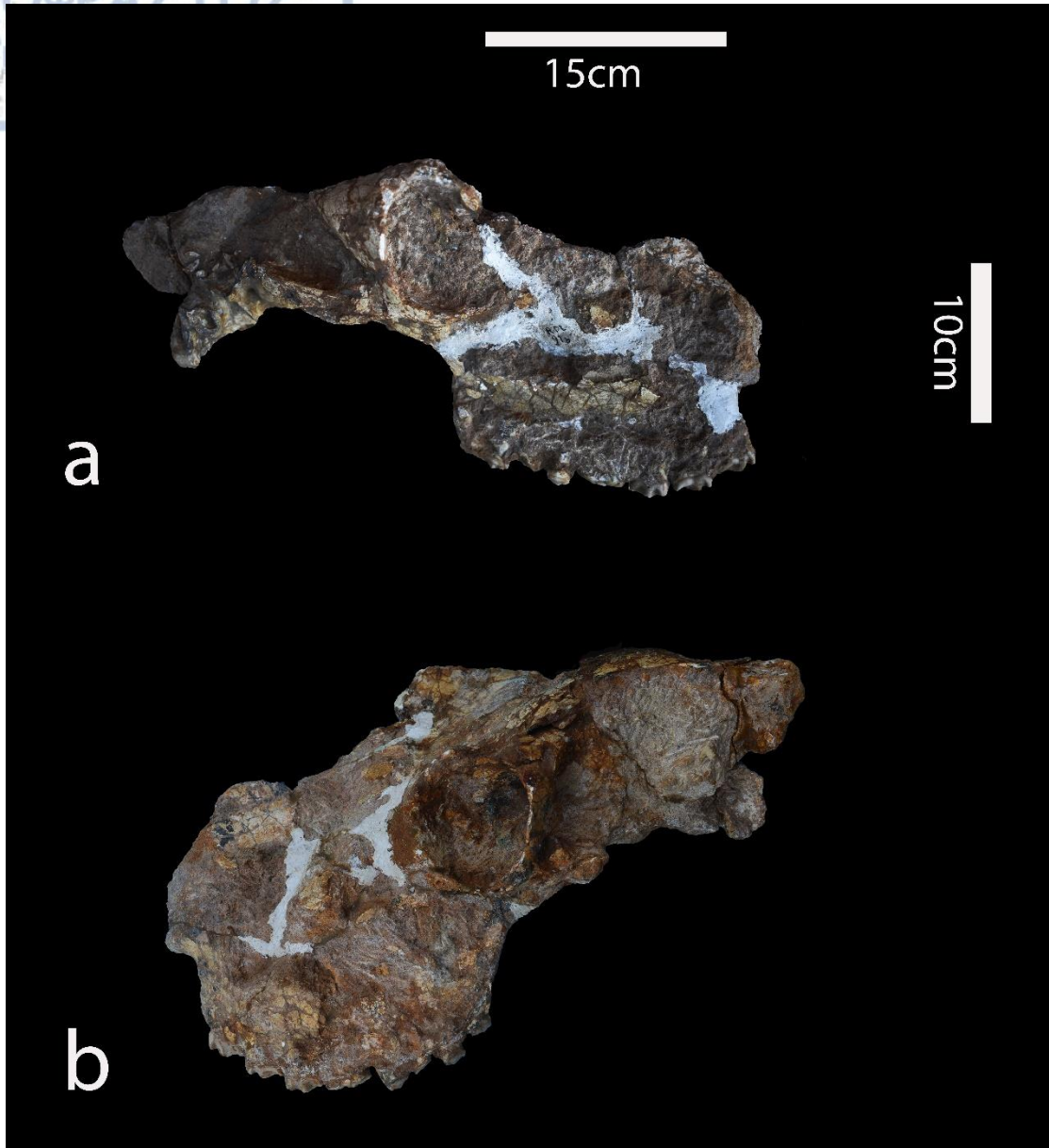








Plate 17

Palaeotragus cf. coelophrys

Ravin de la Pluie Mandible with M₁-M₃ (RPI-104)

- a) Occlusal view
- b) Lingual view
- c) Labial view





Xirochori Mandible Fragment (XIR-24)

- a) Occlusal view
- b) Lingual view
- c) Labial view



5cm

a



b



c

